INTERNATIONAL DOCTORAL
SCHOOL OF THE USC

Nuria
Carmona Ule

PhD Thesis

Nanotechnology applied to translational oncology: Developing tools for liquid biopsy

Santiago de Compostela, 2021

Doctoral Programme in Molecular Medicine

TESE DE DOUTORAMENTO

NANOTECHNOLOGY APPLIED TO TRANSLATIONAL ONCOLOGY: DEVELOPING TOOLS FOR LIQUID BIOPSY

Nuria Carmona Ule

ESCOLA DE DOUTORAMENTO INTERNACIONAL DA UNIVERSIDADE DE SANTIAGO DE COMPOSTELA

PROGRAMA DE DOUTORAMENTO EN MEDICINA MOLECULAR

SANTIAGO DE COMPOSTELA
2021

DECLARACIÓN DEL AUTOR /A DE LA TESIS

D./Dña. **Nuria Carmona Ule**

Título de la tesis: **Nanotechnology applied to translational oncology: developing tools for liquid biopsy**

Presento mi tesis, siguiendo el procedimiento adecuado al Reglamento y declaro que:

1) La tesis abarca los resultados de la elaboración de mi trabajo.
2) De ser el caso, en la tesis se hace referencia a las colaboraciones que tuvo este trabajo.
3) Confirmo que la tesis no incurre en ningún tipo de plagio de otros autores ni de trabajos presentados por mí para la obtención de otros títulos.
4) La tesis es la versión definitiva presentada para su defensa y coincide la versión impresa con la presentada en formato electrónico.

Y me comprometo a presentar el Compromiso Documental de Supervisión en el caso que el original no esté depositado en la Escuela.

En **Santiago de Compostela**, **29 de noviembre de 2021**.

Fdo. Nuria Carmona Ule

AUTORIZACIÓN DEL DIRECTOR/TUTOR DE LA TESIS

Nanotechnology applied to translational oncology: developing tools for liquid biopsy

D. Rafael López López

Dª. Ana Belén Dávila Ibáñez

INFORMA/N:

Que la presente tesis, se corresponde con el trabajo realizado por Dª. Nuria Carmona Ule, bajo mi dirección/tutorización, y autorizo su presentación, considerando que reúne los requisitos exigidos en el Reglamento de Estudios de Doctorado de la USC, y que como director de esta no incurre en las causas de abstención establecidas en la Ley 40/2015.

De acuerdo con lo indicado en el Reglamento de Estudios de Doctorado, declara también que la presente tesis doctoral es idónea para ser defendida en base a la modalidad de Monográfica con reproducción de publicaciones, en los que la participación del doctorando/a fue decisiva para su elaboración y las publicaciones se ajustan al Plan de Investigación.

En Santiago de Compostela, 29 de noviembre de 2021.

Fdo. Rafael López López
(Director y tutor)

Fdo. Ana Belén Dávila Ibáñez
(Directora)

I, Nuria Carmona Ule, author of this thesis, have no conflict of interest to declare.

The studies described in this thesis were performed within the framework of the Roche-CHUS Join Unit of the Translational Medical Oncology Group (Oncomet), Health Research Institute of Santiago de Compostela (IDIS) at the University Hospital Complex of Santiago de Compostela, Spain.

The work in this thesis was financially supported by the Galician Agency of Innovation (GAIN), Consellería de Economía, Emprego e Industria, Roche Pharma. I, Nuria Carmona Ule, was financially supported by Axudas Predoutorais do IDIS.

A mis padres, Esther y Julio

A mi tío, Santiago L. Ule Garrido

“Imagination is the Discovering Faculty, pre-eminently.
It is that which penetrates into the unseen worlds around us, the worlds of Science”
– Ada Lovelace

“Those who are inspired by a model other than Nature, labour in vain”
– Leonardo da Vinci

Table of contents

TABLE OF CONTENTS

Abbreviations and acronyms

ABBREVIATIONS AND ACRONYMS

CDX · CTC Derived Xenograft

CH · Cholesterol

CK · Cytokeratin

CQAs · Critical Quality Attributes

CTCs · Circulating Tumour Cells

ctDNA · Circulating DNA

ctRNA · Circulating RNA

DLS · Dynamic Light Scattering

EGFR · Epidermal Growth Factor Receptor

EMT · Epithelial-mesenchymal transition

EpCAM · Epithelial cell adhesion molecule

EPISPOT· Epithelial ImmunoSPOT

ER · Estrogen Receptor

FAO · Fatty Acid Oxidation

FDA · Food and Drug Administration

FFAs · Free fatty acids

HER2 · Human Epidermal growth factor Receptor 2

HPLC · High-performance liquid chromatography

HPLC-ESI-MS · HPLC-electrospray ionization tandem mass spectrometry

LDs · Lipid droplets

MACS · Magnetically Activated Cell Sorting

mCTCs · CTC-derived cell line

mRNA · Messenger RNA

MET · Mesenchymal-epithelial transition

NEs · Nanoemulsions from this thesis made of OA, PC, and CH

NGS · Next-generation sequencing

NPs · Nanoparticles

NTA · Nanoparticle Tracking Analysis

OA · Oleic Acid

OS · Overall survival

O/W · Oil in Water

PBMCs · Peripheral mononuclear blood cells

PC · Phosphatidylcholine

PCA · Principal Component Analysis

PdI · Polydispersity index

PDX · Patient-Derived Xenograft

PEG · Polyethylene glycol

PFS · Progression-free survival

PLL · Polylysine

PR · Progesterone Receptor

RBCs · Red Blood Cells

ROS · Reactive Oxygen Species

RT-qPCR · Quantitative Reverse Transcription PCR

TEM · Transmission Electron Microscopy

UCP 2 · Uncoupling protein 2

W/O · Water in Oil

ζ-potential · Zeta potential

Resumen *in extenso*

RESUMEN *IN EXTENSO*

La nanotecnología es un campo que permite el diseño de estructuras funcionales con dimensiones nanométricas, tales como las nanopartículas (NPs). La importancia de las NPs reside en que presentan un enorme potencial en distintos campos debido a sus propiedades físico-químicas únicas. Además, son fácilmente modulables según la aplicación final deseada. Entre las áreas de investigación dónde se usan las NPs, cabe destacar la oncológica y en particular, la biopsia líquida. La biopsia líquida es la técnica que estudia el material biológico en fluidos corporales como la sangre. Esto en oncología, permite estudiar lo que es conocido como el "circuloma tumoral", es decir, el conjunto de componentes que circulan por los fluidos procedentes del tejido tumoral. Algunos de ellos son ácidos nucleicos tumorales circulantes (ctDNA y ctRNA), vesículas extracelulares o CTCs. Haciendo uso de la biopsia líquida, es posible determinar la heterogeneidad tumoral en distintos momentos de la enfermedad, aportando información en tiempo real sobre la evolución de la misma. En este campo, la nanotecnología aporta herramientas tanto para el aislamiento, como para la detección de este tipo de materiales.

El análisis secuencial de CTCs permite obtener información tanto a nivel molecular (caracterización a nivel proteico, genético o epigenético) como a nivel clínico (sensibilidad farmacológica y monitorización). Actualmente, existen gran cantidad de técnicas para la detección y aislamiento de CTCs y continuamente se publican nuevas estrategias para este fin. Sin embargo, todavía presentan ciertas limitaciones: Por un lado, (i) la muestra inicial presenta pocas células debido a su baja concentración en sangre (1 CTC entre 10^6-10^7 células sanguíneas). Por otro lado, (ii) generalmente se utilizan técnicas de aislamiento basadas en el reconocimiento de antígenos específicos en la superficie de la célula tumoral. Esta selección positiva resulta en la pérdida de subpoblaciones de CTCs. En concreto, la mayoría de las técnicas de aislamiento se basan en marcadores epiteliales a pesar de que una población de CTCs no los expresan o los han perdido previamente a causa de la plasticidad que presentan debido al proceso de transición epitelio-mesénquima (EMT, del

inglés *epithelial-mesenhcymal transition*), y el de transición mesénquima-epitelio (MET, del inglés *mesenchymal-epithelial transition*).

Cabe destacar, que dependiendo de los estudios que se quieran realizar con las CTCs, la elección del sistema de aislamiento es un punto crítico. Muchos de los sistemas empleados para el aislamiento fijan las células al final del proceso, siendo útiles para caracterización a nivel proteico, de genoma, pero no para llevar a cabo estudios funcionales. Para llevar a cabo estos estudios, es necesario liberar las CTCs viables de los sistemas en los que quedan retenidas. Por tanto, es necesario avanzar hacia plataformas que permitan un aislamiento más eficiente de las CTCs sin disminuir su viabilidad. Para mejorar la eficiencia de aislamiento, las nuevas tecnologías utilizan la combinación de diferentes técnicas, como separación física y separación basada en marcadores de las membranas celulares.

Es importante resaltar que, aún con todos estos avances, el uso de las CTCs sigue sin ser incorporado en las guías clínicas, principalmente por la complejidad que representa su uso.

Teniendo en cuenta estos antecedentes, el objetivo de esta tesis es generar herramientas basadas en la nanotecnología para favorecer el estudio de CTCs, permitiendo evaluar la utilidad de estas células para predecir el estado en pacientes con cáncer de mama. Este objetivo general se dividió en tres módulos de trabajo. El primero consistió en generar nanoemulsiones que favorecieran el cultivo *ex vivo* de CTCs. Para ello, se formularon nanoemulsiones con lípidos y ácidos grasos relacionados con proliferación de células tumorales de cáncer de mama. Una vez caracterizadas, se estudió su eficacia para favorecer la proliferación celular en líneas modelo de cáncer de mama. Después de llevar a cabo la optimización del protocolo a seguir con las nanoemulsiones proliferativas, el segundo módulo de trabajo trataba de testar dichas nanoemulsiones para su uso en cultivos *ex vivo* de CTCs, previamente aisladas de pacientes con cáncer de mama metastásico. Con dicho protocolo se pretendía establecer cultivos que permitieran realizar una caracterización molecular de las CTCs cultivadas. Por último, en el tercer módulo, una vez visto el potencial de estas nanoemulsiones para favorecer el mantenimiento de los cultivos de CTCs, se procedió a funcionalizar dichas

nanoemulsiones con péptidos de reconocimiento de marcadores proteicos de la superficie de las células tumorales de cáncer de mama. El objetivo de este último punto consistía en desarrollar NPs biodegradables y biocompatibles que sirvieran para funcionalizar dispositivos de microfluídica y dotarlos de mayor capacidad para aislar CTCs. En concreto, a modo de prueba de concepto para el desarrollo de una plataforma versátil en la que se pudieran emplear distintos péptidos en función de la población celular a la que se quisiera dirigir, se formularon dos formulaciones de nanoemulsiones decoradas con dos péptidos. Por un lado, se usó el péptido Pep10, el cuál reconoce a EpCAM (del inglés *epithelial cell adhesion molecule*) y, por otro lado, se empleó GE11, que reconoce a EGFR (del inglés *epidermal growth factor receptor*).

En la primera parte de la tesis, donde se desarrollaron nanoemulsiones para favorecer el cultivo *ex vivo* de CTCs de pacientes con cáncer de mama, para su formulación se emplearon: colesterol (CH, del inglés *cholesterol*), fosfatidilcolina (PC, del inglés *phosphatidylcholine*) y ácido oleico (OA, del inglés *oleic acid*). De OA se usaron distintas concentraciones, para obtener cuatro formulaciones iniciales. A continuación, se llevó a cabo su caracterización para escoger la mejor formulación, en base a su tamaño, homogeneidad (PdI, del inglés *polidispersity index*) y estabilidad. Las nanoemulsiones escogidas (llamadas NEs) presentaron un tamaño menor a los 200 nm, con carga superficial negativa (-32.2 mV). Además, se determinó la concentración final de NEs mediante la técnica de análisis de seguimiento de NPs (NTA, del inglés *nanoparticle tracking analysis*). También, se analizó su morfología mediante microscopía de transmisión electrónica (TEM, del inglés *transmission electron microscopy*), para comprobar su esfericidad. Por otro lado, mediante la técnica de resonancia magnética nuclear y cromatografía líquida de alta eficacia (HPLC, del inglés *high-performace liquid chromatography*) se determinó que todos los compuestos empleados en el momento de la formulación formaban parte de las NEs. Finalmente, se realizó un estudio de estabilidad, y se comprobó que las NEs eran estables a lo largo de 6 meses de almacenaje a 4 ^{o}C.

Una vez finalizada la caracterización de las propiedades y estabilidad de las NEs, se iniciaron los estudios *in vitro* para comprobar si las

nanoemulsiones seleccionadas en la primera fase (NEs) eran realmente eficaces para favorecer el mantenimiento y la proliferación en cultivos celulares. Para ello, se trataron distintas líneas celulares de cáncer de mama (HCC1143, MDA-MB-231 y MCF-7) con concentraciones crecientes de NEs y se comprobó un aumento de la viabilidad celular, determinada por la técnica del alamarBlue™. Gracias a este ensayo, se escogió la concentración de trabajo a emplear para el resto de los experimentos (2.4×10^9 NPs/mL), estableciendo un protocolo para el uso de estas nanoemulsiones con actividad proliferativa. A continuación, se comprobó la internalización de las NEs en dichas células usando la tinción de Nile Red analizada por microscopía confocal y citometría de flujo.

Una vez comprobado que había un efecto beneficioso en la viabilidad celular al tratar los cultivos con NEs, se realizó un experimento en el que se comparó el efecto de las NEs y el de los compuestos libres empleados en su formulación (CH, PC y OA). Para ello, se usaron CH, PC y OA sin formular, tanto mezclados entre sí como de forma individual a la misma concentración final que en la formulación. De ello se determinó que, estos compuestos sin estar formulados no ejercían los mismos efectos sobre la viabilidad celular. De forma complementaria, se formularon dos nuevas nanoemulsiones, cambiando el OA empleado en las NEs por otros compuestos (vitamina E o migliol 812), con el objetivo de estudiar el efecto de nanoemulsiones con propiedades similares, pero composición diferente. De ello se determinó que dichas formulaciones no aportaban ese incremento en la viabilidad celular conseguido con el uso de NEs. Además, para comprobar que este efecto en el aumento de viabilidad permanecía en el tiempo, se analizó un cultivo de 4 días al que se añadió dos veces NEs (día 0 y día 2) y se observó que el porcentaje de viabilidad siempre superaba el 100 % con respecto a los controles negativos (sin añadir NEs).Es importante destacar en este punto, el hecho de que ya a las 3 horas de incubación con las NEs se observaba un efecto en el aumento de la viabilidad celular medida por alamarBlue™. Dicho efecto podría estar relacionado con la hipótesis deque parte de las NEs estarían siendo dirigidas de manera directa a las mitocondrias para ser oxidadas mediante la vía de oxidación de ácidos grasos (FAO, del inglés *fatty acid oxidation*). Como resultado de esta vía se generan NADPH y

NADH, los cuales estarían provocando la reducción de la resarzurina (el compuesto activo del alamarBlue$^{TM)}$. Por otro lado, se observó como con la segunda adición se restablecía el efecto, validando su uso para futuros protocolos en los que favorecer el cultivo celular.

Una vez determinado el efecto en líneas celulares, se generó una línea modelo de CTCs (mCTCs). El objetivo era validar el efecto de las NEs en un modelo próximo a CTCs de cáncer de mama, pues a diferencia de las líneas empleadas en los experimentos previos, las mCTCs habían estado en circulación de un ratón inmunosuprimido. La línea parental que se usó fue (MDA-MB-231), expresando la proteína fluorescente verde (eGFP, del inglés *enhanced green fluorescent protein*) y el gen de la luciferasa (MDA-MB-231$^{eGFP\text{-}Luciferase}$). Inicialmente se inyectó dicha línea en el ratón y una vez formada la metástasis, se extrajola sangre y finalmente las células fueron aisladas usando EasySep^{TM} mouse T cell isolation kit. La línea mCTCs y su línea parental MDA-MB-231$^{eGFP\text{-}Luciferase}$ se pusieron en cultivo durante 9 días y se estudió el efecto de la adición de NEs con respecto a no incluirlas en el medio celular (usando las condiciones desarrolladas en el grupo para crecimiento de CTCs). En ambos casos, la densidad celular fue mayor en el caso de las células tratadas con NEs, que con respecto a los controles negativos. En concreto, la línea parental tratada se mantenía en la densidad celular de la siembra, mientras que el control se reducía prácticamente a la mitad. Para el caso de mCTCs, se observaba un incremento en la proliferación próximo al 36 % en el caso de tratarlas con NEs. Adicionalmente, para la línea de mCTCs se hizo un análisis de expresión génica para entender el efecto positivo observado con respecto a la proliferación. Del panel de 13 genes analizado por RT-qPCR se observó que solo un gen relacionado con proliferación (*Ki67*) y otro gen relacionado con ciclo celular (*E2F4*), presentaban una expresión relativa mayor con respecto a las mismas células sin tratar.

Para terminar el estudio se propuso un mecanismo de acción para justificar el efecto observado de las NEs. El cual se basó en evidencias experimentales, obtenidas por citometría de flujo y por TEM. En ellas, se estudiaba la dinámica que seguían las NEs dentro de las células. Con ambas técnicas se analizaron 3 tiempos: 4 h, 24 h y 48 h después de haber añadido

las NEs. Por citometría de flujo se determinó de manera cuantitativa que a las 4h las células tratadas presentaban un aumento en la cantidad de compuestos lipídicos en su interior. En el último punto (48 h) se apreció un descenso en la presencia de dichos compuestos en células tratadas con NEs. Estos resultados, junto con lo observado en los estudios de viabilidad, indicaban que el mecanismo de acción de las NEs podía consistir en que una vez en el citoplasma celular, parte de las NEs podrían ir directamente a ser oxidadas en las mitocondrias y otra parte ser convertidas en reservas energéticas, en forma de gotas lipídicas (LDs, del inglés *lipid droplets*). El estudio realizado por TEM verificó dicha hipótesis de manera cualitativa.

El siguiente paso fue emplear las NEs en cultivos de CTCs aisladas de pacientes de cáncer de mama metastásico. El objetivo de esta parte era validar el uso de las NEs en cultivos *ex vivo* de CTCs para favorecer la expansión de dichas células. Una vez se comprobó dicha utilidad, se pudo llevar a cabo la caracterización de las CTCs en cultivo. Además, se determinó que siguiendo el protocolo de cultivo con NEs, se podía asociar la duración de los cultivos de CTCs con la evolución de los pacientes.

Para este módulo de trabajo, se aislaron CTCs usando una técnica de enriquecimiento negativo, en concreto RosetteSep™. Se usaron 50 muestras de sangre periférica obtenidas de 35 pacientes con enfermedad metastásica avanzada de cáncer de mama. Las muestras fueron recogidas longitudinalmente: 32 de las 50 muestras totales (64 %) se recogieron después del inicio de terapia y el 36 % fueron recogidas en el momento del diagnóstico de la metástasis. De las pacientes tratadas, 14 de ellas estaban con primeria-línea de tratamiento y 18 llevaban ≥ 2 líneas distintas de tratamiento. Para los cultivos celulares se usaron placas de baja adherencia y se suplementaron con factores junto con las NEs (protocolo desarrollado por nuestro grupo). En relación a este protocolo, es importante destacar que este es el primer estudio en el que se han usado nanoemulsiones para favorecer el cultivo de CTCs.

El tiempo medio de cultivo fue de 56.35 días para las 50 muestras. Sin embargo, para poder diferenciar un cultivo exitoso (cultivo (+)) de uno fallido (cultivo (–)), se realizó un análisis de curva ROC, estableciendo un corte de 23 días como cultivo (+). Basado en este criterio, los cultivos fueron

exitosos en un 75 % de los casos, mientras otros trabajos indican porcentajes de éxito entre el 13-28 %. Por ello, queda reflejada la mejoría que supone el uso del protocolo de cultivo propuesto en esta tesis.

De forma paralela a la recogida de muestras, en 34 muestras de las 50 totales se hizo una enumeración por CellSearch® system en el punto inicial del cultivo. Con respecto a la enumeración, está establecido en cáncer de mama metastásico que una muestra de 7.5 mL de sangre que presenta ≥ 5 CTCs está asociada a un peor pronóstico para el paciente. Esta asociación puede determinarse con el uso de parámetros tales como la supervivencia libre de progresión (PFS, del inglés *progression-free survival*) y a la supervivencia global (OS del inglés, *overall survival)*. Sin embargo, de este análisis se determinó que no había asociación entre que el cultivo fuera exitoso (cultivo (+)) y el hecho de presentar ≥ 5 CTCs.

Se realizó un estudio fenotípico en algunas muestras aleatorias después de llevar ~ 2 semanas en cultivo. Dicha caracterización se basó en técnicas de inmunofluorescencia, junto con un análisis de expresión génica usando RT-qPCR. Empezando por el estudio de inmunoflurescencia, se usó la siguiente tinción: para marcadores epiteliales se emplearon E-Cadherina, EpCAM y Pancitoqueratina (PanCK, del inglés *pancitokeratin*), mientras que para mesenquimales se estudió la presencia de Vimentina y por último se puso como marcador de células sanguínea CD45. De las muestras analizadas, se observó que los marcadores epiteliales aparecían en un porcentaje bajo (18.18 %, n = 22), mientras que el marcador mesenquimal de vimentina aparecía en mayor grado (47 %, n = 17). Estos resultados coinciden con lo expuesto en trabajos previos donde indican que, después de 14 días en cultivo, gran parte de las CTCs pierden sus características epiteliales y exhiben marcadores mesenquimales.

Con respecto a los estudios de expresión génica, a partir de un panel de 20 genes, se hizo una comparativa de las muestras en dos puntos: una vez aisladas (antes del cultivo) y después del cultivo (~ 2 semanas en cultivo). Los genes seleccionados agrupaban tales como: epiteliales, mesenquimales, marcadores de célula madre, específicos de cáncer de mama y otros genes relacionados con vías del ciclo celular. Del estudio realizado, mediante el

análisis de agrupación jerárquica y el de componente principal (PCA, del inglés *principal component analysis*), se concluyó que las CTCs analizadas antes y después de cultivo presentaban un patrón de expresión génica diferente. Se estableció que las CTCs recién aisladas de la sangre, mostraban mayor expresión de marcadores epiteliales. Asimismo, se detectó expresión de *CD45* en las muestras y para descartar que la contaminación estuviera afectando al análisis génico, en 4 de las 6 muestras analizadas se realizó el estudio para la fracción de células mononucleares de sangre periférica (PBMCs, del inglés *peripheral blood mononuclear cells*), aislada y cultivada con las mismas condiciones descritas. Tanto por el análisis de agrupación jerárquica como por el análisis de PCA se vio que la expresión de los PBMCs presentaba un patrón completamente distinto al de las CTCs. Algunos de los genes que presentaban una expresión relativa superior en las muestras de CTCs después del cultivo estaban relacionados con EMT (como *GDF15* y *CTNNB1*), con fenotipo de célula madre (*ALDH1A1*) y con transporte de ácidos grasos (*CD36*).

Para identificar marcadores con valor pronóstico, se realizó un análisis de supervivencia. Dicho análisis se basó en la observación de dos parámetros: por un lado, la duración del cultivo y, por otro lado, la presencia de eritrocitos (RBCs, del inglés *red blood cells*) al inicio del cultivo. Con respecto al primer parámetro, se determinó cómo la duración del cultivo podía predecir la PFS, siendo ésta la primera vez que se describía en cáncer de mama. En concreto, cultivos (+) presentaban una peor PFS. Con respecto a la presencia de ≥ 5 CTCs por CellSearch®, en este estudio este sistema no fue capaz de predecir la PFS. Relacionado con esta observación, es importante destacar el hecho de que en este estudio solo el 53% de las muestras habían presentado inicialmente CTCs usando CellSearch®. Por ello, la falta de asociación de estos resultados se vio influenciada por la manera de aislar las muestras de cultivo (aislamiento negativo), pudiendo recoger tanto células con fenotipos epiteliales como de célula madre o mesenquimales. En cambio, las muestras de CellSearch® solo capturaron las de fenotipo epitelial. En sentido opuesto, en el caso de analizar OS, se apreció como el hecho de que el cultivo durara más de 23 días no fue predictivo, en cambio la presencia de ≥ 5 CTCs por CellSearch® si que pudo predecirla.

De manera independiente al efecto de las NEs en los cultivos, se determinó la presencia de RBCs llamando a las muestras que presentaban gran cantidad RBCs (+) mientras a las que presentaban casi inapreciable o no presencia RBCs (–). En este caso, observamos como la cantidad de RBCs predecían PFS y OS. Relacionado con dicha observación, en otros estudios se ha descrito como pacientes oncológicos presentan anemia y problemas de coagulación, aunque falta por conocer en detalle las causas de ello.

Como resultado de esta segunda parte, se demuestra como en cultivos de CTCs aisladas de pacientes de cáncer mama puede resultar de gran utilidad el protocolo de NEs proliferativas. Tanto a la hora de establecer cultivos a corto-plazo como para determinar el pronóstico de los pacientes.

En último lugar, una vez demostrado el uso de las NEs para favorecer el cultivo de CTCs de cáncer de mama, se decidió funcionalizar las nanoemulsiones con ligandos específicos. El objetivo consistía en dotarlas con capacidad de reconocimiento de receptores de membrana de CTCs, para finalmente formar parte de un sistema de aislamiento para dispositivos de microfluídica. Como primera aproximación, se modificaron las superficies de las nanoemulsiones, incorporando péptidos dirigidos a EpCAM y EGFR. El diseño de la unión se basó en el enlace covalente entre el grupo reactivo éster de N-hidroxisuccinimida (NHS) de las nanoemulsiones y las aminas primarias presentes en los péptidos. Para ello, a diferencia de las nanoemulsiones de los capítulos anteriores (NEs), éstas se formularon añadiendo, CH asociado a una cadena de PEG con el grupo reactivo NHS al final de dicha cadena. En este caso, a las nanoemulsiones formuladas se las llamó PEG-NEs, y una vez llevada a cabo la conjugación con los péptidos: Pept-NEs. Específicamente, se les llamó Pep10-NEs o GE11-NEs, en función de si llevaban el péptido Pep10 (anti-EpCAM) o el GE11 (anti-EGFR), respectivamente.

En este trabajo se determinaron las propiedades físicas de estas partículas. Todas las formulaciones presentaron tamaños menores de 200 nm, presentaron homogeneidad de tamaño de partículas, con valores inferiores a 0.2 de PdI. Además, se pudo determinar la concentración de ambas formulaciones por NTA, presentado valores muy similares (para

GE11-NEs de $1.63x10^{11}$ NPs/mL y para Pep10-NEs $1.61X10^{11}$ NPs/mL). Del mismo modo, empleando curvas patrón con concentraciones conocidas de ambos péptidos se determinaron las concentraciones finales de péptido en cada una de las dos formulaciones (GE11-NEs, $3.87x10^{-3}$ mg/mL y Pep10, $9.44x10^{-3}$ mg/mL).

Una vez hecha la caracterización física, se determinó si este tipo de NPs servían para ser inmovilizadas sobre superficies. Por ello, durante la estancia realizada en el centro de investigación iNANO, en Aarhus (Dinamarca), se utilizó la microbalanza de cristal de cuarzo con medida de disipación (QCM-D, del inglés *Quartz cristal microbalance with dissipation*), que permite determinar comportamientos de adsorción de manera precisa. En dicho estudio, se utilizaron distintas condiciones (varias superficies (oro, sílice o polilisina (PLL)) en combinación con varios buffers (agua MQ, dPBS o HEPES2) y se determinó que la única condición que aportaba una monocapa estable era usando PLL y las nanoemulsiones dispersas en agua MQ. Aprovechando la gran utilidad de este equipo, se decidió emplearlo también para determinar el reconocimiento específico de las dos Pept-NEs por sus dianas. En este caso, primero se inmovilizaron las Pept-NEs y luego se pasó un flujo con las proteínas de interés en una solución de agua MQ por separado (EpCAM y EGFR). Con dicho análisis se determinó un reconocimiento específico para ambas formulaciones. Adicionalmente, se hizo un estudio por microscopía de fluorescencia usando las líneas MCF-7 y MDA-MB-231, las cuales expresaban altos niveles de EpCAM y EGFR, respectivamente. Del mismo modo se justificó la especificidad de cada una de las dos formulaciones de Pept-NEs para dirigirse a sus células diana.

De forma muy relevante, se llevó a cabo un estudio de citotoxicidad que verificó que al poner en contacto las Pept-NEs inmovilizadas en la superficie de placas de cultivos con las células no se detectaba toxicidad. Esto se observó en los 9 días que duró el estudio. De esta forma, se resaltaba el futuro uso de esta aproximación para el cultivo inicial de las células una vez aisladas.

Con todo ello, esta tesis resalta el gran potencial del uso de la nanotecnología para diseñar nanomateriales de aplicación en la biopsia

líquida. La importancia de esta tesis reside en haber empleado nanosistemas biocompatibles a base de lípidos, en concreto nanoemulsiones, logrando abordar dos de los puntos críticos que dificultan el trabajo con CTCs: cultivo *ex vivo* y aislamiento. En relación con el primero, gracias al uso de las NEs proliferativas, desarrolladas y validadas en el capítulo 1, se pudieron emplear en cultivos *ex vivo* de CTCs (capítulo 2). Como consecuencia, bajo el protocolo de cultivo con NEs, se pudieron llevar a cabo la caracterización de CTCs en cultivo y la búsqueda de factores predictivos. En cuanto al segundo punto, aislamiento, en el capítulo 3 se desarrollaron las Pept-NEs con capacidad para reconocer receptores de la membrana celular de dichas células y favorecer su aislamiento. De esta forma, se resalta la versatilidad de dichas nanoemulsiones para convertirse en una plataforma de gran utilidad en biopsia líquida.

Resumo *in extenso*

RESUMO *IN EXTENSO*

A nanotecnoloxía é un campo que permite o deseño de estruturas funcionais con dimensións nanométricas, tales como as nanopartículas (NPs). A importancia das NPs reside en que presentan un enorme potencial en distintos campos debido ás súas propiedades físico-químicas únicas. Ademais, son facilmente modulables segundo a aplicación final desexada. Entre as áreas de investigación onde se usan as NPs, destaca a oncolóxica e en particular, a biopsia líquida. A biopsia líquida é a técnica que estuda o material biolóxico en fluídos corporais, como o sangue. Isto en oncoloxía, permite estudar o que se coñece como o "circuloma tumoral", é dicir, o conxunto de compoñentes que circulan polos fluídos procedentes do tecido tumoral. Algúns deles son ácidosnucleicos tumorais circulantes (ctDNA e ctRNA), vesículas extracelulares ou Células Tumorais Circulantes (CTCs). Facendo uso da biopsia líquida, é posible determinar a heteroxeneidade tumoral en distintos momentos da enfermidade, achegando información en tempo real sobre a evolución da mesma. Neste campo, a nanotecnoloxía aporta ferramentas tanto para o illamento como para a detección deste tipo de materiais.

A análise secuencial de CTCs permite obter información tanto a nivel molecular (caracterización a nivel proteico, xenético ou epixenético) como a nivel clínico (sensibilidade farmacolóxica e monitorización). Actualmente, existen gran cantidade de técnicas para a detección e illamento de CTCs e publícanse continuamente novas estratexias para este fin. Con todo, aínda presentan certas limitacións: por unha banda, (i) a mostra inicial presenta poucas células debido á súa baixa concentración en sangue (1 CTC entre 10^6-10^7 células sanguíneas). Por outra banda, (ii) xeralmente utilízanse técnicas de illamento epitopo dependentes que resultan na perda de subpoboacións de CTCs. En concreto, a maioría das técnicas de illamento baséanse en marcadores epiteliais, a pesar de que existe unha poboación de CTCs que non os expresan ou os perderon previamente por mor da plasticidade celular que posúen, debido ao proceso de transición epitelio-mesénquima (EMT, do inglés *Epithelial-Mesenhcymal Transition*), e o de

transición mesénquima-epitelio (MET, do inglés *Mesenchymal-Epithelial Transition*).

Cómpre destacar que dependendo dos estudos que se queiran realizar coas CTCs, a elección do sistema de illamento é un punto crítico. Moitos dos sistemas empregados para o illamento fixan as células ao final do proceso, sendo útiles para caracterización a nivel proteico, xenoma, pero non para levar a cabo estudos funcionais. Para levar a cabo estes estudos, é necesario liberar as CTCs viables dos sistemas nos que quedan retidas. Por tanto, resulta imprescindible avanzar cara plataformas que permitan un illamento máis eficiente das CTCs sen diminuír a súa viabilidade. Para mellorar a eficiencia de illamento, as novas tecnoloxías apóiansena combinación de diferentes técnicas, como a separación física e a separación baseada en marcadores das membranas celulares.

Aínda con todos estes avances, o uso das CTCs segue sen ser incorporado ás guías clínicas, principalmente pola complexidade que representa a súa aplicación.

Tendo en conta estes antecedentes, o obxectivo desta tese é xerar ferramentas baseadas na nanotecnoloxía para favorecer o estudo das CTCs, permitindo avaliar a utilidade destas células para predicir o estado en pacientes con cancro de mama. Este obxectivo xeral dividiuse en tres módulos de traballo. O primeiro consistiu en xerar nanoemulsións que favorecesen o cultivo *ex vivo* de CTCs. Para iso, formuláronse nanoemulsións con lípidos e ácidos graxos relacionados coa proliferación das células tumorales de cancro de mama. Unha vez caracterizadas, estudouse a súa eficacia para favorecer a proliferación celular en liñas modelo de cancro de mama. Despois de levar a cabo a optimización do protocolo para seguir coas nanoemulsións proliferativas, o segundo módulo de traballo tratou de testar ditas nanoemulsións para o seu uso en cultivos *ex vivo* de CTCs, previamente illadas de pacientes con cancro de mama metastático. Co devandito protocolo, pretendíase establecer cultivos que permitisen realizar unha caracterización molecular das CTCs cultivadas. Por último, no terceiro módulo, unha vez visto o potencial destas nanoemulsións para favorecer o mantemento dos cultivos de CTCs, estas

modificáronse con péptidos de recoñecemento de marcadores proteicos da superficie das células tumorais en cancro de mama. O obxectivo deste último punto consistía en desenvolver NPs biodegradables e biocompatibles que servisen para funcionalizar dispositivos de microfluídica e dotalos de maior capacidade para illar CTCs. En concreto, formuláronse nanoemulsións decoradas por unha banda co péptido Pep10, o cal recoñece a EpCAM (do inglés *epithelial cell adhesion molecule*) e por outra banda, usando GE11, que recoñece a EGFR (do inglés *epidermal growth factor receptor*).

Na primeira parte da tese, onde se desenvolveron nanoelmusións para favorecer o cultivo *ex vivo* de CTCs de pacientes con cancro de mama, para a súa formulación empregáronse: colesterol (CH, do inglés *cholesterol*), fosfatidilcolina (PC, do inglés *phosphatidylcholine*) e ácido oleico (OA, do inglés *oleic acid*). Usáronse distintas concentracións de OA para obter catro formulacións iniciais. A continuación, levouse a cabo a súa caracterización para escoller a mellor formulación, en base ao seu tamaño, homoxeneidade (PdI, do inglés *polidispersity index*) e estabilidade. As nanoemulsións escollidas (chamadas NEs) presentaron un tamaño menor aos 200 nm, con carga superficial negativa (-32.2 mV). Ademais, determinouse a concentración final de NEs mediante a técnica de análise de rastrexo de NPs (NTA, do inglés *nanoparticle tracking analysis*). Tamén se analizoua súa morfoloxía mediante microscopía de transmisión electrónica (TEM, do inglés *transmission electron microscopy*), para comprobar a súa esfericidade. Por outra parte, mediante a técnica de resonancia magnética nuclear e cromatografía líquida de alta eficacia (HPLC, do inglés *high performace liquid chromatography*) determinouse que todos os compostos empregados no momento da formulación formaban parte das NEs. Finalmente, realizouse un estudo de estabilidade e comprobouse que as NEs eran estables ao longo de 6 meses de almacenamento a 4 °C.

Unha vez finalizada a caracterización das propiedades físicas e a estabilidade das NEs, iniciáronse os estudos *in vitro* para comprobar se as nanoemulsións seleccionadas na primeira fase (NEs) eran realmente eficaces para favorecer o mantemento e a proliferación en cultivos celulares. Para iso, tratáronse distintas liñas celulares de cancro de mama (HCC1143,

MDA-MB-231 e MCF-7) con concentracións crecentes de NEs comprobándose o aumento na viabilidade celular, mediante a técnica do alamarBlue™. Grazas a este ensaio, escolleuse a concentración de traballo a empregar no resto dos experimentos (2.4 x 10^9 NPs/mL), establecendo un protocolo para o uso destas nanoemulsións con actividade proliferativa. A continuación, comprobouse a internalización das NEs nas devanditas células usando a tinción de Nile Red analizada por microscopía confocal e citometría de fluxo.

Unha vez comprobado que había un efecto beneficioso na viabilidade celular ao tratar os cultivos con NEs, realizouse un experimento no que se comparou o efecto das NEs e o dos compostos libres empregados na súa formulación (CH, PC e OA). Para iso, usáronse CH, PC e OA sen formular, tanto mesturados entre si como de forma individual á mesma concentración final ca na formulación. A partir disto determinouse que estes compostos, sen estar formulados, non presentaban os mesmos efectos sobre a viabilidade celular. De forma complementaria, formuláronse dúas novas nanoemulsións, cambiando o OA empregado nas NEs por outros compostos (vitamina E ou migliol 812), co obxectivo de estudar o efecto das nanoemulsións con propiedades similares, pero de composición diferente. Os resultados deste ensaio determinaron que ditas formulacións non achegaban ese incremento na viabilidade celular acadado co uso de NEs. Ademais, para comprobar que este efecto no aumento de viabilidade permanecía no tempo, analizouse un cultivo de 4 días ao que se lle engadiron NEs en dúas ocasións (día 0 e día 2) e observouse que a porcentaxe de viabilidade sempre superaba o 100 % con respecto aos controis negativos (sen engadir NEs). É importante destacar neste punto, o feito de que xa ás 3 horas de incubación coas NEs se observaba un efecto no aumento da viabilidade celular medida por alamarBlue™. O devandito efecto podería estar relacionado coa hipótese de que parte das NEs estarían a ser dirixidas de maneira directa ás mitocondrias para ser oxidadas mediante a vía de oxidación dos ácidos graxos (FAO, do inglés *fatty acid oxidation*). Como resultado desta vía xéranse NADPH e NADH, os cales estarían a provocar a redución da resarzurina (o composto activo do alamarBlue™). Por outra banda, observouse como coa segunda adición se restablecía o

efecto, validando o seu uso para futuros protocolos nos que favorecer o cultivo celular.

Unha vez determinado o efecto en liñas celulares, xerouse unha liña modelo de CTCs (mCTCs). O obxectivo foi validar o efecto das NEs nun modelo próximo a CTCs de cancro de mama, pois a diferenza das liñas empregadas nos experimentos previos, as mCTCs estiveran na circulación dun rato inmunocomprometido. A liña parental usada foi MDA-MB-231, a cal expresaba a proteína fluorescente verde (eGFP, do inglés *enhanced Green Fluorescent Protein*) e o xene da luciferasa (MDA-MB-231$^{\text{eGFP-Luciferase}}$). Por tanto estas células foron introducidas en rato, e unha vez formada a metástase, extraéronse do sangue e illáronse usando EasySep$^{\text{TM}}$ mouse T cell isolation kit. A liña mCTCs e a súa liña parental MDA-MB-231$^{\text{eGFP-Luciferase}}$ puxéronse en cultivo durante 9 días, usando as condicións desenvolvidas no grupo para crecemento de CTCs. En ambos casos, a densidade celular foi maior no caso das células tratadas con NEs, con respecto aos controis negativos. En concreto, a liña parental tratada mantíñase na densidade celular que o cultivo presentaba inicialmente, mentres que o control se reducía practicamente á metade. No caso de mCTCs, observábase un incremento na proliferación próximo ao 36% no caso das células tratadas con NEs. Adicionalmente, para a liña de mCTCs fíxose unha análise de expresión xénica para entender o efecto positivo observado con respecto á proliferación. Do panel de 13 xenes analizado por RT-qPCR observouse que un xene relacionado con proliferación (*Ki67*) e outro xene relacionado con ciclo celular (*E2F4*), presentaban unha maior expresión relativa con respecto ás mesmas células sen tratar.

Para rematar o estudo propúxose un mecanismo de acción baseado nas evidencias experimentais, obtidas por citometría de fluxo e por TEM. Nelas, estudamos a dinámica que seguían as NEs dentro das células. Con ámbalas dúas técnicas analizáronse tres tempos: 4 h, 24 h e 48 h despois de engadir as NEs. Por citometría de fluxo determinouse de maneira cuantitativa que ás 4 h as células tratadas presentaban un aumento na cantidade de compostos lipídicos no seu interior. No último punto (48 h) apreciábase un descenso na presenza de compostos lipídicos en células tratadas con NEs. Estes resultados, xunto co observado nos estudos de viabilidade, indicaban que o

mecanismo de acción das NEs podía consistir en que unha vez no citoplasma celular, parte das NEs poderían ser oxidadas directamente nas mitocondrias e outra parte ser convertidas en reservas enerxéticas, en forma de pingas lipídicas (LDs, do inglés *Lipid Droplets*). Os estudos por TEM verificaron esta hipótese de maneira cualitativa.

O seguinte paso foi empregar as NEs en cultivos de CTCs illadas de pacientes de cancro de mama metastático. O obxectivo desta parte foi validar o uso das NEs en cultivos *ex vivo* de CTCs, para favorecer a expansión das devanditas células. Unha vez comprobada a súa utilidade, púidose levar a cabo a caracterización das CTCs en cultivo. Ademais, determinouse que seguindo o protocolo de cultivo con NEs, foi posible asociar a duración dos cultivos de CTCs coa evolución dos pacientes.

Para este módulo de traballo, illáronse CTCs usando unha técnica de enriquecemento negativo, denominada RosetteSep™. Usáronse 50 mostras de sangue periférico obtidas de 35 pacientes con enfermidade metastática avanzada de cancro de mama. As mostras foron recollidas lonxitudinalmente: 32 das 50 mostras totais (64 %) recolléronse despois do inicio de terapia e o 36 % foron recollidas no momento do diagnóstico da metástase. Das pacientes tratadas, 14 delas atopábanse con primeira liña de tratamento e 18 levaban ≥ 2 liñas distintas de tratamento. Para os cultivos celulares usáronse placas de baixa adherencia e ademais, estes cultivos foron suplementándose con factores de crecemento xunto coas NEs (protocolo desenvolvido polo noso grupo). En relación a este protocolo, é importante destacar que este é o primeiro estudo no que se usan nanoemulsións para favorecer o cultivo de CTCs.

O tempo medio de cultivo foi de 56.35 días para as 50 mostras. Con todo, para poder diferenciar un cultivo exitoso (Cultivo (+)) dun non exitoso (cultivo (–)), realizouse unha análise de curva ROC, establecendo un corte de 23 días como cultivo (+). Baseándose neste criterio, os cultivos foron exitosos nun 75 % dos casos, mentres outros traballos indican porcentaxes de éxito entre o 13-28 %. Por iso, queda reflectida a melloría que supón o uso do protocolo de cultivo proposto nesta tese.

De forma paralela á recollida de mostras, en 34 mostras das 50 totais fíxose unha enumeración polo sistema CellSearch® no punto inicial do cultivo. Con respecto á enumeración en cancro de mama metastático, está establecido que cando unha mostra de 7.5 mL de sangue que presenta ≥ 5 CTCs está asociada a un peor prognóstico para o paciente. Esta asociación pode determinarse co uso de parámetros tales como a supervivencia libre de progresión (PFS, da inglés *Progression-Free Survival*) e a supervivencia global (OS de o inglés, *Overall Survival*). Con todo, desta análise determinouse que non había asociación entre que o cultivo fose exitoso (cultivo(+)) e o feito de presentar ≥ 5 CTCs.

Así mesmo, realizouse un estudo fenotípico nalgunhas mostras elixidas aleatoriamente despois de levar 2 semanas en cultivo. Dita caracterización baseouse en técnicas de inmunofluorescencia, xunto cunha análise de expresión xénica usando RT-qPCR. Empezando polo estudo de inmunoflurescencia, usouse a seguinte tinción: para marcadores epiteliais empregáronse E-Cadherina, EpCAM e pancitoqueratina (PanCK, do inglés *pancytokeratin*), mentres que para a análise de marcadores mesenquimais estudouse a presenza de vimentina. Por último, empregouse CD45 como marcador de células sanguíneas. Das mostras analizadas, observouse que os marcadores epiteliais aparecían nunha porcentaxe baixa (18.18 %, n = 22), mentres que o marcador mesenquimal vimentina aparecía en maior grao (47 %, n = 17). Estes resultados coinciden co exposto en traballos previos onde se indican que, despois de 14 días de cultivo, gran parte das CTCs perden as súas características epiteliais e exhiben marcadores mesenquimais.

Con respecto aos estudos de expresión xénica, a partir dun panel de 20 xenes, fíxose unha comparativa de mostras unha vez illadas (antes do cultivo) e despois do cultivo (2 semanas en cultivo). Os xenes seleccionados agrupaban tales como: epiteliais, mesenquimais, stem, específicos de cancro de mama e outros xenes relacionados con vías do ciclo celular. Do estudo realizado, mediante a análise de agrupación xerárquica e o de compoñente principal (PCA, do inglés *Principal Component Analysis*), concluíuse que as CTCs analizadas antes e despois do cultivo presentaban un patrón de expresión xénica diferente. Estableceuse que as CTCs recentemente illadas do sangue presentaban maior expresión de marcadores epiteliais.

Ademais, detectouse expresión de CD45 nas mostras e para descartar que a contaminación estivese afectando á análise xenética, en 4 das 6 mostras analizadas realizouse o estudo para a fracción de células mononucleares de sangue periférico (PBMCs, do inglés *peripheral blood mononuclear cells*), illadas e cultivadas nas mesmas condicións descritas. Tanto pola análise de agrupación xerárquica, como pola análise de PCA viuse que a expresión dos PBMCs presentaba un patrón completamente distinto ao das CTCs. Algúns dos xenes que presentaban unha expresión relativa superior nas mostras de CTCs despois do cultivo estaban relacionados con EMT (como *GDF15* e *CTNNB1*), con fenotipo de célula nai (*ALDH1A1*) e con transporte de ácidos graxos (*CD36*).

Para identificar marcadores con valor prognóstico, realizouse unha análise de supervivencia. A devandita análise baseábase na observación de dous parámetros: por unha banda, a duración do cultivo e, por outra banda, a presenza de eritrocitos (RBCs, da inglés *Red Blood Cells*) ao comezo do cultivo. Con respecto ao primeiro parámetro, determinouse como a duración do cultivo podía predicir a PFS, sendo esta a primeira vez que se describía en cancro de mama. En concreto, cultivos (+) presentaban unha peor PFS. Con respecto á presenza de ≥ 5 CTCs por CellSearch®, neste estudo non predicía a PFS. Relacionado con esta observación, está o feito de que neste estudo só o 53 % das mostras presentasen CTCs mediante CellSearch® inicialmente. Por iso, a falta de asociación destes resultados vén influenciada pola maneira de illar as mostras para o seu cultivo (illamento negativo), podendo recoller tanto células con fenotipos epiteliais, como de célula nai ou mesenquimais. En cambio, as mostras de CellSearch® só capturaron as de fenotipo epitelial. Pola contra, no caso da OS, apreciouse como o feito de que o cultivo durase máis de 23 días non era preditivo, mentres que a presenza de ≥ 5 CTCs por CellSearch® si que era capaz de predicila.

De maneira independente para o efecto das NEs nos cultivos, determinouse a presenza de RBCs. As mostras que presentaban gran cantidade de RBCs denomináronse RBCs (+), mentres que as que presentaban niveis case inapreciables ou non presencia chamáronse RBCs (–). Neste caso, observamos como a cantidade de RBCs predicía PFS e OS. Relacionado coa devandita observación, noutros estudos describiuse como

pacientes oncolóxicos presentan anemia e problemas de coagulación. Non obstante, aínda non se coñecen con detalle as causas desta observación.

Como resultado desta segunda parte, demóstrase como a os cultivos de CTCs illadas de pacientes de cancro mama pódenlle resultar de gran utilidade o protocolo de NEs proliferativas, tanto á hora de establecer cultivos a curto prazo, como para determinar o prognóstico dos pacientes.

En último lugar, unha vez demostrado o uso das NEs para favorecer o cultivo de CTCs de cancro de mama, decidiuse funcionalizar as nanoemulsións con ligandos específicos. O obxectivo consistía en dotalas con capacidade de recoñecemento de receptores de membrana de CTCs para finalmente formar parte dun sistema de illamento para dispositivos de microfluídica. Como primeira aproximación, modificáronse as superficies das nanoemulsións, incorporando péptidos dirixidos a EpCAM e EGFR. O deseño da unión baseouse na ligazón covalente entre o grupo reactivo éster de N- hidroxisuccinimida (NHS) das nanoemulsións e as aminas primarias presentes nos péptidos. Para iso, a diferenza das nanoemulsións dos capítulos anteriores (NEs), estas formuláronse engadindo, CH asociado a unha cadea de PEG co grupo reactivo NHS ao final da devandita cadea. Neste caso, as nanoemulsións formuladas denomináronse PEG- NEs, e unha vez levada a cabo a conxugación cos péptidos denomináronse Pept- NEs. Especificamente, chamóuselles Pep10-NEs ou GE11-NEs, en función de se levaban o péptido Pep10 (anti-EpCAM) ou o GE11 (anti-EGFR), respectivamente.

Neste traballo determináronse as propiedades físicas destas partículas. Todas as formulacións presentaron tamaños menores de 200 nm, presentaron homoxeneidade de tamaño de partículas, con valores inferiores a 0.2 de PdI. Ademais, púidose determinar a concentración de ambas as formulacións por NTA, presentado valores moi similares (para GE11-NEs $1.63x10^{11}$ NPs/mL e para Pep10-NEs $1.61x10^{11}$ NPs/mL). Do mesmo xeito, empregando curvas patrón con concentracións coñecidas de ámbolos péptidos determináronse as concentracións finais de péptido en cada unha das dúas formulacións (GE11-NEs, $3.87x10^{-3}$ mg/mL e Pep10, $9.44x10^{-3}$ mg/mL).

Unha vez feita a caracterización física, determinouse se este tipo de NPs servían para ser inmobilizadas sobre superficies. Por iso, durante a estancia realizada no centro de investigación iNANO, en Aarhus (Dinamarca), utilizouse a microbalanza de cristal de cuarzo con medida de disipación (QCM-D, do inglés *Quartz crystal microbalance with dissipation*), que permite determinar comportamentos de absorción de maneira precisa. No devandito estudo, utilizáronse distintas condicións (varias superficies (ouro, sílice ou polilisina (PLL)) en combinación con varios *buffers* (auga MQ, dPBS ou HEPES2) e determinouse que a única condición que achegaba unha monocapa estable era usando PLL e as nanoemulsións dispersas en auga MQ. Aproveitando a gran utilidade deste equipo, decidiuse empregalo tamén para determinar o recoñecemento específico das dúas Pept-NEs polas súas dianas. Neste caso, primeiro inmobilizáronse as Pept-NEs e logo pasouse un fluxo coas proteínas de interese nunha solución de auga MQ por separado (EpCAM e EGFR). Con estes resultados púidose determinar que o recoñecemento era específico para ambas formulacións. Adicionalmente, fíxose un estudo por microscopia de fluorescencia, en concreto usáronse as liñas MCF-7 e MDA-MB-231, as cales expresaban altos niveis de EpCAM e EGFR, respectivamente. Do mesmo xeito xustificouse a súa especificidade.

De forma moi relevante, levouse a cabo un estudo de toxicidade asociada ao feito de que as Pept-NEs estivesen inmobilizas e en contacto coas células e determinouse que durante un cultivo de 9 días nesas condicións non había toxicidade. Por tanto, evidenciábase que esta aproximación é ademais óptima para o cultivo inicial das células unha vez illadas.

Con todo iso, esta tese resalta o gran potencial do uso da nanotecnoloxía para deseñar nanomateriais de aplicación na biopsia líquida. A importancia desta tese reside en empregar nanosistemas biocompatibles a base de lípidos, en concreto nanoemulsións, logrando abordar dous dos puntos críticos que dificultan o traballo con CTCs: cultivo *ex vivo* e illamento. En relación co primeiro, grazas ao uso das NEs proliferativas, desenvolvidas e validadas no capítulo 1, puidéronse empregar en cultivos *ex vivo* de CTCs (capítulo 2). Como consecuencia, baixo o protocolo de cultivo

con NEs, púidose levar a cabo a caracterización de CTCs en cultivo e a procura de factores preditivos. En canto ao segundo punto, o illamento, no capítulo 3 desenvolvéronse as Pept-NEs con capacidade para recoñecer receptores da membrana celular das devanditas células e favorecer o seu illamento. Desta forma, resáltase a versatilidade de ditas nanoemulsións para converterse nunha plataforma de gran utilidade en biopsia líquida.

Summary

SUMMARY

Nanotechnology allows the design of functional structures with nanometric dimensions, such as nanoparticles (NPs). NPs present an enormous potential in different fields due to they possess unique physico-chemical properties. In addition, they can be easily modulated according to the desired final application. Among the research fields where NPs are used, it is essential to highlight their role in oncology and specifically, in the liquid biopsy. Liquid biopsy is the technique that allows the study of biological material from body fluids such as blood. This in oncology allows the study of what is known as the "tumour circulome", that is, the set of components that circulate through the fluids coming from the tumour tissue. Some of them are circulating tumour nucleic acids (ctDNA and ctRNA), extracellular vesicles or circulating tumour cells (CTCs). By using the liquid biopsy, it is possible to determine tumour heterogeneity at different times of the disease, providing information in real time. In this field, nanotechnology provides tools for both, the isolation, and the detection of this circulating material.

The sequential analysis of CTCs allows obtaining molecular information (characterization at protein, genetic or epigenetic level) and relevant clinical data (pharmacological sensitivity and monitoring). Currently, there are many techniques for the detection and isolation of CTCs and new strategies are continually being described for this purpose, although they still have certain limitations. On the one hand, (i) the initial sample shows low concentration of cells in blood (1 CTC between 10^6-10^7 blood cells). On the other hand, (ii) isolation techniques based on the recognition of specific antigens on the surface of the tumour cell are generally used. This positive selection results in the loss of certain subpopulations of CTCs. Specifically, most isolation techniques are based on epithelial markers even though some populations of CTCs do not express them. This is related to the plasticity of CTCs due to the epithelial-mesenchymal transition process (EMT) and the mesenchymal-epithelial transition (MET).

It should be noted that depending on the studies to be carried out with the CTCs, it is a key point the selection of a specific isolation approach. Since in many of the systems the cells are fixed during the isolation process,

it is possible to perform characterization at a protein and genome level, but not for carrying out functional studies. To perform these studies, it is necessary to release viable CTCs from the systems in which they are retained. Therefore, it is necessary to move towards platforms that allow more efficient isolation of CTCs without reducing their viability.To improve isolation efficiency, new technologies take advantage of the combination of different methodologies, such as physical separation and marker-based separation of cell membranes.

It is also important to highlight that, even with all these advances, the use of CTCs is still not incorporated into clinical guidelines, mainly due to the complexity referred to their use.

Against this background, the objective of this thesis is to develop tools based on nanotechnology to favour the study of CTCs in breast cancer. This general objective was divided into three work modules. The first was the development of nanoemulsions that supported the *ex vivo* culture of CTCs. To do this, nanoemulsions were formulated with lipids and fatty acids related to proliferation of breast cancer cells. Once characterized, their efficacy to promote cell proliferation in a breast cancer model was validated. After the optimization for the use of NEs was achieved, the second work module was the translation of this protocol to use it in *ex vivo* CTC cultures isolated from patients with metastatic breast cancer. The objective was to support the establishment of CTC cultures, to allow the downstream analysis of this cells (molecular characterization of the expanded CTCs). Finally, in the third module, once the potential of these nanoemulsions to favour the maintenance of the cultures of CTCs was confirmed, peptide decorated nanoemulsions were designed to specifically recognize surface proteins of breast cancer cells. The objective of this last point was to develop biodegradable and biocompatible NPs that would serve to functionalize microfluidic devices and provide them with a greater capacity to isolate CTCs. Specifically, as a proof of concept for the development of a versatile platform in which different peptides could be used depending on the cell population to be targeted, two formulations of nanoemulsions decorated with two peptides were formulated. On the one hand, the peptide Pep10 was used, which recognizes the epithelial cell adhesion molecule (EpCAM) and, on the

other hand, GE11 was used, which recognizes the epidermal growth factor receptor (EGFR).

In the first part of the thesis, nanoemulsions were developed to support the *ex vivo* culture of CTCs from breast cancer patients, using for its formulation: cholesterol (CH), phosphatidylcholine (PC) and oleic acid (OA). Different concentrations of OA were used to obtain four initial formulations. Next, they were characterized to choose the best formulation based on its size, homogeneity (polydispersity index, PdI) and stability. The chosen nanoemulsions (called NEs) presented a particle size less than 200 nm, with a negative surface charge (-32.2 mV). In addition, the final concentration of NEs was determined using the nanoparticle tracking analysis (NTA) technique. Also, its spherical morphology was determined by transmission electron microscopy (TEM). On the other hand, using the nuclear magnetic resonance technique and high-performance liquid chromatography (HPLC) it was determined that all the compounds used at the time of formulation were part of the NEs. Finally, a stability study was performed, and it was confirmed that the NEs were stable at least 6 month of storage at 4 ºC.

After the characterization of the properties and stability of the NEs was completed, *in vitro* studies were carried out to verify if the nanoemulsions selected in the first part (NEs) were effective in supporting the maintenance and proliferation of breast cancer cell cultures. For this, different breast cancer cell lines (HCC1143, MDA-MB-231 and MCF-7) were treated with an increasing concentration of NEs and it was found that this desired increase in cell viability was obtained, determined by the technique of the alamarBlue™. Thanks to this test, it was selected the optimal concentration to be used for the rest of the experiments (2.4×10^9 NPs/mL), establishing a protocol for the use of these proliferative NEs. Subsequently, the internalization of the NEs in these cells was verified using the Nile Red stain analysed by confocal microscopy and flow cytometry.

Once it was verified that there was a beneficial effect on cell viability when treating cultures with NEs, it was tested the effect of NEs and that of the free compounds used in their formulation (CH, PC and OA). For this, unformulated CH, PC, and OA were used, both mixed together and

individually at the same final concentration as in the formulation. It was determined that, without being formulated, the effect of the increment on cell viability was not observed. Additionally, two extra nanoemulsions were formulated, changing the OA used in NEs for other compounds (specifically, vitamin E and Miglyol 812 were used). The aim of this experiment was to study the effect of nanoemulsions with similar properties, but different composition. It was determined that these two formulations did not provide that increase in cell viability achieved with the use of NEs. Then, to verify that this effect on the increase in viability could remain over time, cell viabilities were monitored over 4 days adding NEs at time 0 and 2 days. It was observed that the cell viability percentage was always above 100 % related to negative controls (without NEs). It is important to highlight the effect observed at one of the earliest time points (3 hours after NEs addition). This effect could be related to the hypothesis that part of the NEs would be being directly sent to the mitochondria to be oxidized through the fatty acid oxidation (FAO). As a result of this pathway, NADPH and NADH were produced, which would be the responsible of the reduction of resarzurin (the active compound of alamarBlue^{TM}). Moreover, when new NEs were added, the positive effect in cell viability was re-established, validating its use for a new protocol to support breast cancer cell culture.

Once the effect in cell lines was determined, a model line of CTCs (mCTCs) was generated. The objective was to validate the effect of the NEs in a model of CTCs in breast cancer, since, unlike the lines used in previous experiments, the mCTCs had been in circulation in an immunosuppressed mouse. To obtain the mCTCs line, the parental line (MDA-MB-231), expressing the green fluorescent protein (eGFP) and the luciferase gene (MDA-MB-231$^{eGFP\text{-}Luciferase}$) was injected in the mouse. After metastasis was detected, cells were extracted from the blood and isolated using the EasySep^{TM} mouse T cell isolation kit. The mCTCs line and its parental line, MDA-MB-231$^{eGFP\text{-}Luciferase}$ were put in culture for 9 days, using the conditions developed in the group for the growth of CTCs. In both cases, the cell density at the end of the experiment was higher in cells treated with NEs. Specifically, the parental line treated with NEs maintained the initial seeding cell density, while the control was reduced by nearly a half. In the

case of mCTCs, an increase in proliferation close to 36 % was observed in NEs condition. Additionally, for the mCTCs line, a gene expression analysis was performed to understand the positive effect observed with respect to proliferation. From the panel of 13 genes analysed by RT-qPCR, it was observed that only one gene related to proliferation (*Ki67*) and another gene related to cell cycle (*E2F4*), presented higher relative expression in mCTCs treated with NEs.

To conclude the study, a mechanism of action based on experimental evidence, obtained by flow cytometry and TEM, was proposed. The dynamics of NEs followed in cells was studied. With both techniques, 3 time points were analysed: 4 h, 24 h, and 48 h after NEs addition. Quantitatively, it was determined by flow cytometry that at 4h the treated cells presented an increase in the amount of lipids. At the last point (48 h), a decrease in the presence of lipid compounds was observed in cells treated with NEs. These results, together with what was observed in the viability studies, indicated that the mechanism of action of the NEs could consist in that once in the cell cytoplasm, part of the NEs could be sent to be oxidized in the mitochondria and another part is storage in lipid droplets (LDs). The TEM analysis qualitatively confirmed the hypothesis.

The next step was to use NEs in cultures of CTCs isolated from metastatic breast cancer patients. The objective of this part was to validate the use of NEs in *ex vivo* cultures of CTCs, to favour the expansion of these cells. Once its value was proven, CTCs in culture were characterized. In addition, it was determined that following the culture protocol with NEs, the ability to grow of CTC cultures was associated with the evolution of the patients.

For this working module, CTCs were isolated using a negative enrichment technique, specifically RosetteSep™ was used. 50 peripheral blood samples obtained from 35 patients with advanced metastatic breast cancer were used. The longitudinal samples were collected at different time points through the disease: 32 of the 50 total samples (64 %) were collected after the start of therapy and 36 % were collected at baseline (diagnosis of metastasis). Of the treated patients, 14 were first-line and 18 had ≥ 2 lines of

treatment. Low adherence plates were used for cell cultures that were supplemented with factors and NEs (protocol developed by our group). In relation to this protocol, it is important to highlight that this is the first study in which nanoemulsions are used to support the culture of CTCs.

The mean time of cell culture was 56.35 days for the 50 samples. However, to differentiate a successful culture (culture (+)) from one failed (culture (-)), a ROC curve analysis was performed, establishing a cutoff of 23 days as culture (+). Based on this criterion, the cultures were successful in 75 % of the cases, while other studies indicate success rates between 13-28 %. For this reason, it is observed an improvement associate to the protocol proposed in this thesis.

In 34 out of 50 samples, paired CTC enumeration was carried out by CellSearch® system at the starting point of culture. Regarding enumeration, it is established in metastatic breast cancer that a 7.5 mL blood sample that presents ≥ 5 CTCs is associated with a worse prognosis. This association can be determined using parameters such as progression-free survival (PFS) and overall survival (OS). However, from this analysis it was determined that there was no association between the successful culture group (culture (+)) and the fact of having ≥ 5 CTCs.

A phenotypic characterization was performed in some random samples after ~ 2 weeks of cell culture. The characterization was carried out using immunofluorescence techniques, together with a gene expression analysis by RT-qPCR. First, for the immunofluorescence study, the following staining was used: for epithelial markers E-Cadherin, EpCAM and Pancytokeratin (PanCK) were used, while for mesenchymals the presence of Vimentin was studied and finally it was used a white blood cell marker CD45. Of the analysed samples, the epithelial markers were detected in low percentage (18.18 %, n = 22), while the mesenchymal marker of vimentin appeared in a higher percentage (47 %, n = 17). This result is in agreement with previous published studies that show that after 14 days of culture, a large part of the CTCs lose their epithelial characteristics and exhibit mesenchymal markers.

Regarding gene expression studies, from a customised panel of 20 genes, a comparison of samples before (once isolated) and after culture (~ 2

weeks in culture) was performed. Selected genes included: epithelial, mesenchymal, stem, breast cancer specific and other genes related to cell cycle pathways. The hierarchical clustering and the principal component analysis (PCA) diagrams determined that CTCs before and after culture presented a different gene expression pattern. It was observed that the CTCs freshly isolated from the blood presented higher expression of epithelial markers. Moreover, it was detected *CD45* expression in the samples and to establish whether blood cells contamination was influencing the genetic expression analysis, in 4 of the 6 samples it was analysed the expression of peripheral blood mononuclear cells (PBMCs) before and after culture using the same conditions. Both the hierarchical clustering and the PCA analysis showed that the expression of the PBMCs presented a completely different pattern from that of the CTCs. Some of the genes that showed higher relative expression in CTCs samples after culturing were related to EMT (such as *GDF15* and *CTNNB1*), stem cell phenotype (*ALDH1A1*) and fatty acid transport (*CD36*).

To identify markers with prognostic value, a survival analysis was performed. This analysis was based on the observation of two parameters: on the one hand, the cultivability of CTCs and, on the other hand, the presence of red blood cells (RBCs) at the beginning of the culture. Regarding the first parameter, it was determined how the duration of the culture could predict PFS, this being the first time that is has been described in breast cancer. Specifically, culture (+) presented a worse PFS. Regarding the presence of ≥ 5 CTCs by CellSearch®, in this study it did not predict PFS. Related to this observation, in this study only 53 % of the samples initially presented CTCs using CellSearch®. For this reason, the lack of association between these results is influenced by the isolation approach used (negative isolation), being able to collect cells with epithelial as well as stem or mesenchymal phenotypes. In contrast, the CellSearch® system only captured those with the epithelial phenotype. Regarding OS, it was appreciated that culture (+) was not a predictive factor in these samples, whereas the presence of ≥ 5 CTCs by CellSearch® was linked with shorter OS.

Independently of the effect of NEs in the cultures, we considered the presence of RBCs in the culture, establishing the criterion of RBCs (+) or RBCs (–) based on the amount of RBCs in cultures. We observed that the number of RBCs predicted PFS and OS. Related to this observation, in other studies it has been described that cancer patients display anaemia and coagulation problems, although the causes are unknown.

As a result of this second part, it is demonstrated the valuable use of proliferative NEs in CTCs cultures from breast cancer patients for establishing short-term cultures and to determine the prognosis of patients.

Lastly, once the use of NEs to support the expansion of breast cancer CTCs was demonstrated, NEs were decorated with specific ligands. The objective was to provide them with the ability to recognize surface proteins of CTCs, to finally use them in microfluidic devices for CTC capture.

As a first approach, the surfaces of the NEs were modified, incorporating peptides targeting EpCAM and EGFR. The design of the functionalization was based on the covalent bond between the reactive N-hydroxysuccinimide ester (NHS) group of the nanoemulsions and the primary amines present in the peptides. For this, NEs were formulated by adding CH associated to a chain of PEG with the NHS reactive group at the end. In this case, the formulated nanoemulsions were called PEG-NEs, and once the conjugation with the peptides was carried out: Pept-NEs. Specifically, they were called Pep10-NEs or GE11-NEs, depending on whether they carried the peptide Pep10 (anti-EpCAM) or GE11 (anti-EGFR), respectively.

In this work the physical properties of these particles were determined. All the formulations were less than 200 nm, and presented good monodispersity, with PdI lower than 0.2. In addition, the concentration of the two formulations were determined by NTA, presenting very similar values (for GE11-NEs of $1.63x10^{11}$ NPs/mL and for Pep10-NEs $1.61X10^{11}$ NPs/mL). Similarly, using standard curves with known concentrations of both peptides, the final peptide concentrations were determined in each of the two formulations (GE11-NEs, $3.87x10^{-3}$ mg/mL and Pep10, $9.44x10^{-3}$ mg/mL).

Once the physical characterization was done, an immobilization study on different surfaces was performed. For this reason, during the research stay at the iNANO center, in Aarhus (Denmark), the quartz crystal microbalance with dissipation measurement (QCM-D) was used. This equipment allows the determination of adsorption behaviours. In this study, different conditions were used (various surfaces (gold, silica or polylysine (PLL)) in combination with various buffers (MQ water, dPBS or HEPES2) and it was confirmed that the only condition that provided a stable monolayer was using PLL and MQ water. Taking advantage of the great utility of this equipment, it was also used to study the specific recognition of the two Pept-NEs formulations against their targets. Hence, the Pept-NEs were first immobilized and then a flow of MQ water and the proteins of interest (EpCAM and EGFR) were used. As a result, it was confirmed the specific recognition for both formulations. Additionally, a study was carried out using fluorescence microscopy and the breast cancer cell lines: MCF-7 and MDA-MB-231, which expressed high levels of EpCAM and EGFR, respectively, and their specificity was confirmed.

Notably, a toxicity study of the immobilized Pept-NEs on the surface of cell culture plates in contact with cells was performed. It was observed that during 9 days of culture under these conditions there was no toxicity associated. This result allows a future approach in which it is possible to perform an initial culture of the cells isolated in the device functionalized with Pept-NEs that has been used for the isolation.

All in all, this thesis highlights the great potential of the use of nanotechnology to design nanomaterials for their application in liquid biopsy. The relevance of this thesis lies in having used lipid-based biocompatible nanosystems, specifically nanoemulsions, managing to address two of the critical points that make challenging the use of CTCs in translational studies: *ex vivo* culture and isolation. Regarding the first, thanks to the use of proliferative NEs, developed and validated in Chapter 1, they could be used in *ex vivo* cultures of CTCs (Chapter 2). Consequently, using the protocol based on NEs addition, it is possible to expand these cells for their characterization and to predict patient outcome. Regarding the second point, isolation, in Chapter 3 Pept-NEs were developed to recognize

receptors on the surface membrane of CTCs. Therefore, it is highlighted the versatility of these nanoemulsions to become a valuable platform in liquid biopsy.

Introduction

INTRODUCTION

1. Nanotechnology and nanoemulsions

1.1. Historical background and overview of nanoparticles classification

In 1959, Richard Feynman introduced the concept of nanotechnology in his lecture *"There's plenty of room at the bottom"*, in which he considered to manipulate matter on the atomic scale[1]. However, was Norio Taniguchi who first used the term nanotechnology in 1974, to describe manufacturing processes exhibiting control on the order of a nanometer. Few years later, in 1986, Eric Drexler proposed the idea of a nanoscale assembler in his book *"Engines of creation: The coming era of nanotechnology"*[2].

Currently, nanotechnology is the popular term for the construction and use of functional structures with at least one characteristic dimension measured in nanometers. Historically, the term "nanometer" was coined by Richard Zsigmondy who won the Nobel Prize in chemistry in 1925[3], defining a nanometer as one billionth of a meter (10^{-9}); for instance, proteins are 1–20 nm in size. Nevertheless, is important to remark that nano is not the smallest scale; further down the power of ten are angstrom (=0.1 nm), pico, femto, atto and zepto[2]. As an example, dimensions of various objects in scale are represented in **Figure 1**.

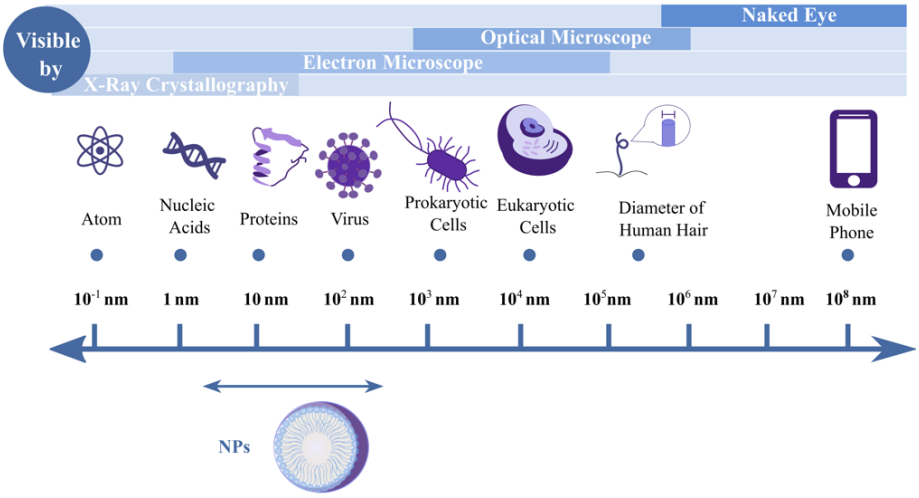

Figure 1. Size scale for most nanoparticles (NPs) as compared to other objects. Representation of different objects in scale visible by X-ray crystallography, electron microscope, optical microscope, and naked eye.

Nanoparticles (NPs) present a strong use in several fields, including physics, materials science, chemistry, biology, medicine, computer science, and engineering. The main reason for that is their unique physico-chemical properties, such as: (i) their high surface area to volume ratio compared with their macromolecular counterparts and (ii) the diversity of shapes and sizes that can be synthesised. Hence, NPs are broadly divided into various categories depending on their composition, morphology, size, among others. When it comes to their composition, NPs can be classified into inorganic and organic NPs. In **Figure 2** are represented some examples of each group.

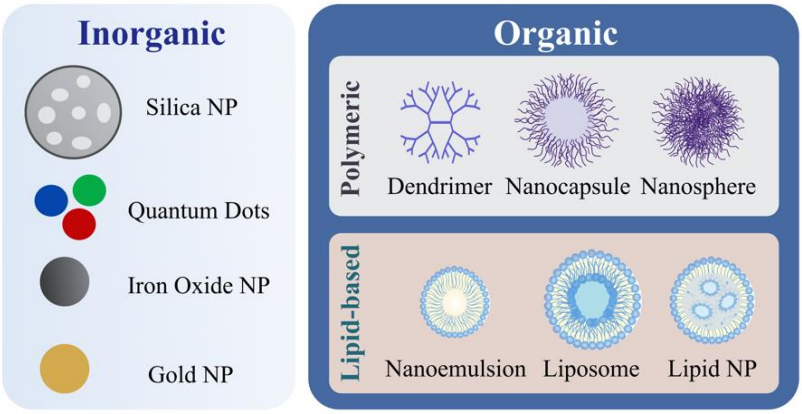

Figure 2. Groups of NPs based on their principal composition: inorganic and organic NPs. Representation of some examples of the most common groups of NPs (inorganic and organic NPs) and their subclasses (Polymeric and Lipid-based, in case of organic NPs).

In terms of inorganic materials, gold, iron, and silica have been widely used to synthesize NPs for various drug delivery and imaging applications. Among all of them, gold NPs and iron oxide NPs are two of the most well studied. They can be functional in several structures such as nanospheres, nanorods, nanostars, and nanoshells. In case of using organic materials, polymeric NPs or lipid-based NPs can be obtained. Regarding polymeric NPs, they can be synthesized from natural or synthetic materials, as well as monomers or preformed polymers. The most common forms of polymeric NPs are nanocapsules (cavities surrounded by a polymeric membrane or shell) and nanospheres (solid matrix systems). With reference to the last group, lipid-based NPs, includes various subset structures such as nanoemulsions, liposomes, and lipid-NPs. They offer many advantages including formulation simplicity, self-assembly, biocompatibility, high bioavailability, and a range of physicochemical properties that can be controlled to modulate their biological characteristics. For these reasons, lipid-based NPs are the most common class of nanomedicines approved by the Food and Drug Administration (FDA)[4,5].

1.2. General aspects of nanoemulsions and their formulation

1.2.1. Classification of nanoemulsions

Nanoemulsions are one subclass of lipid-based NPs. A Nanoemulsion is a biphasic dispersion of two immiscible liquids (**Figure 3**): either water in oil (W/O) or oil in water (O/W) droplets[6], although O/W nanoemulsions are much more commonly utilized than W/O ones[7]. Depending on constituents and relative distribution of the internal dispersed phase(s) and the more ubiquitous continuous phase, nanoemulsions are termed as biphasic (O/W or W/O) or multiple nanoemulsions (W/O/W). When it comes to the mean droplet diameter attained is usually between 20 and 200 nm[7]. Small droplet size gives them a clear or hazy appearance which differs from milky white colour associated with coarse emulsion (whose micron sized droplets partake in multiple light scattering).

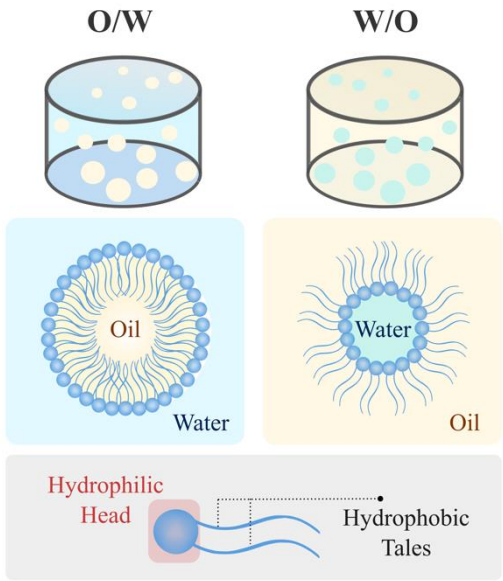

Figure 3. Representation of the two types of biphasic nanoemulsions: Oil in Water (O/W) and Water in Oil (W/O). At the bottom it is indicated the structure of a phospholipid: a hydrophobic head and hydrophobic tales.

When it comes to formulating nanoemulsions, interaction of various components making up the nanoemulsion must be taken into consideration. In terms of composition, nanoemulsions include two phases: the oil phase and the aqueous phase. The oil phase may be composed of various components such as free fatty acids, for instance the oleic acid (OA), or essential oils, among others. In case of the aqueous phase is typically composed primarily of water but might also contain other ingredients (e.g. buffers)[7].

However, more ingredients are often needed, due to nanoemulsions cannot usually be formulated by simply homogenizing an oil and aqueous phase together. In fact, the system would rapidly separate into its component phases in absence of other compounds such as emulsifiers. Hence, their main goal is to stabilize the final formulation. Emulsifiers are amphiphilic molecules (**Figure 3**) that stabilize emulsions in two ways: first, by providing an electrostatic repulsion between droplets, and second, acting as a steric barrier increasing the thermodynamic energy required to coalesce[8]. A common surfactant employed in nanoemulsions are phospholipids, such as the phosphatidylcholine (PC) derived from egg yolk or soybean[9]. Phospholipids are the major component of cell membrane and they have a head–tail morphology characterized by a positively charged phosphate head and two fatty acid tails. Furthermore, ultra-low negative interfacial tension is required for nanoemulsion formation. For this purpose, co-surfactants or co-solvents are also used. Co-surfactants or co-solvents that are generally used in formulation of nanoemulsion systems are polyethylene glycol (PEG), propylene glycol, ethanol, and propanol[10].

1.2.2. Formulation of nanoemulsions

A wide range of fabrication methods have been developed to formulate nanoemulsions, which can be roughly divided into (i) high-intensity methods (as high-pressure homogenization, microfluidization or ultrasonication) and (ii) low-intensity methods (including phase inversion emulsification and the spontaneous emulsification (also called "self-nanoemulsification") methods)[11]. One of the most used techniques is the spontaneous

emulsification method, which was firstly developed, and used for a long time, to prepare NPs by polymerization[12]. However, it is also used to obtain lipid-based NPs, and in this case, instead of polymer, oil is used. Briefly, the procedure involves separately preparation of two phases and then, organic phase is added drop wise to aqueous stirred phase (adding water to oil is equally feasible in case of W/O emulsions) to form small drops. In some cases, small amount of external energy may still be required, and it can be supplied by a magnetic stirrer, even though the actual process of emulsification occurs spontaneously. In fact, mild magnetic stirring is helpful in setting up tiny convection currents which consistently distribute oil droplets in bulk so that any new surface generated by solvent diffusion is immediately covered by surrounding surfactant molecules[6].

1.2.3. Functionalization of nanoemulsions

Along with the optimization of physicochemical properties, nanotechnologists have focused their attention on surface modification of nanoemulsions with different ligands, which is known as functionalization of nanoemulsions. For example, molecular fluorophores can be included for purposes of fluorescent imaging. Moreover, ligands can be used to bind specific receptors on the surface of target cells, which is referred to as active targeting (**Figure 4**). For the last case, in the active targeting design, it is of great importance selecting receptors which are overexpressed on target cells but not on the rest, to enable specificity[13].The aforementioned targeting agents that may be broadly classified as ligands include proteins, peptides, vitamins, and carbohydrates. For example, one of the commonly used ligands for cancer targeting is the high affinity vitamin folic acid (folate) since folate receptors are frequently overexpressed in different tumour cells[14].

In order to link these ligands to the surface of the nanoemulsions, giving functionality to the surface of the nanoemulsion is the most common followed approach. Although attachment could be related to other properties like surface charge or hydrophobicity (**Figure 4**), to obtain surface functionality, crosslinking technique is often used. It refers to the process of

chemically linking two or more molecules by a covalent bond[15]. Crosslinkers are molecules that contain reactive ends to specific functional groups (primary amines), which are present on proteins or other molecules. Therefore, the availability of several chemical groups in protein and peptides make them key targets for conjugation using crosslinking methods[15].

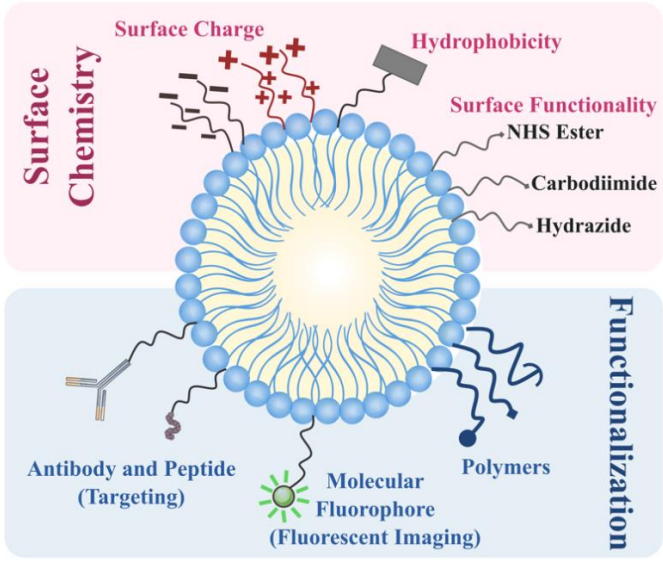

Figure 4. Schematic representation of different approaches used in surface chemistry design and functionalization of nanoemulsions. The attachment of different molecules on the surface of a nanoemulsions can be done by surface chemistry design based on surface charge, hydrophobicity or giving surface functionality using reactive chemical groups.

In this context, it is essential to highlight that the most important property of a crosslinker is its reactive chemical group, which establishes the method for chemical modification. Usually, reactions such as PEGylation or biotinylation are employed for protein modifications. For example, in case of protein PEGylation, the covalent attachment of PEG to proteins is achieved by the presence of a reactive group at one terminus and a chemical moiety at the other end of the PEG chain. The functional groups that are commonly targeted for bioconjugation are represented in **Table 1** and

include primary amines, sulfhydryls, carbonyls, carbohydrates and carboxylic acids.

Table 1. Some of the main crosslinker reactive groups for protein/peptide conjugation.

Reactivity Class	Target Functional Group	Reactive Chemical Group
Amine-Reactive		
	$-NH_2$	NHS ester Imidioester Hydroxymethyl phosphine
Carboxyl-to -Amine Reactive		
	-COOH	Carbodiimide (EDC)
Sulfhydryl-reactive		
	-SH	Maleimide Pyridyldisulfide Vinylsulfone
Aldehyde-reactive		
	-CHO	Hydrazide Alkoxyamine
Azide-Reactive		
	$-N_3$	Phosphine

1.2.4. Characterization of properties and stability in nanoemulsions

Adherence to a strict particle size is a perquisite for fabricating nanoemulsions, and following formulation, size estimation is mandatorily performed. This required under the European Union regulations, applies for research and industry[16]. Other important parameter is the polydispersity index (PdI), which measures uniformity of droplet size distribution; low PdI indicates low size distribution in the nanoemulsions. Usually, a formulation of nanoemulsions is considered monodisperse if the PdI is < 0.2 nanoemulsions. Particle size and PdI parameters can be measured by dynamic light scattering (DLS). Making use of the Brownian motion of colloidal particles, a DLS instrument scatters the light to find the diffusion coefficient of the particle[17]. However, microscopic techniques are essential

to obtain reliable data about the actual morphology of the system. In this sense, transmission electron microscopy (TEM) and scanning transmission electron microscopy had proven to be useful to observe the structure of the nanoemulsions. In the characterization process it is also important knowing the surface charge of the nanoemulsions. In this regard, the zeta potential (ζ-potential) is used for gauging charge on nanoemulsion surface, which provides clues towards its long-term stability and in some cases, their potential interaction with targets through electrostatic forces. It is determined indirectly using principle of electrophoretic mobility[6].

Significantly, the main limitation for developing applications for nanoemulsions is their stability, related to the different destabilizing mechanisms: creaming, sedimentation, flocculation, coalescence, and Ostwald Ripening (**Figure 5**). These mechanisms are followed by phase separation and therefore, the breakdown of the nanoemulsions. Although practically all literature indicates that nanoemulsions can be stable even by years, the small droplet size makes nanoemulsions break by the Ostwald Ripening mechanism[18–20]. This specific process occurs in the formulation when large droplets grow and small droplets shrink due to diffusion of oil molecules from small droplets to large droplets to the intervening continuous phase[21]. In contrast, nanoemulsions have stability to creaming and sedimentation (gravitational separation), (**Figure 5**). Regarding creaming and sedimentation, they are usually reversible processes with a minimal energy input.

In this line, stability studies are mandatory to properly characterize the nanoemulsions. The stability of the formulation is usually measured by their storage at 4.0 and 25.0 ºC for a period of three to six months. Sample characteristics such as particle size, PdI, ζ-potential, and efficiency of drug encapsulation are usually analysed once a month. No significant modifications of the nanoemulsion parameters should be found in order to confirm that the nanometric emulsion is stable under the storing conditions[11].

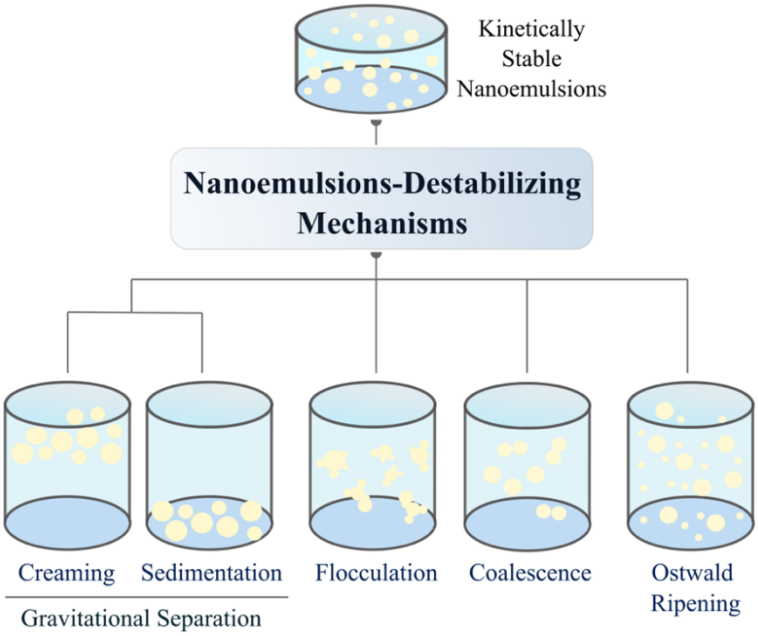

Figure 5. Scheme of the destabilizing mechanisms of nanoemulsions. In blue is represented the continuous phase, and in yellow the dispersed phase. Creaming and sedimentation are two types of gravitational separation. Flocculation is the process whereby droplets (two or more) associate with each other and form clusters. In contrast, coalescence is the process whereby a number of droplets collide and merge together, leading to the formation of a larger droplet. Ostwald Ripening is the growth of larger droplets at the expense of smaller droplets by diffusion of dispersed phase through the continuous phase.

2. Breast cancer and liquid biopsy

2.1. Breast cancer: incidence and subtypes

Cancer is commonly defined as the abnormal uncontrolled growth of the cells with inherent ability to spread to other tissues of the human body. In 2020, female breast cancer surpassed lung cancer as the most commonly diagnosed cancer worldwide, with an estimated 2.3 million new cases (11.7%), followed by lung (11.4%), colorectal (10.0%), prostate (7.3%), and stomach (5.6%) cancers[22].

Breast cancer is a heterogeneous disease and differs greatly among different patients (intertumour heterogeneity) and even within each individual tumour (intratumour heterogeneity). Different factors can be used to study the disease course: (i) routinely assessed pathological (lymph node status, grading, tumour size and extent) and (ii) molecular features, predominantly the steroid hormone receptor status (Progesterone Receptor (PR), Estrogen Receptor (ER), Human Epidermal growth factor Receptor 2 (HER2) expression/amplification status and Ki67 (proliferation index). The assessment of PR, ER, HER2, and Ki67 status allows the subclassification into four clinically distinct subtypes: luminal-A, luminal-B, HER2-positive ($HER2^+$), or triple negative[23]. In **Figure 6** are indicated the principal characteristics of each subtype. About 20% of breast cancers are triple negative, that means they are PR^-, ER^-, and $HER2^-$. These tumours are often aggressive and have poor prognosis[24].

Currently, the basis for an specific treatment is the expression of the established prognostic and predictive biomarkers, hormone receptors, and HER2[25]. The approach followed in a luminal-like disease is using endocrine therapy before chemotherapy. In case of triple negative breast cancers, the treatment is chemotherapy. Furthermore, immunotherapies show early signs of improving survival. For $HER2^+$ patients, it is preferred to use approaches such as HER2 pathway blockade and chemotherapy.

More effective therapeutic targets and novel biomarkers are still needed to find new therapeutic strategies and to improve the overall survival (OS) of breast cancer patients. Potential strategies to overcome treatment resistance include targeting driver mutations and deleterious passenger mutations, together with modulating the tumour microenvironment and immunotherapy[26].

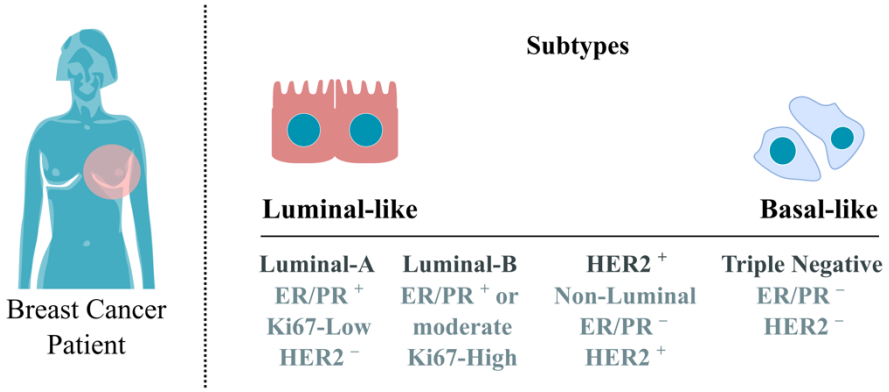

Figure 6. Subtypes of breast cancer. Main characteristics of the four subtypes of breast cancer. ER = Estrogen Receptor, PR = Progesterone Receptor, HER2 = Human Epidermal growth factor Receptor 2.

2.2. The complexity of breast cancer metastasis

2.2.1. The metastatic journey: main steps

Almost 90% of the mortality associated with cancer is due to the metastasis rather than to the primary tumour[27]. Although it is the most important mechanism of cancer aggressiveness, it is still poorly understood[28]. The metastatic breast cancer is also called advanced breast cancer or stage IV.

Cancer metastasis comprises a series of processes where cancer cells, on their way to metastasize, use and exploit three main bodily fluids: blood, lymph, and interstitial fluid. **Figure 7** shows a schematic representation of the main steps in blood. Firstly, breast carcinomas (primary tumours) induce

the formation of new blood vessels to facilitate the supply of nutrients and oxygen for growth[29,30]. This process called angiogenesis, often results in leaky vessels caused by weak interconnections of the endothelial cells at the vessels and intercellular openings[31]. Due to outward pushing of the tumour during growth, single or clusters[32] of tumour cells can be forced through the leaky vessels, thus ending up in the blood circulation (intravasation). Once in the bloodstream these cells are called Circulating Tumour Cells (CTCs). Next, when transported in the bloodstream (circulation), as single CTC or as CTC cluster, cells are subjected to various mechanical forces. For example, high shear forces exerted on CTCs can induce mechanical stress, leading to cell fragmentation and death, whereas intermediate shear forces have been shown to favour CTCs intravascular arrest and extravasation. Then, some cells will eventually survive the local immune response from the organ microenvironment to colonize and form micrometastases. In fact, this process is highly inefficient, with an estimated 1 out of 10,000 cells successfully achieve extravasation and homing to a distant site[33].

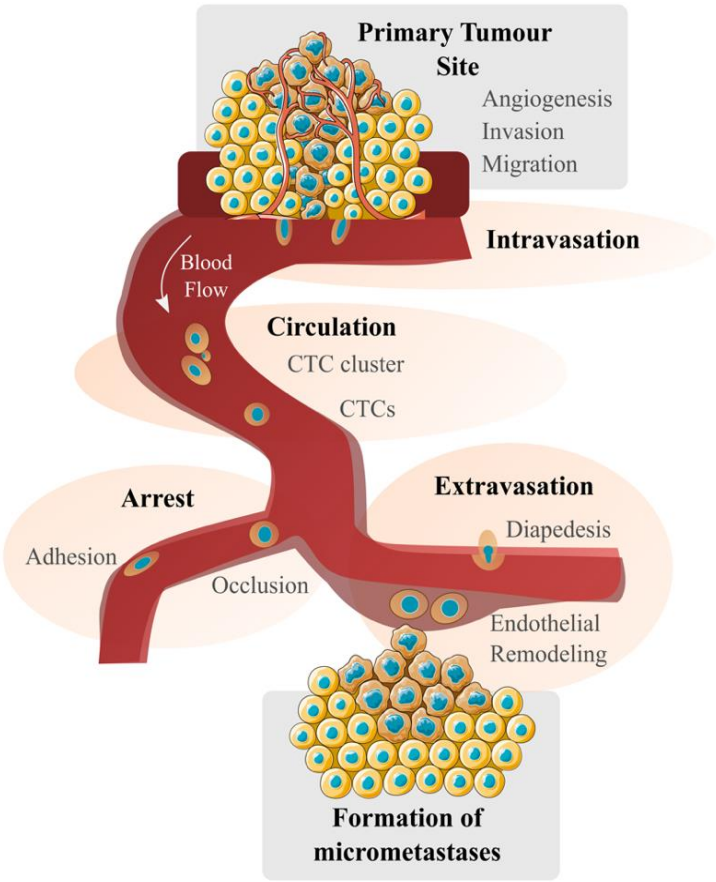

Figure 7. Scheme of the key steps in metastasis. Cancer cells from the primary tumour site break the basement membrane and invade into the surrounded tissues. Angiogenesis in the primary tumour stimulates the formation of blood vessels. Cells become motile and invade surrounding tissue through the extracellular matrix. Then, cancer cells migrate towards blood vessels. Metastatic cancer cells enter the circulation system by intravasation process. These Circulating Tumour Cells (CTCs) can travel through the circulation as a CTC cluster or as single CTCs to reach a distant organ. During the circulation of these cells, they can be arrest by an active process (adhesion) or by a passive process (occlusion). CTCs can finally extravasate (for example using diapedesis), invade, undergo endothelial remodelling, and proliferate to form micrometastasis (secondary tumour).

2.2.2. The epithelial-mesenchymal plasticity

One of the first steps of the metastasis is the detachment of cancer cells from primary tumours, due to the loss of intercellular contacts and cell motility. This process can be driven by the epithelial-mesenchymal transition (EMT), characterized by the decrease of epithelial and increasement of mesenchymal cell markers. In this context, the downregulation of epithelial proteins such as E-Cadherin has been shown to support mechanisms that induce stemness in carcinomas[34].This stem cell-like cells have a propensity to invade surrounding tissues. However, disseminated mesenchymal cancer are also capable to undergo the reversion of EMT (the mesenchymal-epithelial transition (MET)) to support more epithelial states in distant metastases[35]. Nonetheless, despite the contribution of EMT to CTCs release, it is clear today that not all CTCs express canonical EMT markers. Alternatively, EMT can generate a spectrum of cellular states displaying mixed epithelial and mesenchymal features that lie between these two extremes, which may also account for the CTC heterogeneity[36,37]. In **Figure 8** it is represented the most important markers related to this cellular plasticity.

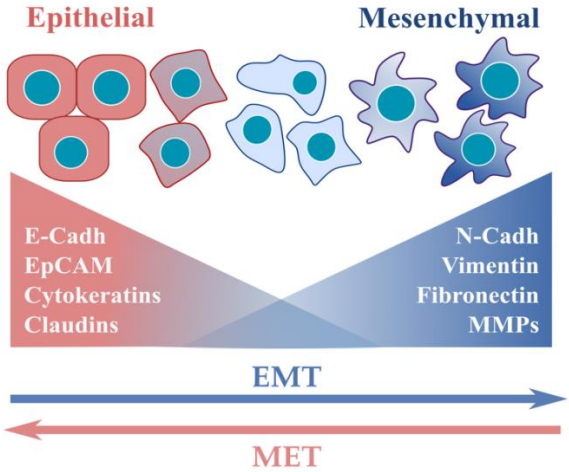

Figure 8. Spectrum of cellular states along the epithelial-mesenchymal transition (EMT) and the mesenchymal-epithelial transition (MET) programs. Some markers for each phenotype (epithelial and mesenchymal) are represented. E-Cadh = E-Cadherin, N-Cadh = N-cadherin, MMPs = Matrixmetalloproteinases.

2.2.3. Implications of the lipid metabolism in metastasis

In 2000, Hanahan and Weinberg outlined hallmarks that characterized the capabilities acquired during tumour development[38]. The six hallmarks originally proposed were: sustaining proliferative signalling, evading growth suppressors, activating invasion and metastasis, enabling replicative immortality, inducing angiogenesis, and resisting cell death. Some years later, in 2011, they added four new hallmarks[39]: avoiding immune destruction, tumour-promoting inflammation, genome instability and mutation, and deregulating cellular energetics. Related to this last hallmark, over the past decade, it has become more relevant that metabolic reprogramming represents a key event in promoting tumour progression. Initially, Otto Warburg in 1920s reported that cancer cells employed much more glucose for glycolysis compared to normal cells, even in normoxic condition (phenomenon known as "Warburg effect")[40]. However, while most attention was focused on glucose metabolism, in the last decade lipid metabolism has increasingly been recognized as another important property of tumour cells. For instance, it is known that lipid accumulation increase the invasiveness, migration, and progression of various cancers including breast cancer[41,42]. Classically, de *novo* lipogenesis (using glucose and glutamine as substrates) was the only known way for energy production and lipid accumulation in cancer cells; nevertheless, it is now apparent that cancer cells can acquire exogenous free fatty acids (FFAs). In this context, the tumour microenvironment has been described as an important source of metabolites for tumour cells. In fact, breast cancer cells are able to activate lipolysis in tumour-surrounding adipocytes, to obtain FFAs[43]. Then, FFAs and lipids are taken up by tumour cells and mainly stored as neutral lipids in lipid droplets (LDs). Moreover, this increased fatty acid uptake was not just observed in primary tumour surrounds, but also in CTCs[42,44].

Nowadays, it is well-known the relevance of the diet in lipid availability (**Figure 9**). Actually, the increasing incidence of obesity results in a significant challenge for the clinical management of breast cancer, specifically due to obesity reduces response to chemotherapy[45]. Several pre-clinical models find that high fat diets increase secondary tumour sites in

breast cancer mouse models. Therefore, lipid availability may enhance metastases by providing lipid substrates for energy production and for biosynthetic processes supporting cell proliferation[46]. As represented in **Figure 9** tumour cells present different ways to internalized extracellular lipids and FFAs. Among the several fatty acid transporters, CD36 (a fatty acid translocase) has been identified as an important mediator for lipid-driven metastatic cell adaptation for survival[47]. Regarding this lipid availability, metastatic tumours exhibit increased Fatty Acid Oxidation (FAO), increased lipid storage in LDs, and subsequently decreased Reactive Oxygen Species (ROS) production[48]. Moreover, when disseminated cells travel through the lymphatic system, which has been shown to be rich in OA (a well-known fatty acid), their lymph metastases also express an altered lipid profile (**Figure 9**). Due to increased OA uptake, lymph metastases have been shown to present decreased ROS production[49]. Certainly, numerous mechanisms could be taking part in lipid-mediated metastasis, supporting secondary tumour development in tissues such as the brain, lung, liver, and bone[46], (**Figure 9**).

In some cancers enhanced FAO is coupled to adenosine triphosphate (ATP) production, but specifically in breast cancer, the observed enhanced FAO is uncoupled from ATP production. Actually, in previous studies where breast cancer cells were co-cultivated with adipocytes, it was observed a decrease in mitochondrial respiration associated with decreased ATP content. This result was related to the enhanced expression of uncoupling protein (UCP) 2[50], (**Figure 9**). Increased FAO associated with decreased mitochondrial respiration could therefore contribute to the accumulation of acetyl-CoA[51]. Accordingly to the increasing evidence demonstrating links between acetyl-CoA, histone acetylation, and control of gene expression[52,53], FAO-derived product could contribute to epigenetic changes favouring the pro-invasive effect of adipocytes[50,54,55]. Moreover, acetyl-CoA is involved in the synthesis of ketone bodies, FFAs, and cholesterol (CH)[56]. **Figure 9** shows how FAO is also involved in NADPH production, which is a critical to maintain redox balance and survival of cells[57].

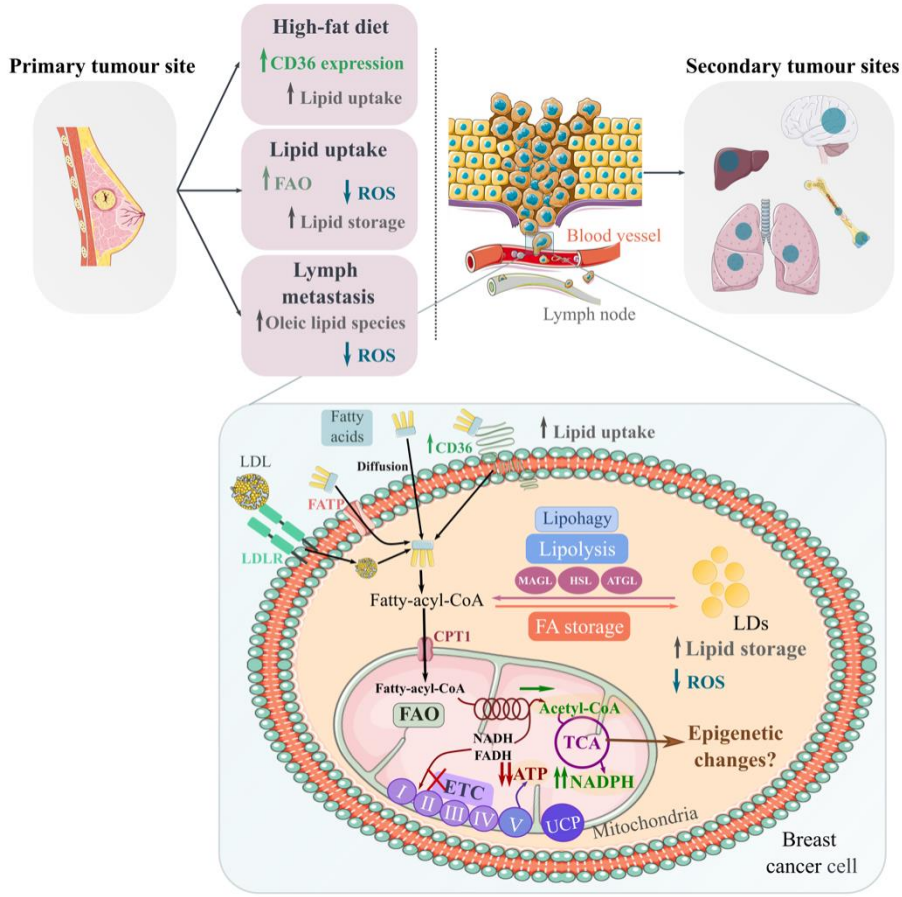

Figure 9. Lipid metabolism mechanisms involved in metastatic breast cancer. Common sites of spread are represented: bone, the liver, the lungs, and the brain. Free fatty acid (FFA) can be uptake by several processes (LDLR, FATP, diffusion, and CD36). Then can be stored as lipid droplets (LDs) or directly transferred to the mitochondria to be oxidized. Tumour cells can also release FFA over time through LDs store mobilization by lipolysis or lipophagy. Once inside the mitochondria, FFAs are oxidized to produce redox coenzymes and acetyl-CoA, which enter the tricarboxylic acid (TCA) cycle. In different cancers (melanoma, ovarian, and gastric) use the Fatty Acid Oxidation (FAO) process, where redox coenzymes are used in the electron transport chain (ETC) for ATP production. However, in breast cancer FAO could be uncoupled from ATP production. Hence, the accumulation of metabolites, such as acetyl-CoA, resulting from this uncoupling could induce epigenetic changes. Abbreviations: ATGL, adipose triglyceride lipase; CPT1, carnitine palmitoyltransferase 1; FA, fatty acid; FABP, fatty acid binding protein;

FATP, fatty acid transport protein; FAO, fatty acid oxidation; HSL, hormone-sensitive lipase; MAGL, monoacylglycerol lipase; ROS, reactive oxygen species; UCP, uncoupling protein. Adapted with permission from[46] and [51].

2.3. Liquid biopsy and circulating tumour cells (CTCs)

2.3.1. Application of liquid biopsy in cancer

Traditional tissue biopsy presents some key related issues such as patient risk, sample preparation, low-sensitivity, procedural costs, and invasive testing. In this context, liquid biopsy has emerged as a powerful non-invasive tool in detection and monitorization of cancer patients. It appears as a complementary tool to conventional tissue biopsies. Significantly, liquid biopsy captures intratumour and metastatic genetic heterogeneity, while tissue biopsy fails to do it[58]. To date, approved clinical use of liquid biopsy is limited but expanding, with a few approved tests for cancer screening or for identification of specific actionable mutations that guide cancer drug treatment, especially when tissue biopsy is not possible. Multiple studies are under way for early diagnosis, monitoring of tumour recurrence, evaluation of treatment response, and identification of emerging targets or resistance indicators during disease progression[59].

In other words, liquid biopsy represents a powerful tool to support precision medicine, allowing the study of the "tumour circulome"[60]. This term has been used to describe the subset of circulating components that derived from cancer tissue and can be directly or indirectly used as a source of cancer biomarkers[61]. The biomarkers that can be obtained using liquid biopsy include: circulating tumour proteins, circulating tumour nucleic acids (ctDNA and ctRNA), CTCs, extracellular vesicles, and tumour-educated platelets. Among all these circulating materials, CTCs represent one of the most promising biomarkers of liquid biopsy; although other biomarkers may be more easily detected and measured (for example ctDNA and ctRNA), CTCs are advantageous for identifying treatment targets for clinical testing or drug development mainly because they represent cancer cells that survive after drug therapy.

2.3.2. CTCs: isolation, detection, and characterization techniques

As already mentioned, CTCs have great potential for the diagnosis, monitoring, prognosis, and prediction of response to therapy in the cancer management[61]. Moreover, they offer essential potential for the discovery of novel drug targets. Historically, this biomarker was discovered by Ashworth in 1869[62]. However, there was not much interest in tumour cells in the bloodstream after this first report, mainly due to the lack of the technology required to isolate them. CTCs are challenging because they are infrequent, appearing at an estimated level of one against the background of millions (10^6-10^7) of surrounding normal peripheral mononuclear blood cells (PBMCs)[63].

To date, a wide range of technologies are being used for the (i) isolation, (ii) detection, and (iii) characterization of CTCs in blood (**Figure 10)**. Firstly, regarding (i) isolation of CTCs (also called enrichment), one of the most important milestones in the field was reached in 2004, when the CellSearch® system was introduced in the clinical use as the only technology approved by the FDA for enumeration of CTCs in breast, prostate and lung cancer. This technology is based on differential expression of cell surface proteins between tumour cells and blood cells.

When it comes to technologies to isolate CTCs, they can be roughly classified into two groups (**Figure 10**). One major group is (i,a) label-dependent CTC isolation (such as CellSearch®) that utilize surface markers to distinguish CTCs from their surrounding blood cells. In this context, the most used approach is by positive selection, which consists in directly targeting cancer-specific markers on the cell surface of CTCs (is used mainly Epithelial Cell Adhesion Molecule (EpCAM)). Notwithstanding, while these methods show very good specificity, they present a limited sensitivity most likely due to the failure in recognizing cells undergoing EMT. For that reason, platforms relying on the depletion of leukocytes (negative selection), are being investigated and used to overcome this bias from positive selection. One example of negative selection would be RosetteSep™ cell isolation kit. The other group, differentiates CTCs from

blood cells based on physical properties of CTCs, they are called (i,b) label-independent CTC isolation techniques. They take advance of the differences in size, density, electrical charge or/and deformability of tumour cells and non-malignant blood cells.

Following isolation, CTC populations may still present hundreds to thousands of leukocytes, requiring the use of reliable methods to identify them. Therefore, regarding (ii) detection of CTCs (**Figure 10**), it is possible to identify these cells using (ii,a) immunological techniques (antibodies to membrane and cytoplasmic antigens, including epithelial, mesenchymal, tissue-specific and tumour-associated markers). The most used approach is the same identification as the FDA-approved CellSearch® (cells stained with fluorescently labelled antibodies to epithelial cytokeratins (CKs) and DAPI for cell nucleus detection, while staining of CD45 is used for leukocyte exclusion)[59]. Morphologic investigation together with fluorescence immunocytochemistry is also a common procedure for the identification and enumeration of CTCs after enrichment. Furthermore, CTCs can be identify using (ii,b) molecular biology techniques. In this field, the gold standard method is the quantitative reverse transcription PCR (RT-qPCR) assays for detection of low-abundance messenger RNA (mRNA) transcripts. Moreover, (ii,c) *in vitro* functional assays such as the Epithelial ImmunoSPOT (EPISPOT) assay might be useful for CTC detection[64].

Finally, in-depth analysis can be carried out, performing the (iii) characterization of CTCs **(Figure 10)**. The most widely used approach to study the (iii,a) proteome, is immunophenotyping with antibodies to proteins of interest. Nevertheless, more comprehensive analyses can be carried out through (iii,b) genome analysis by single-cell isolation, followed by amplification of the whole genome. This method allows assessments of copy number aberrations and specific mutations by for example next-generation sequencing (NGS) technologies. Unlike bulk-cell approaches, single-cell analysis have the advantage of assessing the cellular heterogeneity[65]. Furthermore, it is also possible to study the (iii,c) transcriptome by different techniques, such as multiplex RT-qPCR, RNA sequencing or *in situ* RNA hybridization. Lastly, as part of (iii,d) functional studies, CTCs can be utilized at *in vitro* and *in vivo* levels. It is essential to achieve enough CTCs

for down-stream analyses, so a key step once isolated these rare cellular subpopulations, is to expand them using *ex vivo* CTC cultures[59]. Furthermore, CTCs can be injected in xenografts to generate Patient-Derived Xenograft (PDX) models (also known as CTC Derived Xenograft (CDX)). These assays can provide information about secondary sites of metastasis and treatment-decision drug screening. However, the development of PDXs usually takes several months and for that, *ex vivo* CTC culture provide an attractive alternative. Most of these cultures are short-term, lasting from 3 days to 14 days[66–72]. Only a few long-term cultures have reported successfully established CTC lines with demonstrated immortality that could be cultured stably for many passages[73–76].

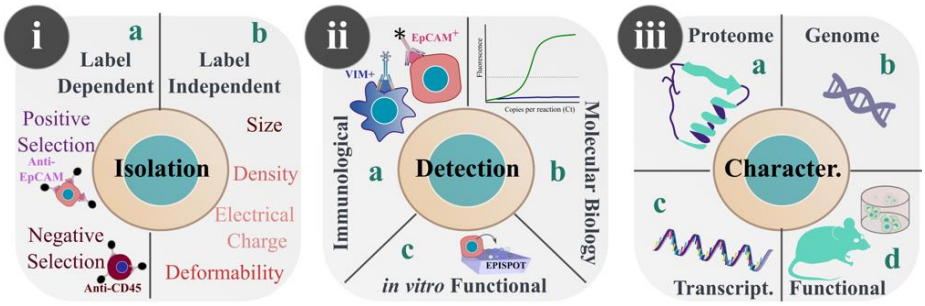

Figure 10. Technologies for the isolation, detection, and characterization of CTCs. CTCs can be isolated (i) by (a) label-dependent or (b) label-independent approaches. Next, (ii) detection of CTCs can be performed by (a) immunological, (b) molecular biology assays or using *in vitro* functional studies. Then, an in-depth analysis can be performed by characterization of CTCs at a (a) proteome, (b) genome, (c) transcriptome levels or by (d) functional assays.

2.3.3. Clinical implications and therapeutic application of CTCs in breast cancer

The easiest information obtainable from CTCs is their number, that is a prognostic predictor for many cancers, including breast, colon, and prostate[77]. On one hand, in case of non-metastatic breast cancer patients a CTC count ≥ 1 cells per 7.5 mL of blood is associated with decreased progression-free survival (PFS) and OS[78]. On the other hand, in metastatic breast cancer patients a count ≥ 5 per 7.5 mL of blood is associated with significantly inferior PFS and OS[79]. Apart from that, also in metastatic breast

cancer patients, CTC counts allows prediction after therapy due they are correlated with PFS and OS[80,81].

Even though these currently applications, CTCs have not been included into clinical guidelines[82], and their clinical utility remains to be determined in clinical trials[83].

3. Nanotechnology assistance in liquid biopsy: enrichment and analysis of CTCs

3.1. Nanoparticles for isolation and detection of CTCs

In terms of the application of nanotechnology to the liquid biopsy field, the most well-known approach is the CellSearch® system. This technology is based on magnetic NPs functionalized with antibodies (immunomagnetic separation) against an epithelial marker.

So far, a variety of NPs have been developed for CTC isolation and detection, although three types could be the most relevant: (1) magnetic NPs, (2) quantum dots, and (3) gold NPs. Regarding the (1) magnetic NPs, they are one of the leading methods for CTC isolation based on immunolabel capture. These magnetic NPs bind to cells and can be separated in the presence of an external magnetic field. The most known are: CellSearch® system[80], Magnetically Activated Cell Sorting (MACS)[84], Adna Test[85], Dynabeads®[86], and EasySep™[87]. The CellSearch® and Adna Test platforms utilize magnetic NPs attached to antibodies to EpCAM. However, Adnatest employs additional tumour-specific antibodies depending on the requirement[88]. Moreover, CellSearch® uses downstream immunostaining to identify CTCs, while the Adnatest employs cell lysis and RT-qPCR to measure tumour-associated gene expression. Compared to CellSearch®, AdnaTest exhibits improved enrichment efficiency, due to the usage of two antibodies and the size of magnetic particles. However, neither of these technologies allows for further live-cell phenotypic analysis, due to captured cells are either fixed or lysed. Another variation of the use of magnetic NPs

in liquid biopsy is MACS (MiltenyiBiotec, BergischGladbach, Germany). This differs from CellSearch® and AdnaTest in using superparamagnetic iron NPs combined with a magnetized steel-wool column. By removing the column from the external magnetic field, cells can be recovery from the column. The advantage of this technique is the combined usage of magnetic NPs (so-called beads) coupled with various antibodies and the possibility to label cells with fluorescent antibodies. Thereby, direct enrichment and evaluation of captured cells without further detaching or staining procedures can be performed. All these examples are based on positive selection, but a draw-back of this approach is that CTCs not expressing the targeted markers will not be recognized and isolated. This key issue can be partly addressed by using a negative depletion strategy with magnetic beads, such as EasySep™ technology. Referring to (2) quantum dots, this type of NPs has been widely used for CTC detection. The reason is their inherent fluorescence with tuneable emission wavelengths. Quantum dots display longer fluorescence lifetimes compared with organic fluorophores[89], which is important to enhance the sensitivity of surface marker–dependent CTC capture. However, their toxicity affects cell viability, so no further functional assays can be performed after them. Regarding (3) gold NPs, they present enhanced light-absorption and scattering properties. Accordingly, binding between gold NPs and CTCs can be monitored quantitatively via photoacoustic signals or surface plasmon resonance shifts. The advantage of this type of technology is that detection can be controlled by laser, the drawback is they are non-biodegradables.

3.2. Nanoparticle-based microfluidic devices for isolation and detection of CTCs

Nanotechnology-assisted CTC isolation and analysis using microfluidic devices has attracted more and more attention as it combines the advantages of both nanotechnology and microfluidics fields (**Figure 11**). Hence, a promising approach for isolation and detection of CTCs is provided by the integration of NPs into microfluidic chips, due to nanostructured-assisted devices for CTC capture provide increased contact area between the cell

surface and the nanomaterial of the device. This results in more binding sites and more efficient affinity capture[90].

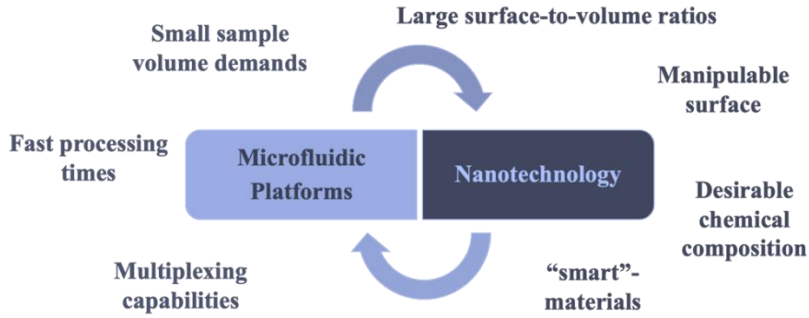

Figure 11. Main advantages of using microfluidic platforms combined with nanotechnology. On the left is represented the advantages involved with microfluidic devices and on the right the ones related to nanotechnology.

Overall, microfluidics provides many attractive advantages for CTCs studies such as continuous sample processing to reduce target cell loss and easy integration of various functions into a chip, making "do-everything-on-a-chip" possible.

When it comes to functionalization of microfluidic devices, all the previous NPs mentioned (magnetic NPs, quantum dots or gold NPs) can be incorporated into them. Some examples of microfluidic approaches based on immunocapture would be Herrinbone (HB) chip, GEDI chip, Isoflux, and CTC-iChip. In terms of taking advantage of physical properties, some isolation microfluidic devices are: Parsortix™ (Angle plc) and Vortex VTX-Q[91].

At date, most of the analysis of CTCs is done by directly lysing the cells on the surface of the microfluidic device to measure DNA, mRNA, and proteins[92]. However, captured CTCs can give more information. One of the essential steps of CTC downstream analyses is to release the captured CTCs from trapping structures while keeping cells unperturbed and viable[93]. Therefore, great efforts have been devoted to release CTCs from microfluidic devices and some of the possibilities are using the following approaches: (1) flowing fluid-mediated, (2) light-controlled, (3) thermal-

controlled, (4) electrochemical, (5) ligand-competition, and (6) enzymatic degradation[92]. Each one has a different impact in parameters like capture efficiency, release efficiency, and post-release cell viability. Therefore, it is essential to highlight that each method has their respective strengths and weaknesses, so their selection should be done depending on the downstream application. Next, all kind of analyses can be carried out in this type of platforms such, CTC morphologic, CTC genomic, CTC transcriptomic, CTC protein, and CTC functional analyses. For instance, Pang's group proposed a micropillar chip-assisted multifunctional-nanosphere system for the capture and analysis of heterogeneous single CTCs. Using red fluorescent magnetic nanospheres modifying anti-EpCAM and green fluorescent nanospheres modifying anti-HER2 antibody were targeted to two kinds of CTC biomarkers of breast cancer, allowing simultaneous magnetic labelling and fluorescent measure[94].

Altogether, nanotechnology-assisted microfluidic chip represents a powerful tool due to their unique properties, showing higher sensitivity and better compatibility with downstream analysis. Therefore, might be useful for guiding personalize anticancer therapy. However, most of the technologies are still in the stage of laboratory research, so the currently challenge is to arrive to clinical practice.

Hypothesis

HYPOTHESIS

It is possible to formulate biocompatible and biodegradable NPs that will address two of the critical points that make challenging the use of CTCs in translational studies of breast cancer: *ex vivo* culture and cell isolation. Both are essential tools used in liquid biopsy to better understand the metastatic process. Using nanoemulsions that are composed of a specific combination of lipids involved in the proliferation of breast cancer cells, we can obtain an increase in the cell viability and proliferation of the limited number of CTCs obtained initially. Then, these CTC cultures can be employed as the starting material for different downstream analyses. Furthermore, in terms of isolation, the nanoemulsions can be decorated using different peptides in order to recognize cell surface proteins of CTCs.

Objectives

OBJECTIVES

The global aim of this thesis is to develop innovative NPs that can provide a source of CTCs for translational studies, which contribute to a better understanding of the processes involved in metastasis. The main objectives of this thesis are:

1. To design and develop nanoemulsions using a specific combination of lipids, in order to facilitate the expansion of breast cancer cells in cell culture.

2. To study the influence of the nanoemulsions on cell viability and proliferation of *in vitro* cell cultures of breast cancer cells.

3. To use the proliferative nanoemulsions to develop an *ex vivo* short-term culture protocol of CTCs isolated from metastatic breast cancer patients, allowing downstream CTC analysis.

4. To functionalize the proliferative nanoemulsions with peptides, in the interest of allowing them to specifically recognize breast cancer CTCs for their isolation.

To achieve these aims, the experimental part was divided in the following work modules:

Phase 1: formulation and characterization of nanoemulsions consisting of a mix of different lipids and oils. Different nanoemulsions were formulated and analysed to select the most suitable, regarding their stability and positive effect on breast cancer cell viability. This data is presented in Chapter 1.

Phase 2: application of the proliferative nanoemulsions developed in Chapter 1 to establish *ex vivo* short-term CTCs cultures from metastatic breast cancer patients, and the subsequent use of this CTC cultures in different analyses (immunofluorescence characterization and gene expression analysis). Additionally, analysis of the correlation with clinical

data was performed to test the prognostic value of expanded CTCs cultured with the proliferative nanoemulsions. This data is presented in Chapter 2.

Phase 3: functionalization of nanoemulsions with peptides able to interact with cell surface biomarkers characteristic from CTCs, and anchoring to a microfluidic chip for their efficient isolation and culture. Two peptides against EpCAM and Epidermal Growth Factor Receptor (EGFR) were used. Once performed the characterization of the Peptide-functionalized nanoemulsions, analyses of immobilization on surfaces were carried out to determine their potential use in microfluidic systems. Furthermore, their specific binding affinity was validated. Results from this part are presented in Chapter 3.

Chapter 1

Chapter 1.

Nanoemulsions to support *ex vivo* cell culture of breast cancer CTCs

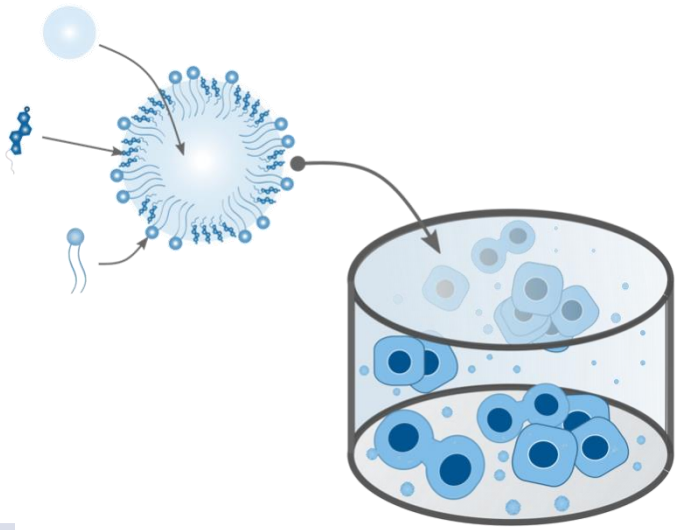

CHAPTER 1

Nanoemulsions to support *ex vivo* cell culture of breast cancer CTCs

The results from this chapter have been adapted/extracted from our previous published article[95].

Nanoemulsions to support *ex vivo* cell culture of breast cancer circulating tumor cells

Nuria Carmona-Ule[1], *Carmen Abuín-Redondo*[1], *Clotilde Costa*[1,2], *Roberto Piñeiro*[1], *Thais Pereira-Veiga*[1], *Inés Martínez-Pena*[1], *Pablo Hurtado*[1], *Rafael López-López*[1,2, 3], *María de la Fuente* [2,4], *and Ana B. Dávila-Ibáñez*[1].

[1]Roche-Chus Joint Unit, Translational Medical Oncology Group (Oncomet), Health Research Institute of Santiago de Compostela (IDIS), Hospital Gil Casares, Travesía da Choupana, s/n Cp:15706 Santiago de Compostela, Spain.

[2]Cancer Network Research (CIBERONC), 28029 Madrid, Spain.

[3]Translational Medical Oncology Group (Oncomet), Health Research Institute of Santiago de Compostela (IDIS), Hospital Clínico Universitario de Santiago de Compostela (SERGAS); Travesía. Choupana s/n 15706, Santiago de Compostela, Spain.

[4]Nano-Oncology Unit, Health Research Institute of Santiago de Compostela (IDIS), SERGAS; Travesía. Choupana s/n 15706, Santiago de Compostela, Spain.

Materials Today Chemistry. 16. 100265. ISSN: 2468-5194
Elsevier Ltd, 03/04/2020.
Full-text available: https://doi.org/10.1016/j.mtchem.2020.100265

Abstract

As cancers spread, they shed CTCs into the bloodstream of breast cancer patients. Isolating and analysing CTCs can provide insight into the understanding of the metastasis process, response to treatment or new potential therapeutic targets. For that, CTCs can be expanded using *ex vivo* cell cultures to perform different studies. However, the *ex vivo* culture of CTCs still represents a big challenge in translational research. In this work, we present a new methodology based on the use of nanotechnology to support *ex vivo* culture of CTCs. To achieve that, we have formulated O/W nanoemulsions which can help increasing cell viability on different breast cancer cell lines. Moreover, we have generated a CTC model from breast cancer mice xenografts, to prove the ability of the NEs to facilitate their culture and expansion. Additionally, we have postulated a mechanism of action based on the cell consumption of the NEs, which are acting as energy suppliers, driving proliferation. This work corroborates the potential of nanotechnology to provide valuable tools for liquid biopsy and shows the potential of our nanoemulsions to improve proliferation of breast cancer CTCs for the establishment of standardized CTCs culture protocols.

Graphical abstract

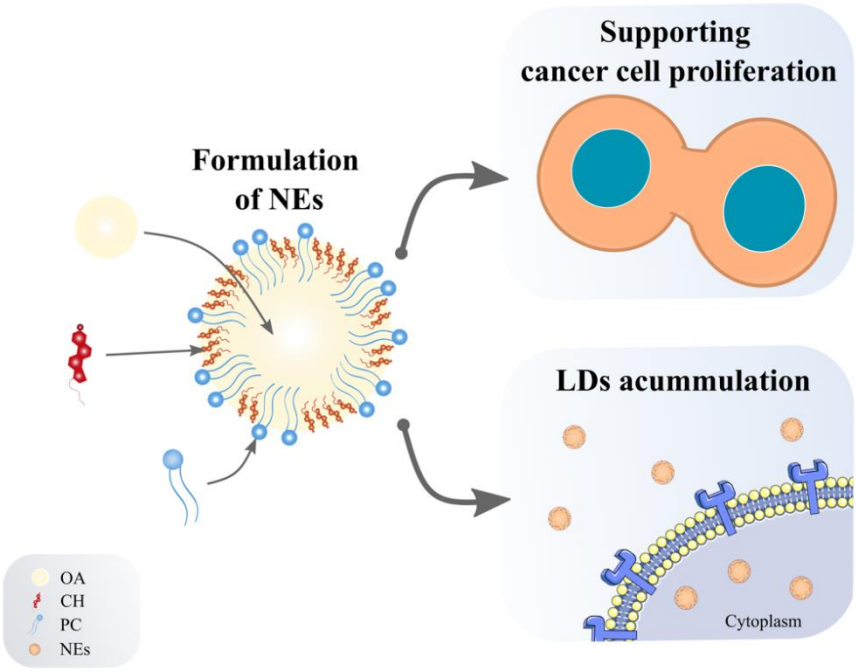

1.1. Introduction

Cancer is one of the major causes of mortality worldwide, with >14.1 million new cases and 8.2 million deaths each year[96]. Among females, breast cancer is the most frequent malignancy diagnosed worldwide. The worldwide incidence of breast cancer has been rising with annual increases of 3.1%, starting with 641,000 cases in 1980 and increasing to >1.6 million in 2010. In this context, efforts are being made to improve current diagnosis and therapeutic strategies to increase patient survival[97–99].

By means of liquid biopsy, it is possible to analyse circulating tumour material: circulating DNA or RNA, exosomes, and CTCs; obtaining real-time information related to the state and progression of the disease. The importance of this material is that support the improvement of cancer diagnosis and treatment, and ultimately the outcome of cancer patients. Especially relevant is the analysis of CTCs, which are those cells that abandon the primary tumour and circulate through the vascular system in the body to eventually colonize distant organs and originate the formation of distal metastasis. However, the molecular analysis of CTCs is still a challenge due to the difficulty to expand them *in vitro*. The main challenges of CTCs isolation and culture relate to the fact that CTCs are infrequent (1 CTC against 10^6-10^7 of surrounding normal PBMCs and they usually present a non-proliferative state when isolated[100].

The first to describe the establishment of primary cultures of CTCs isolated from blood samples of metastatic breast cancer patients was Zhang *et al.*[101]. Then, Alix-Panabières group[74] established a permanent cell line from CTCs isolated from a metastatic colon cancer patient that presented a high number of CTCs (≥300 CTC). Since then, many research groups have been working on the development of novel expansion techniques. However very few studies report to have achieved short-term (about 3-30 days)[72,102–104], and long-term cultures (≥6 months)[105]. Therefore, there is still much room for innovation, in order to find new strategies to potentiate cultures of CTCs.

To this end, we focused our attention on the potential role of lipids and fatty acids to improve cell growing to favour the culture and expansion of breast cancer CTCs. It is well-known that lipids are important cellular components involved in several steps related to cell metabolism, through modulation of several physiologic and pathophysiologic processes[106–108]. Some lipids, as for example PC, cholesterol (CH), and ceramide-1-phosphate, have been described to play a role in cell proliferation, tumour growth, survival and metastasis progression[109–114]. Fatty acids, as for example OA, are also related with cancer cell metabolism since they are required for energy storage, membrane proliferation, and production of phosphoglycerides[114]. Indeed, LDs, which are intracellular vesicles constituted by neutral lipids and fatty acids, are important resources of energy and storage[115]. Consequently, LDs are related with cancer metabolism and progression, by acting as energy suppliers[48].

Based on this data, our hypothesis is that by increasing the intracellular concentration of certain lipids it would be possible to stimulate and enhance the survival and proliferation of CTCs. To this purpose, we propose the use of nanotechnology to improve the delivery of these lipids to breast cancer cells. To the best of our knowledge, the use of biocompatible lipidic NPs to support CTC cultures, by improving their proliferation capacity, has not been reported to the date. Among the different types of NPs, O/W nanoemulsions are well studied ones in biomedicine that can be formulated with different oils and lipids. They have the ability to mediate an interaction with cancer cells and improve the intracellular delivery of different encapsulated molecules[116]. Additionally, the composition of nanoemulsions might be conveniently adjusted to have a similar composition to LDs. Consequently, inspired by LDs involvement in tumour progression, we propose the use of nanoemulsions made from bioactive lipids and fatty acids, to improve their intracellular delivery and to support proliferation of CTCs. The workflow followed in this study is represented in **Figure 12**.

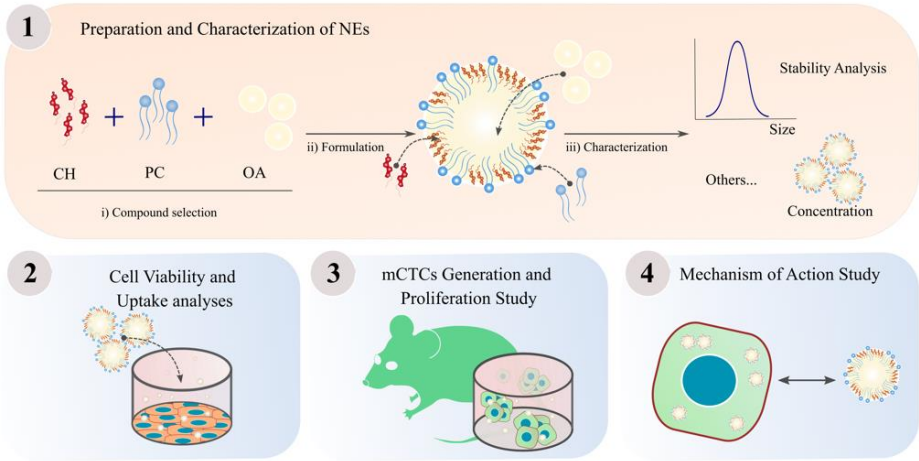

Figure 12. Workflow for the development and characterization of nanoemulsions (NEs) to support culture of breast cancer Circulating Tumour Cells (CTCs). (1) NEs were prepared using a specific combination of lipids and fatty acids, based on previous research. Then, NEs were characterized in terms of their physical and chemical properties; (2) Cell viability studies and uptake analysis were carried out; (3) a CTC model (mCTCs) was generated to validate the proliferative effect of the NEs; (4) NEs mechanism of action, regarding uptake and cytoplasmatic storage of NEs and gene expression analysis.

1.2. Materials and methods

1.2.1. Materials

Lipoid® S100 a soybean PC (18:0/18:1) (94%) was a gift from Lipoid GmbH. OA, CH, phosphotungstic acid, dimethylsulfoxide (DMSO), Mowiol mounting medium, trypsin with EDTA solution, fetal bovine serum, penicillin-streptomycin, Nile Red, Acrodisc® PSF Syringe Filters, progesterone, and β-estradiol were purchased from Sigma-Aldrich. Miglyol812 and Vitamine E (Vit E) were provided by Croda. Ethanol absolute was purchased from Scharlau. Distilled water was deionized using ultrapure Millipore® Direct-Q® 3 with UV system. NucBlue™ (Hoechst 33342 dye), paraformaldehyde (PFA), and alamarBlue™ were purchased from ThermoFisher. Dulbecco's phosphate buffered saline (dPBS), DMEM-High glucose, and RPMI 1640 L-glutamine medium were purchased from Biowest. Milli-Q water (MQ-water) was purified by Millipore® Direct-Q® 3 with UV system. Tissue culture dishes (100mm) and 24-well plates were provided by VWR. Black and white 96-well plates, ultra-low attachment p96, ultra-low attachment p24, and ultra-low attachment flasks were purchased from Corning. White 6 well-plates were provided by SPL Life Sciences. BD Pharmlyse™ lysis buffer and EDTA vacutainer tubes were obtained from BD Biosciences. MammoCult™ Human Medium Kit, EasySep™ Mouse T Cell Isolation Kit, heparin, and hydrocortisone were purchased from STEMCELL™. UltraGRO™ was obtained from AventaCell BioMedical Co. B-27 Supplement (50X) and recombinant basic Fibroblast Growth Factor (bFGF) were purchased from gibco. Recombinant epidermal growth factor (EGF) was provided by Sino Biological.

1.2.2. Cell cultures

All the cell lines used were purchased from Sigma-Aldrich. The human breast cancer MCF-7, MDA-MB-231 cell lines were cultured in DMEM-High glucose medium, whereas HCC1143 cells were cultured in RPMI-1640. Both, DMEM-High glucose and RPMI-1640 were supplemented with 10% fetal bovine serum and 1% penicillin-streptomycin. The cells were

cultured at 37 °C in a humidified atmosphere containing 5 % CO_2. At 85 % confluence, cells were harvested using 0.05 % Trypsin-EDTA (5 min, 37 °C).

1.2.3. Formulation of nanoemulsions

Nanoemulsions were prepared at 1mL scale by low-energy spontaneous emulsification O/W method. Briefly, stock solution of OA (100 mg/mL), PC (10 mg/mL), and CH (10 mg/ml), were prepared in ethanol and mixed in different ratios from 10:1:1 to 40:1:1 to prepare the organic phase for four different nanoemulsions. Then the organic phase (100 µL) of each mix was quickly injected into the deionized water (900 µL), under magnetic stirring at room temperature. After 15 minutes stirring was stopped and the four nanoemulsions were obtained. To obtain the nanoemulsions from **section 1.3.5** of this chapter, instead of OA, miglyol 812 or Vit E at ratio 10:1:1 were used separately. Based on their suitable properties, formulation of nanoemulsions at ratio 10:1:1 (using OA) was chosen for the rest of the study, from now on referred to as NEs. **Figure 13** shows schematically how to prepare the NEs. Formulations were stored at 4 °C and analysed after more than one year to determine their shelf-life (long-term stability study). Moreover, the short-term stability of the NEs was determined by centrifuging 600 µL at 3,000 rpm. Stability of the different formulations were tested by analysing droplet size, cracking, creaming, and phase separation before and after centrifugation (**Supporting Figure S1**).

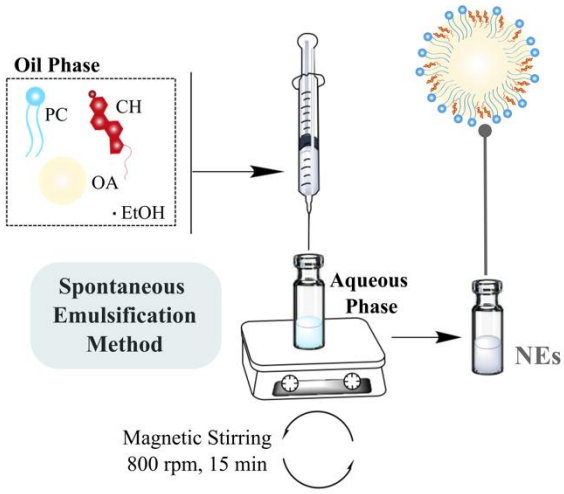

Figure 13. Formulation of the nanoemulsions (NEs). The oil phase (containing phosphatidylcholine (PC), cholesterol (CH), and oleic acid (OA) dissolved in ethanol (EtOH)) is added to the aqueous solution (MQ-Water). Then magnetic stirring is used to set up tiny convection currents to distribute oil droplets in bulk.

1.2.4. Characterization of nanoemulsions

Size and PdI of the nanoemulsions were measured by DLS using Malvern® Zetasizer® (Nano ZS90, Malvern). ζ-potential was determined using zeta cells (Malvern). All measurements were taken using a 1:100 v/v dilution ratio in MQ-water. The critical quality attributes (CQAs) of nanoemulsions were established based on previous knowledge, and recommendations (**Table 2**). TEM measurements were done on a Philips CM20 microscopy at an acceleration voltage of 100 kV. For the preparation of the samples, NEs were previously stained with phosphotungstic acid MQ-water: phosphotungstic acid (1:10); then a drop of the dispersion was placed on Cu grid, letting the liquid evaporate at room temperature. Nanoparticle Tracking Analysis (NTA) was performed in a NanoSight instrument (Malvern), measurements were done in water at room temperature with a dilution factor of 1 X 10^3.

Table 2. Critical Quality Attributes (CQAs) of the nanoemulsions.

CQAs	Target	Justification	Ref.
Particle Size	20 – 200 nm	The mean droplet diameter in nanoemulsions	7
PdI	≤ 0.2	Physicochemical properties that guarantee reproducibility	17
ζ-potential	–60 to +60 mV	Adequate values to ensure a longer stability	117

To determine the composition of the NEs, HPLC and NMR were performed by the *Centro de Apoyo Científico-Tecnológico* (CACTUS) at the University of Santiago de Compostela. High-performance liquid chromatography/electrospray ionization tandem mass spectrometry (HPLC-ESI-MS) analysis was performed using a HPLC 1200-ESI-QTOF-MS (Agilent G6410B). Standard were added by syringe injection and separation was performed in a Zorbax Eclipse XDB-C18 column (4.6x150mm and 5 μm particle size). Liquid chromatographic analysis was carried out using a flux of 1 mL/min in isocratic conditions with water: methanol: ammonium at 0.15 %. To perform HPLC analysis the samples were prepared by dissolving the NEs in ethanol (1:12). Nuclear Magnetic Resonance (NMR) experiments were conducted on a Bruker NEO 17.6 T spectrometer (proton resonance 750 MHz) (Agilent), equipped with a 1H/13C/15N triple resonance probe and shielded PFG z-gradient at 25 °C. The spectrometer control software was TopSpin 4.x. For samples prepared in H_2O, free of ethanol (for PC, CH, and OA the solvent used was Methanol-d4 (CD3OD)), proton spectra (1H) was measured with the 1D NOE with presaturation sequence (sequence *noesygppr1d* of the Bruker library) during the prescan delay for the suppression of the HDO peak at ~4.7 ppm. Proton diffusion filtered spectrum (1HD Dfilter spectrum) was measured for NEs sample with the bipolar-gradient stimulated echo sequence incorporating Longitudinal Eddy Current Delay and presaturation (BPP-LED-STE experiment, sequence *ledbpgppr2s1d* of the Bruker library). All the spectra were processed with MestreNova software v12.0 (*Mestrelab Research Inc.).* The chemical shifts were referenced automatically with respect to the deuterium lock. A

diffusion ordered spectroscopy (DOSY) spectrum was measured according to Segredo-Morales[118]. After Fourier transformation in the ^{1}H dimension, several peaks were selected for the analysis of the self-diffusion coefficient. In each case the peak intensity along the diffusion dimension was fitted to the mono-exponential Stejskal-Tanner equation using software Origin 8.0 (*Originlab inc.*) to determine the self-diffusion coefficient.

1.2.5. *In vitro* cell proliferation studies

Cells were seeded in 96-well culture plates using two concentrations: 1 x 10^3 cells/well in the case of cell seeding at low-density experiments and 5 x 10^3 cells/well in case of the rest, in 90 µL of media and were let to adhere overnight at 37 °C in a 5% CO_2 atmosphere inside an incubator. (a) For the study of the effect in proliferation at different NEs concentrations, HCC1143, MDA-MB-231 and MCF-7 cells were incubated within the range of NEs selected for 24h. (b) For the study of the free compounds addition, OA, PC, and CH were dispersed in MQ-water at the same concentration as the one used with NEs, added directly to HCC1143 cells and cultured for 24h. (c) Otherwise nanoformulations ($2.14x10^9$ nanoparticle/mL (NP/mL) per well) were added to the cells dispersed in 10 µL of cell medium. Then cells were let to interact with NEs for 4h, 24h, 48h, and a total of 4 days in the case of low-density seeding experiments. For all the experiments after the incubation time, cells were washed twice with fresh cell medium. Next, 100 µL of fresh media and 10 µL alamarBlue™ were added to each well and incubated for 3 h at 37 °C in a 5% CO_2 atmosphere. Finally, 100 µL of the solution from each well was transferred to a new black 96-well plate and fluorescence was read on FLUOstar OPTIMA (BMG LABTECH) multimode plate reader (fluorescence excitation wavelength, 544 nm and fluorescent emission wavelength, 590 nm). Experiments were performed in three independent repeats. In all the experiments data was normalized using control cells.

1.2.6. Nile Red lipid droplet staining

Experiments were performed using confocal microscopy and flow cytometry. MDA-MB-231, MCF-7 and HCC1143 cells were grown into 24-well plates (seeded $3.2x10^4$ cells/well) for confocal microscopy analysis, and in 12 well-plates (seeded $8x10^4$ cells/well) for flow cytometry experiments, in both cases cells were let to attach overnight. Afterward, the NEs were added ($3.35x10^9$ NP/mL per well in confocal microscopy experiment and $2.14x10^9$ NP/mL per well in flow cytometry analysis) and let to interact for 4 hours. After this time, cells were washed twice with PBS and fresh media was added. Before staining, Nile Red was dissolved in DMSO (1mg/mL) and then filtered using 0.2 µm syringe filter. Then Nile Red was diluted in the corresponding cell culture media at 1 µg/mL per well. Afterward cells were incubated with the lipid dye at 37 °C, 5% CO_2 for 20 min. For flow cytometry experiments, after that, samples were washed and detached using trypsin to finally be dispersed in 1x PBS. Later, fluorescence intensity was measured using a BD FACS AriaIIu (BD, Bioscience). For MDA-MB-231 cell line, measurements were also done at 24 and 48 after NEs addition. Flow cytometry experiments were done in three independent repeats. For confocal microscopy images, the same lipid staining protocol for flow cytometry experiments, was also employed. Afterward, cells were washed with PBS and fixed with 4% cold PFA in PBS for 15 min. NucBlue™ (Hoechst 33342 dye) was used for nucleus staining. After fixation, coverslips were mounted with Mowiol and analysed by confocal microscopy (Leica TCS SP5 X) for Nile Red (yellow emission 590-620 nm and red emission 638-700 nm) and for Hoechst 33342 (414-479 nm); using the objective HCX PL APO CS 63.0x1.30.

1.2.7. Orthotopic mouse xenograft to generate a CTC-Model (mCTCs)

This part of the work was performed in collaboration with the modelling line of the Roche-Chus joint unit. Mice experimental protocols were approved by the Ethical Committee of the University of Santiago de Compostela (15010/2015/001). Mice were housed in the animal facility at

the Center for Research in Molecular Medicine and Chronic Diseases (CiMUS, University of Santiago de Compostela) and given food and water ad libitum, in accordance with CiMUS guidelines (ES150780275701). SCID beige mice were obtained from the Barcelona Biomedical Research Park (PRBB, Barcelona). After mice arrival and before carrying out the experiments, at least one week of acclimation was considered. For these experiments, triple negative MDA-MB-231 cells were used, which stably expressed the enhanced green fluorescent protein (eGFP) and the luciferase gene (MDA-MB-231$^{eGFP\text{-}Luc}$). The researchers in charge of the modelling line of the Roche-CHUS joint unit orthotopically injected MDA-MB-231$^{eGFP\text{-}Luciferase}$ cells ($2x10^6$ cells) into the mammary fat pad of the mice and allowed to grow into macroscopic tumour and form metastasis. Tumour and metastasis development were followed by bioluminescence signal in the IVIS spectrum system after intraperitoneal luciferin injection. Once metastases were established, mice were sacrificed and blood was extracted by cardiac puncture to isolate MDA-MB-231$^{GFP\text{-}Luciferase}$ CTCs, similar to previous protocols[119,120].

Since here, we proceeded to lyse the blood from one mouse orthotopically injected. EasySep™ Mouse T Cell Isolation Kit (StemCell technologies) was used for CTC isolation. Then, we generate a stable CTC cell line (from now on referred to as mCTC) by protocols established in our research group. Afterward, isolated cells were seeded in a 96-well low attachment culture plate in a final volume of 200µL of Mammocult™ supplemented media (heparin (0.8 µg/mL), hydrocortisone (0.05 µg/mL), bFGF (20ng/mL), EGF (0.04 µg/mL), B27 (4% (v/v)), progesterone (0.4 µg/mL), β-estradiol (0.4 µg/mL), UltraGRO^{TM} (5% (v/v) and pen/strep (1% (v/v)) to propagate the cell culture. Then, sample was initially cultured under hypoxia conditions and maintained in a humidified atmosphere at 37 °C for one week, replacing media every two days. After a week, the culture was removed from hypoxia and subcultured to a 24-well low attachment culture plate and Mammocult™ supplemented media. Under these conditions, mCTC grew indefinitely, forming aggregates in suspension.

1.2.8. *In vitro* experiments with the mCTCs

The mCTCs generated from MDA-MB-231$^{eGFP\text{-}Luciferase}$ murine model, were grown in ultra-low attachment 24 well-plates in a final volume of 1 mL DMEM-High glucose complete medium (seeded at $10x10^3$ cells/well). Afterward the NEs ($6.7x10^8$ NP/well) were added to the cultures and were maintained in a humidified 95 % O_2, 5 % CO_2 atmosphere at 37 °C during 9 days since the cell seeding. The number of NEs added was settled based on the concentration in the cell viability experiments for MDA-MB-231 cell line, considering the number of cells seeded and the final volume of medium per well. Cell media was added to the cultures every 2 days and in the case of the treated cells, fresh NEs were added with the new medium. On the last day of the experiment cells were collected and counted using a hemocytometer (Neubauer Chamber).

1.2.9. Gene expression analysis

The mCTCs from the *in vitro* experiment (9 days in DMEM-HG) were used for the genetic expression analysis. AllPrep DNA/RNA Mini Kit was used for RNA extraction (mCTCs treated with NEs and mCTCs controls (without NEs)), following the manufacturer's protocol. An amount of 11 µL of total RNA were retrotranscribed into cDNA with SuperScript III. Samples were preamplified with Taqman Preamp Master Mix. Gene expression analysis for a custom panel of 13 genes (**Table 3**) was performed with probes and Master Mix TaqMan on a LightCycler 480 II (Roche Diagnostics). The relative expression was calculated considering *B2M* as a reference gene. To compare gene expression data between control cells and cells treated with NEs, relative normalized expression was calculated using $2^{-\Delta\Delta CT}$.

Table 3. Probes of the listed genes for Gene Expression Custom Panel and their functional gene grouping.

TaqMan Probes	Reference	Functional Gene Grouping
ALDH1A1	Hs00946916_m1	Stem cell-like phenotype
BCL11A1	Hs01093197_m1	Stem cell-like phenotype
CCND1	Hs00765553_m1	Proliferation/Cell cycle regulation
CD36	Hs00169627_m1	Cell metabolism
E2F4	Hs00608098_m1	Proliferation/Cell cycle regulation
EpCAM	Hs00158980_m1	Epithelial
GDF15	Hs00171132_m1	Proliferation/Cell cycle regulation
Ki67	Hs00171132_m1	Proliferation/Cell cycle regulation
PALB2	Hs00226617_m1	Breast cancer associated
PROM1	Hs01009257_m1	Stem cell-like phenotype
SNAI1	Hs00195591_m1	EMT
VIM	Hs01675818_s1	EMT
B2M	Hs00187842_m1	Housekeeping gene

1.2.10. Cells and NEs interaction study by TEM

MDA-MB-231 cells were grown in 6 well-plates (seeded $3x10^5$ cells/well) and incubated at 37 °C in a humidified atmosphere containing 5 % CO_2. The NEs were added 24 h post-seeding to a final concentration of $2.14x10^9$ NP/mL per well and incubated for 4 h. After incubation, cells were washed twice with dPBS. The analysis was carried out at times: 4 h, 24 h and 48 h post-addition of the NEs, so at the corresponding time cells were detached using 0.05 % trypsin-EDTA solution. Cells were fixed with a mixture of 2.5 % (weight per volume [w/v]) glutaraldehyde, 7mM ClK, 1.24 mM $CaCl_2$, and 2.48 mM Cl_2Mg in 0.05 M cacodylate buffer for 3 hours at 4 °C. Post-fixation was carried out using 1 % O_4Os in 0.1 M cacodylate buffer, followed by embedding in 2 % agarose. Samples were dehydrated by immersion in an increasing gradient of ethanol. Then, were embedded in Epon. Ultrathin sections were cut using an ultra-microtome (Leica Ultracut UCT). Grids were stained with 1 % uranyl acetate and Pb-citrate. Finally, the sections were examined with a TEM (JEOL JEM 1011) from the *Centro*

de ApoyoCientíficoTecnológico (CACTUS) at the University of Santiago de Compostela.

1.2.11. Statistical analysis

The significance of differences was assessed by unpaired t test and one-way analysis of variance (one-way ANOVA). Statistical analysis was performed with GraphPad Prism software, using one-way ANOVA for comparison of more than two groups. Student's t test was used for the comparison of the two groups. *p* values of less than 0.05 were considered significant.

1.3. Results and discussion

1.3.1. Selecting the composition of the nanoemulsions to induce proliferation in breast cancer cells

Cancer cells show enhanced lipid avidity by mainly two pathways: i) by increasing the uptake of exogenous lipids, and ii) by upregulating the lipid synthesis. Therefore, we propose a way to increase the lipid content, using the first described mechanism (i) to increase cell proliferation in *ex vivo* cell cultures. Taken this into account and after an extensive bibliographic research, OA, PC, and CH were selected due their reported role in cancer: cell proliferation, survival, angiogenesis, and migration[121–123]. More in detail, the role of OA in cancer cell growth, metastasis[124,125], and in migration of MDA-MB-231 breast cancer cells, was previously described[126]. PC was also chosen due to its specific role in supporting proliferation and survival of MCF-7[127,128]. Finally, CH was selected based on previous works describing the capacity of 27-hydroxycholesterol (a CH metabolite) to stimulate cell proliferation via ERß in prostate cancer cells[129]. A part from that, CH is critical for membrane structures[46].

However, it is well known that long fatty acids, as OA, are poorly internalized by cells due to their hydrophobicity[130,131]. Therefore, previous studies have proposed the formation of OA:bovine serum albumin (OA:BSA) complexes with the aim of promoting its internalization into the cells[44]. In a similar line, we propose developing a formulation with these compounds using nanotechnology.

1.3.2. Formulation and characterization of nanoemulsions

As showed in **Table 4**, different NEs were formulated, using an increasing concentrations of OA (OA:PC:CH ratios were from 10:1:1 to 40:1:1). Particle size increased linearly in OA concentration manner. Data agrees with previous works where the mean size of NEs were dependent on the concentration of emulsifiers and oil present in the formulation[132,133]. However, ζ-Potential values remained constant (from -31.40 to -33.60 mV). The negative surface charge could be explained by OA and PC, which have

a negative charge at the polar heads. Related to PdI, NEs_1 prepared at a ratio 10:1:1 presented the lowest value, and therefore better homogeneity. It was in accordance with CQAs (**Table 2**).

Table 4. Characterization of the nanoemulsions formulated using different OA:PC:CH ratios.

Nanoemulsion sample	OA:PC:CH ratio	Particle size (nm)	PdI	ζ-Potential (mV)
NE_1	10:1:1	175.90 ± 4.06	0.21 ± 0.02	-32.20 ± 1.30
NE_2	20:1:1	281.30 ± 6.80	0.23 ± 0.04	-31.40 ± 0.61
NE_3	30:1:1	377.00 ± 13.57	0.25 ± 0.06	-33.60 ± 0.47
NE_4	40:1:1	482.20 ± 17.28	0.35 ± 0.06	-31.40 ± 0.91

Due to NE_1 presented the most optimal values, this formulation was chosen as the best option for carry on with the study, from now on referred to as NEs. NEs were physical characterized using different methods as are presented in **Figure 14.**

A

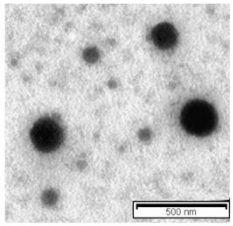

B

Method	Particle Size (nm)	Concentration (NPs/mL)
DLS	175.90 ± 4.06	-
NTA	134.60 ± 34.30	$1.34x10^{11}$
TEM	163.61 ± 16.10	-

Figure 14. Physic characterization of the NEs. (A) Image of the NEs with the TEM equipment; (B) Table summary of the mean size values of the NEs measured by the three techniques: DLS, TEM and NTA.

Then, to determine if all compounds included in the formulation preparation were efficiently included into the NEs, NMR and HPLC-ESI-MS analyses were performed. Starting for the NMR study, proton spectrums for each compound (CH, PC, and OA) were extracted. Then, integrated peaks were assigned to peaks in the NEs sample spectrum. **Figure 15** shows that in case of the CH, it was not available to perform the integration due to

its peak overlapped with PC and OA. Nevertheless, PC and OA were confirmed as part of the NEs formulation.

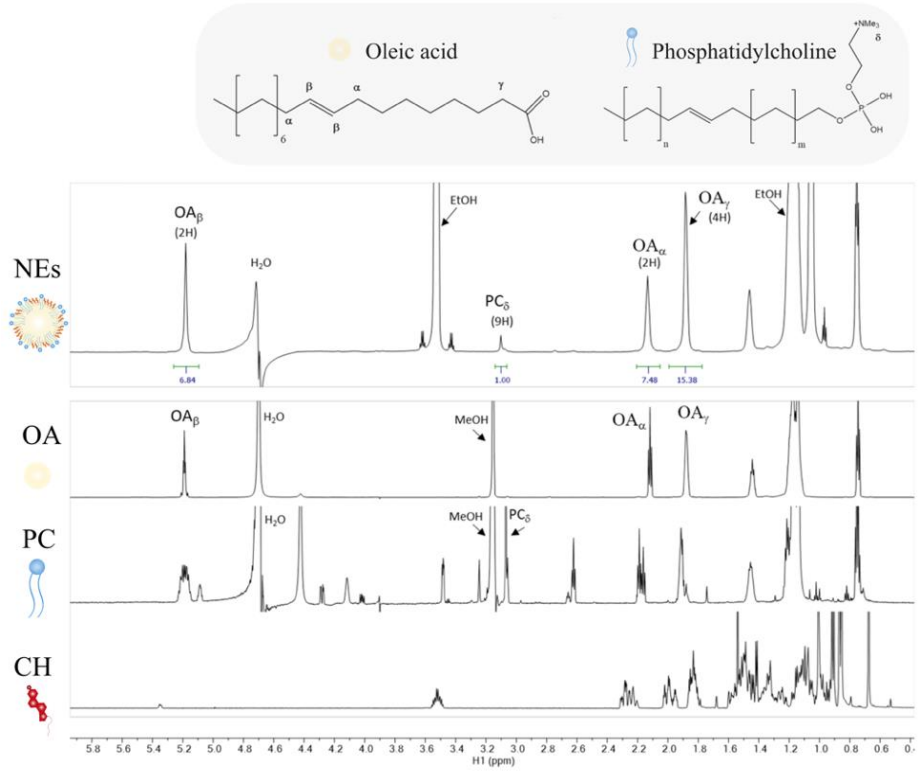

Figure 15. NMR spectrums of NEs analysis. 1H Dfilter spectrum of NEs and 1H spectrums of the standard stocks (OA, PC, and CH). At the top of the figure is represented chemical groups and number of hydrogens that correspond to the peaks highlighted on the spectrums. Methanol (MeOH) and Ethanol (EtOH) refer to the solvents used.

Due to the difficulty to determine the presence of CH by NMR, HPLC-ESI-MS analysis was performed. Firstly, NEs were centrifuged to remove all compounds that were free in the solution. Then, standard stocks (PC, CH, and OA solutions at the same concentration of the final solution) were analysed and extracted the ions of each one. Subsequently, to identify the ions extracted from the previous standard stocks, an EIC (Extracted Ion Chromatogram) was obtained for the NEs sample. It was confirmed that CH and PC were included in the formulation, because peaks of the standard

stocks (CH: *m/z* 369 (loses -OH) and PC: *m/z* 782) were found in the NEs sample **(Figure 16)**. Moreover, DOSY NMR analysis was carried out in the same sample. Then, based on analysis of the self-diffusion coefficient it was possible to verify that all the compounds detected by NMR belong to a bigger structure which correlates with a nanoemulsion (**Supporting Figure S2**).

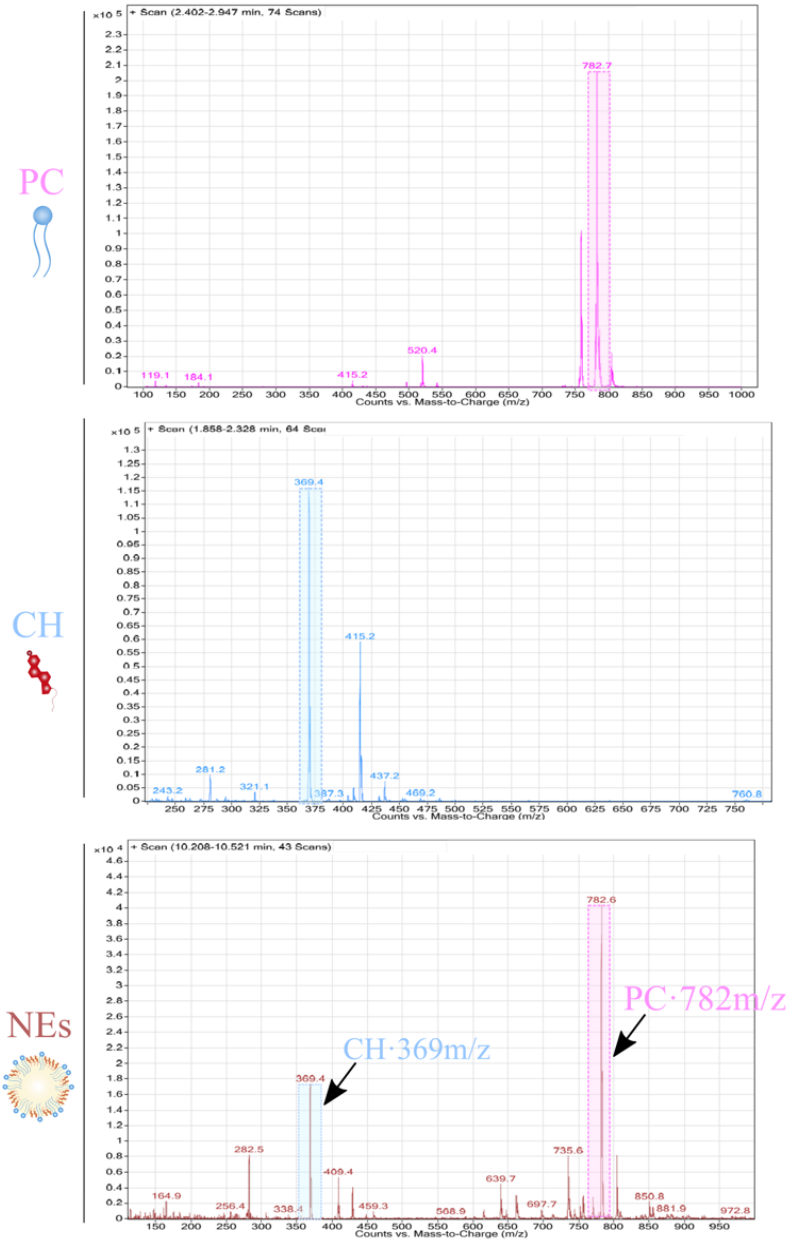

Figure 16. HPLC-ESI-MS spectrums of NEs analysis. Mass peaks extracted from the standards of cholesterol (CH) (*m/z* 369 (loses -OH)) in blue and phosphatidylcholine (PC) (*m/z* 782) in pink, appear in the NEs sample spectrum.

1.3.4. Short-term and long-term stability studies

Two different studies were performed in order to obtain information related to the stability of NEs.

First, a centrifugation stability analysis at room temperature of NEs was carried out. We determined that centrifugal stress had minimal effect on the NEs stability (**Figure 17)**. This might be explained by the rigidity that CH emulsifiers provide to the NEs, as reported for other formulations such as liposomes[134].

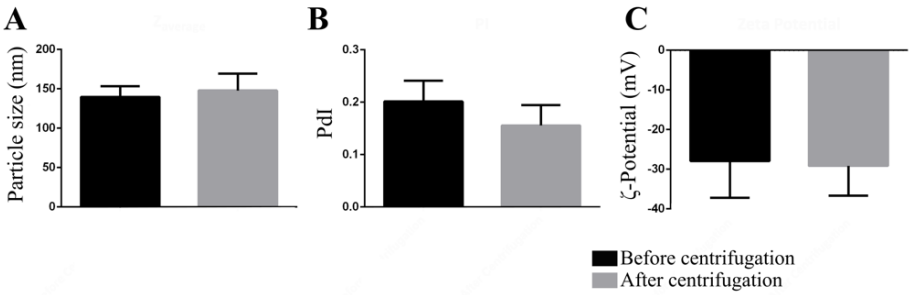

Figure 17. Short-term stability of NEs at room temperature. Values of (A) the particle size, (B) the PdI, and (C) the ζ-Potential. Values represent mean ± SD (n= 4), in black before centrifugation and in grey after centrifugation process.

Due to 4ºC is the usual storage conditions for buffers at laboratory, the second analysis was to determine the long-term stability of NEs; the period monitored was 17 months. It was determined that NEs were stable for at least 6 months at 4ºC, according to particle size, PdI and ζ-Potential **(Figure 18)**. Whereas PdI and ζ-Potential values were stable during the 17 months, particle size value decreased at the last point measured. This observation could be related to the oxidation of the lipids[135,136]. The reduction in the particle size may had started a few months earlier, although having only measured three longitudinal points, it cannot be confirmed. To try to solve this oxidation in the future, a reduction in the concentration of oxygen present while storing must be achieved. For instance, by packing the NEs under vacuum or nitrogen [137].

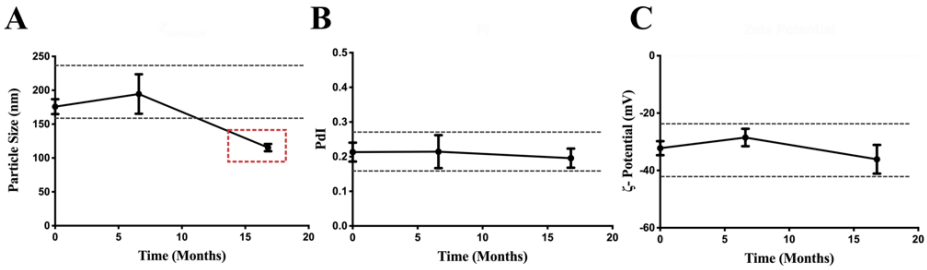

Figure 18. Long-term stability of NEs at 4ºC. Evolution of (A) the particle size, (B) the PdI, and (C) the ζ-Potential of NEs. Grey lines indicate the range within values of each parameter were found and red box highlights the time point where a reduction in the particle size was observed. Values represent mean ± SD (n = 4).

1.3.5. Cell viability studies and uptake analysis of NEs

Cell viability studies after the addition of NEs were performed to choose the optimal working concentration. Three breast cancer cell lines (triple negative HCC1143, triple negative MDA-MB-231, and luminal MCF-7) were chosen because their different molecular subtype and growth rate characteristics[138]. **Figure 19A** shows an increase in cell viability in the three cell lines as a result of adding NEs to the cell medium. It is observed that between the three cell lines, HCC1143 viability achieved higher values than the rest. This cell line reached its highest point of viability at a final concentration of $2.68x10^9$ NP/mL. Strangely enough, HCC1143 was the only one that presented a decreasing trend from this mentioned concentration. Therefore, as it is presented in **Figure 19A**, NEs resulted toxic in HCC1143 when concentration was higher than $4.02x10^9$ NP/mL (<50 % cell viability). This toxicity was not observed in MDA-MB-231 or MCF-7, although at the highest NEs concentration ($5.36x10^9$ NP/mL) there was a decline in their cell viability (**Figure 19A**). These observations may be related to the fact that HCC1143 presents a duplication time almost twice the other two (2.3 vs 1.2 days)[138]. Hence, its growth rate could make more sensitive this cell line to NEs.

Based on this data, the NEs concentration chosen for the following experiments was $2.14x10^9$ NP/mL. This concentration that shows excellent cell viability results should be the one used in consecutive additions in short-

term cultures, avoiding toxicity. The increase in cell viability observed in breast cancer cells when cultured with NEs can be attributed to the energy supply arising from their components that somehow increases the metabolic activity of the cells.

In order to evaluate the uptake of the NEs, we performed confocal microscope and flow cytometry analyses using the previous three breast cancer cell lines. Taking into account that our NEs are made of lipids and fatty acids, the lipophilic dye called Nile Red was used for both analyses. This fluorescent dye is characterized by different emission depending of the hydrophobicity of the lipids (red emission is related to polar lipids, whereas yellow is related to neutral lipids, which are usually present in LDs[139]). In this study, cell lines were incubated with NEs for 4h. In case of confocal microscopy analysis, a higher content of neutral lipids was observed in NEs treated cells at 4h of incubation, compared to their respective negative control (untreated cells), (**Figure 19B**). Whereas MDA-MB-231 negative control cells presented yellow emission, controls of HCC1143 and MCF-7 did not. This indicated a different basal level among the studied cancer cell lines. Related to red emission (**Supporting Figure S3**), it was observed that stayed at the same label with or without NEs treatment. With the aim of quantifying the increase in intracellular lipids and OA delivered, we performed flow cytometry analysis at the same time (t4 (h)). As can be seen from **Figure 19C**, the intracellular lipid content was doubled after NEs treatment in the three breast cancer cell lines. This is reflected by the fold change of two in fluorescence intensity normalized to their negative controls. These results altogether indicate that the enhanced cell viability in treated cells is due to an increase in the LDs content, giving by an effective uptake of the NEs.

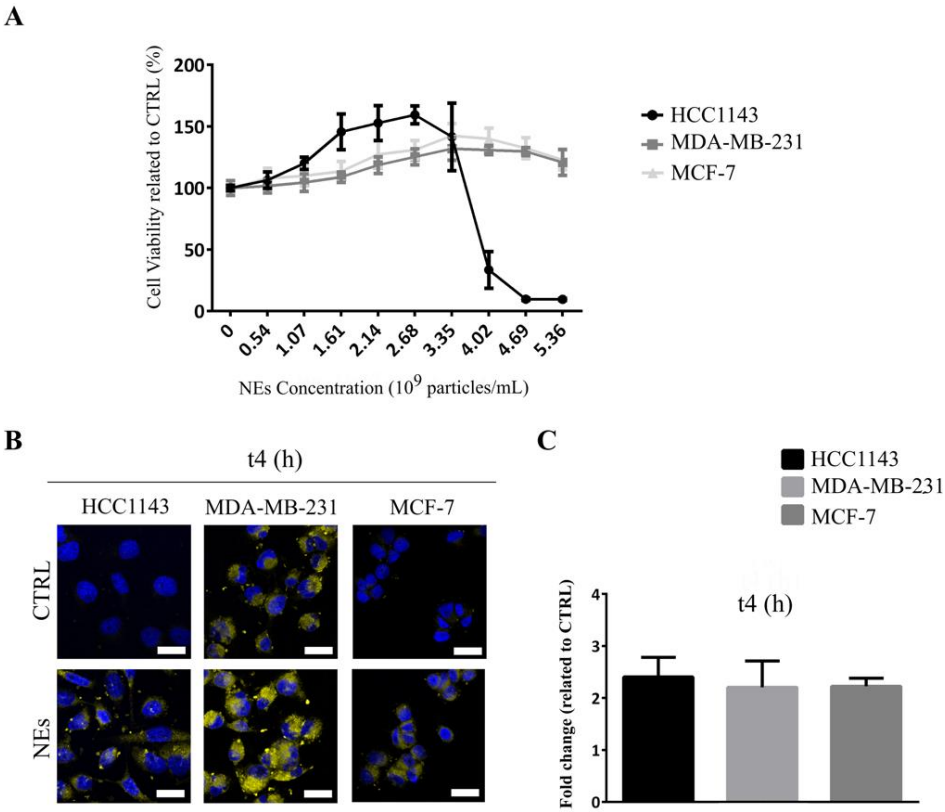

Figure 19. Toxicity analysis of NEs concentrations and uptake of NEs in breast cancer cell lines. (A) Cell viability study towards the three cell lines after 24h of incubation at different concentrations. Results are expressed in percentage related to their negative controls (CTRLs). Values represent mean ± SD (n=3); (B) Confocal microscopy images of lipid content stained by Nile Red after 4h of NEs incubation. Stained neutral lipids are in yellow and cell nuclei are in blue. Size bars represent 25µm; (C) Flow cytometry results of stained lipid content using Nile Red. Results are expressed in fold change values (relative to their corresponding CTRLs). Values represent mean ± SEM (n = 3).

In order to verify that the increment in cell viability observed was a consequence of the chosen compounds formulated as NEs, we performed two additional studies. To this end, we only used HCC1143 cell line, because was the one that previously presented the strongest effect after 24h of incubation with NEs (**Figure 19A**).

For the first experiment, solutions of the three different compounds used for the NEs formulation (alone or mixed) were used at the same final concentration of the one in NEs samples. As **Figure 20** shows, the increase in cell viability is observed in NEs condition only ($p < 0.0001$). It is important to highlight that the mixed compounds (CH+OA+PC) did not achieve the effect of the same combination but formulated as NEs. This experiment demonstrates that the concentration of OA and PC required in the NEs is much lower than the one necessary to achieve the same effect on viability, when used as free compounds[125,127].

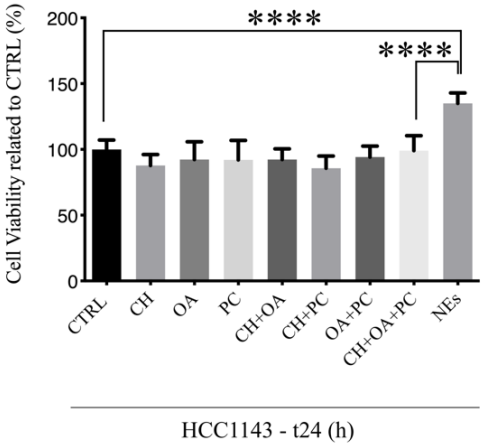

Figure 20. Cell viability analysis in HCC1143 after the addition of the free compounds, their combination, as well as the three compounds formulated as NEs (24h of NEs incubation). Combination of different compounds are indicated as (+). Values represent mean ± SD (n = 3). Statistical comparison was performed using an ordinary two-way ANOVA. Statistical differences are represented as **** ($p < 0.0001$) and *** ($p < 0.001$). CH = Cholesterol, OA = Oleic Acid, PC = Phosphatidylcholine.

Likewise, for the second experiment, we wanted to validate that the effect observed was due to the composition chosen and not because of an easier uptake effect due to be a NP. To this end, three different formulations with similar properties were made changing the compounds, but at the same final concentration (**Figure 21A and B**). As indicated in **Figure 21A**, VitE-NEs and Mygliol-NEs were formulated with the same surfactants (PC-CH), but different oil cores (instead of using OA, Vitamin E and Mygliol 812

were used, respectively). **Figure 21C** shows that the increment in the cell viability only was achieved in case of NEs treatment ($p < 0.0001$); other formulations did not support a rise in viability.

Overall, it is demonstrated that both parameters, the composition (CH, PC, and OA) and use nanoemulsion as delivery vehicle, result beneficial for increasing cell viability. This effect is probably related to their role in cell metabolism and proliferation of cancer cells[124–129140–144].

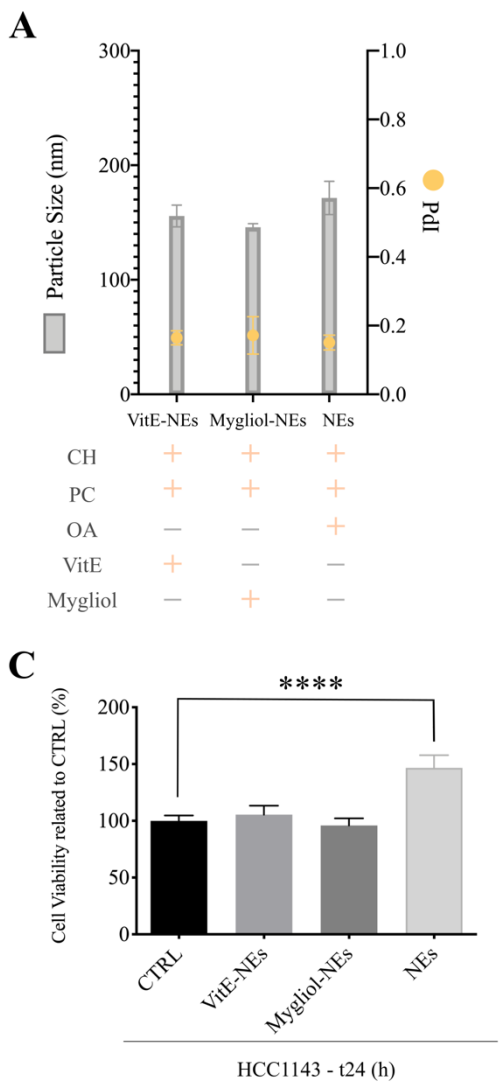

Figure 21. Different nanoemulsions characterization and ther associated cell viability studies at 24h NEs incubation. Values of (A) the particle size and the PdI, and in (B) the ζ-Potential are indicated. Values represent mean ± SD (n=3); (C). Values represent mean ± SD (n = 3). Test of cell viability in HCC1143 treated with different nanoemulsions. Statistical comparison was performed using an ordinary two-way ANOVA. Statistical differences are represented as **** ($p < 0.0001$). CH = Cholesterol, OA = Oleic Acid, PC = Phosphatidylcholine, VitE = Vitamin E, and SM = Sphingomyelin.

Lastly, since the final aim of NEs development is to support CTC culture over time, we wanted to prove the ability of NEs to maintain their positive effect in terms of cell viability increment. Therefore, a low-density seeding of the three previous cell lines (HCC1143, MDA-MB-231, and MCF-7) were plated and allowed to attach overnight. Then, their cell viabilities were monitored by alamarBlue™ over 4 days, adding NEs at time 0 and 2 days (24h and 72h after the seeding). **Figure 22** shows that at one of the earliest time points (t3h after NEs addition), the effect of rising cell viability is already observed. Moreover, after every NEs addition there is an increasing trend of cell viability in every cell line. Above all, it is important to highlight that cell viability percentage is always above the 100 % (related to negative controls). Generally, **Figure 22** represents that the effect observed at t3 h, continued at 1 day after, where it is appreciated a slightly downward trend. Then, when new NEs are added, as previously mentioned, an upward trend it is observed, so the positive effect can be re-established. Strangely enough, the cell viability of MDA-MB-231 cell remain constant (the decreasing trend observed in the rest was not seen). A possible explanation for this quick observable effect might be referred to the lipid metabolism of breast cancer cell lines. AlamarBlue™ measures viability based on the reduction of its active ingredient, resazurin, which can be reduced by NADPH and NADH[145]. Therefore, as a consequence of the enhanced FAO, which is involved in NADPH production and accumulation in cells[57], (**Figure 9, Introduction)**, what we might be observed in our experiments is the reduction of resazurin due to abundant presence of NADPH and NADH in treated cells compared to cells without NEs.

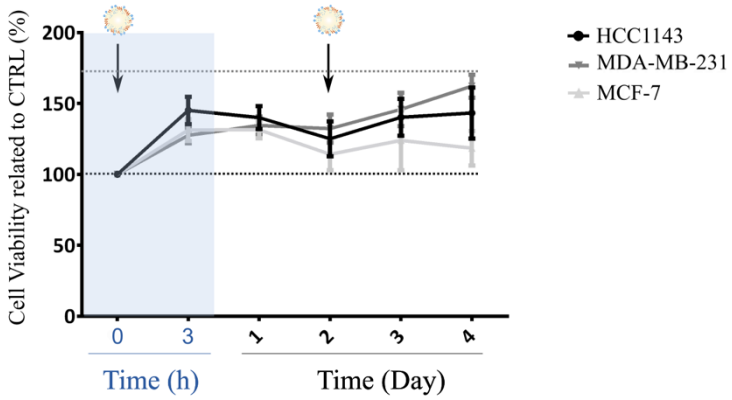

Figure 22. Cell viability analysis in breast cancer cell lines in 4 days culture with NEs additions. HCC1143, MDA-MB-231, and MCF-7 were seeded, let overnight to let to attach, and then NEs were added in two occasions (t0 and t2 (days)). NEs additions are indicated by arrows. Values represent mean ± SD (n=3).

1.3.6. Validation of the effect in cell viability of NEs using the CTC-derived cell line (mCTCs)

To determine the NEs effect in improving the proliferation of CTCs, we established a CTC-derived cell line (mCTCs). To this end, the researchers in charge of the modelling line of the Roche-CHUS joint injected MDA-MB-231$^{eGFP\text{-}Luciferase}$ cells into the mammary fat pad of immunosuppressed mice. Then, metastases were detected 2 months later, and mice were sacrificed. From the blood of one mouse, MDA-MB-231$^{eGFP\text{-}Lucifersase}$ were isolated, we processed the samples using the EasySep^{TM} Mouse T Cell Isolation Kit. MDA-MB-231$^{eGFP\text{-}Luciferase}$ CTCs were expanded in culture. Due to the generation of mCTCs, it was observed that cells grew in suspension mainly forming clusters and for an unlimited time.

Consecutively, to prove the proliferative effect of NEs in the mCTCs (a model closer to CTCs), cells were grown in suspension using the conditions previously mentioned. For this study the parental cell line (MDA-MB-231$^{eGFP\text{-}Lucifersase}$) and mCTCs were used for a cell culture of 9 days. NEs were added every two days (6.7 x 10^8 NP/mL) while cell media was refreshed. As **Figure 23A** shows, for both cases, parental cell line and

mCTCs, cells treated with NEs presented a higher density of cells ($p < 0.01$ and $p < 0.0001$, respectively) at the last point (9^{th} day) of the experiment. Importantly, when cells were counted, we found a percentage of proliferation (related to negative controls) close to 36% in mCTCs treated with NEs **(Figure 23B,** $p < 0.01$**)**. Curiously, in the parental cells treated with NEs, the final cellular density was almost the same as the seeding density, whereas negative control cells presented a decline of almost half.

Taken together, these results suggest that NEs presents a beneficial effect in parental cell lines, promoting survival of these cells when cultured in *non*-adherent conditions. In case of mCTCs, a proliferation effect is observed in cells treated with NEs. It is important to highlight that both cells have different standard culture conditions, specifically the parental cell line grow in adherence while mCTCs cell line does in suspension. Consequently, for the parental cell line there is an extra difficulty for their growth. Altogether, our data proves that NEs maintain cell survival under adverse cell culture conditions (observed in parental cell line), as well as increase proliferation of mCTCs.

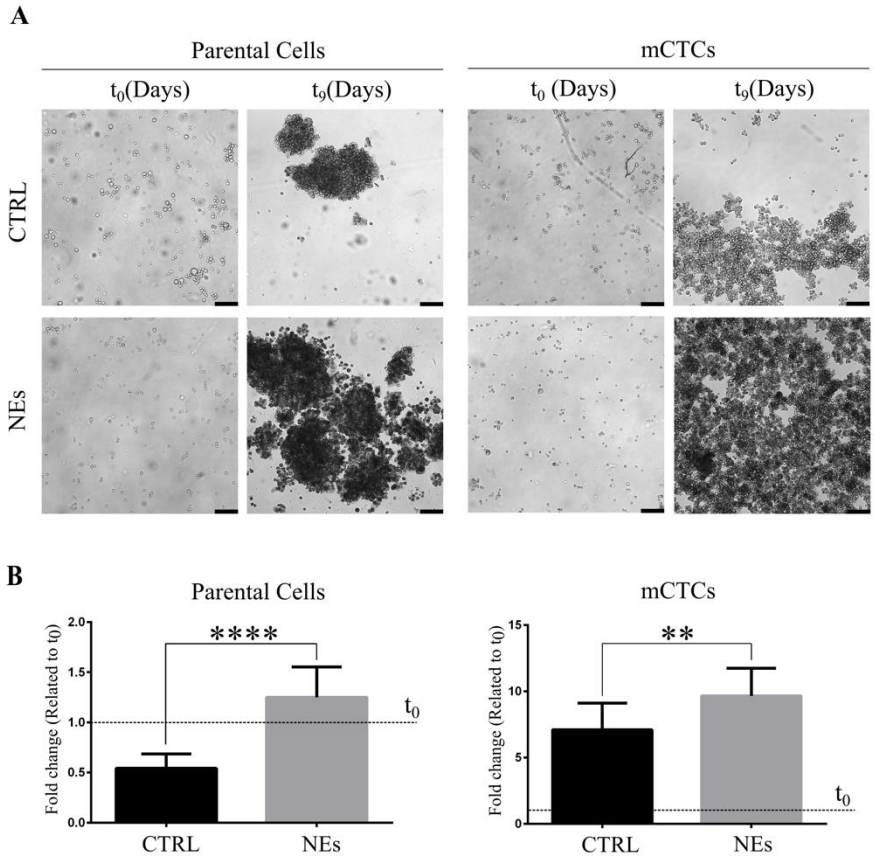

Figure 23. NEs proliferative effect study in parental cell line (MDA-MB-231$^{eGFP\text{-}Luciferase}$) and in mCTCs. (A) Brightfield images after cell seeding (t_0 (Days)) and the last time point of the study (t_9 (Days)). Scale bar represents 150 µm; (B) Fold change values of parental cells and mCTCs after 9 days of culture (related to t_0). Values represent mean ± SD (n = 4). Statistical comparison was performed using unpaired t-tests. Statistical differences are represented as ** ($p < 0.01$) and **** ($p < 0.0001$). NEs are cells treated with NEs and CTRL are cells without treatment.

1.3.7. NEs mechanisms study: gene expression analysis and flow cytometry and TEM Studies

1.3.7.1. Gene expression analysis

In order to understand the positive effect in proliferation for mCTCs, an expression analysis with a customised panel of 13 selected genes was performed in samples from the previous experiment. Selected genes included epithelial (*EpCAM*), mesenchymal (*Snail1* and *VIM*), stem (*Prom1* and *ALDH1A1*), breast specific (*PALB2*), and other genes related to cell cycle/cancer pathways (*Ki67*, *CCND1*, *E2F4*). **Figure 24** shows that from all the genes studied, only one gene related to proliferation (*Ki67*) and other associated with cell cycle (*E2F4*), presented higher relative expression in mCTCs treated with NEs. This observation suggests that the proliferation observed in the previous *in vitro* experiment could be related to this genetic expression. Moreover, *ALDH1* presented an increase; despite it presents a big error bar.

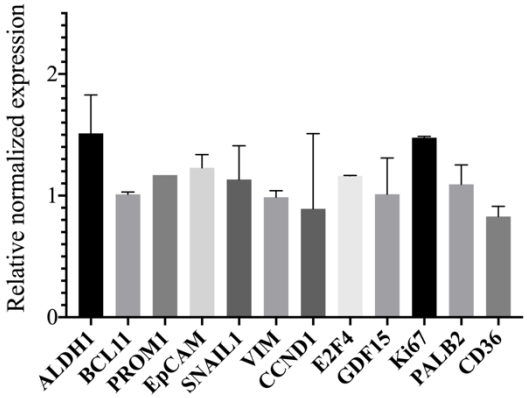

Figure 24. Relative expression levels selected genes in mCTCs treated with NEs. To compare gene expression data between control cells and cells treated with NEs, relative normalized expression was calculated using $2^{-\Delta\Delta CT}$. Values are represented as the mean fold change ± SD from two independent experiments.

1.3.7.2. Flow cytometry and TEM studies

Taking into consideration the previous observations related to LDs formation in breast cancer cells due to NEs addition, we carried out flow cytometry and TEM analyses. Both studies were done with MDA-MB-231 (the one employed to generate the mCTC). Hence, cells were incubated for 4 h with NEs and then, NEs were removed from the cell medium. Monitorization times were: 4 h, 24 h, and 48 h. In the one hand, Nile Red was used for flow cytometry study. As can be seen from **Figure 25A**, fluorescence intensity was higher in cells treated with NEs than their negative control (untreated cells) at 4 h from NEs incubation. This fact indicates that the lipid content was raised because of the NEs incubation. After 24h, there is an increasing trend in both cases, NEs treated cells and negative control cells. Although it was observed this rise in both conditions, lipid content was much higher in case of NEs treated cells ($p < 0.05$). These data suggest that control cells could be increasing the uptake of exogenous lipids from cell medium. Previously, Lesli E. Lupien *et al.* had observed by flow cytometry that breast cancer cells that do not express the protein for triglycerides hydrolysis, lipoprotein lipase, can acquire it from FBS in the cell medium[146]. An additional explanation could be associated to the capacity of cancer cells to reactivate *de novo* lipogenesis. Nevertheless, these cells did not reach the level of LDs of NEs treated, due to the efficient uptake of NEs in comparison with free lipids in solution. Finally, at 48 h, lipid content remains growing for control cells, whereas dropped in case of NEs treated cells. This observation agrees with the previous cell viability studies, where we found a decrease in the effect at 48 h from the NEs addition, as response to the LDs consumption by cells.

In the other hand, related to TEM analysis, images at 4 h, 24 h, and 48 h were taken. **Figure 25B** shows small oil droplets in the cell cytoplasm indicated by blue arrows. Likewise results from flow cytometry, higher cytoplasmatic lipid content was observed in case of cells treated with NEs than in control cells. After 24 h, some of the LDs began to fusion (increasing their size), while others started to become clearer in response to their consumption (orange arrows, t48 h).

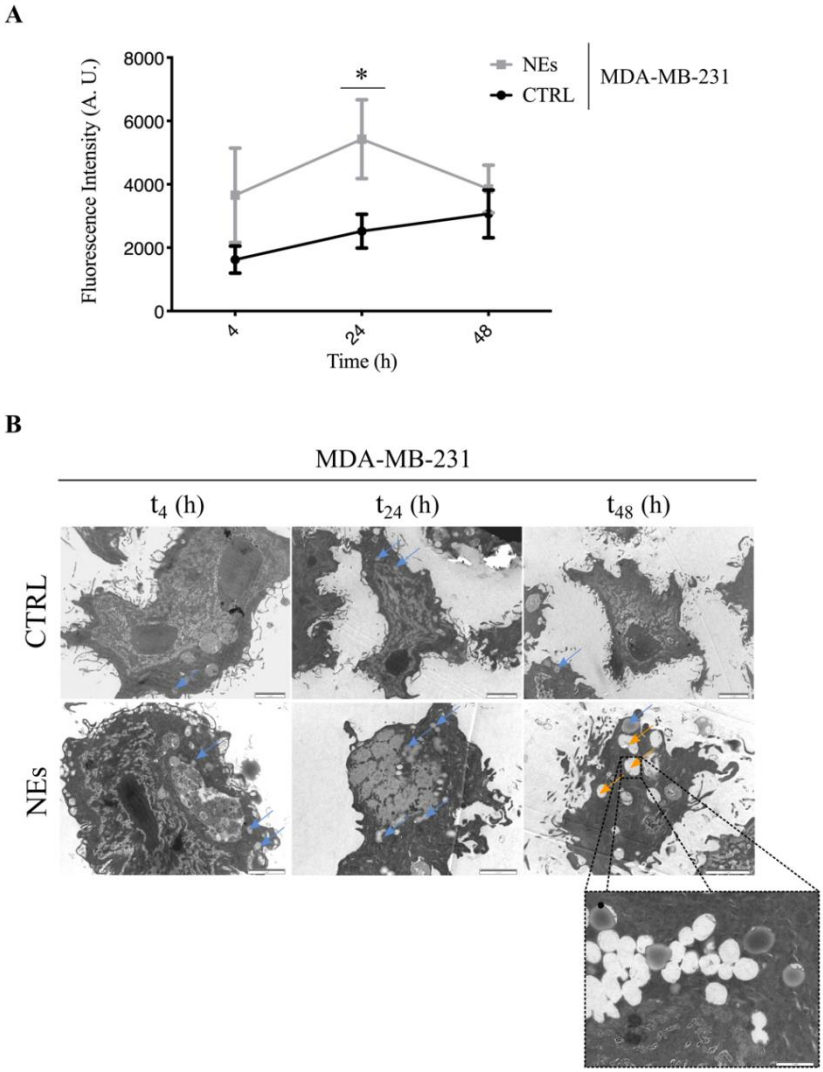

Figure 25. Lipid droplets (LDs) monitorization at t4, t24, and t48 (h) from NEs addition in MDA-MB-231. (A) LDs content measured in terms of fluorescence intensity by flow cytometry using Nile Red staining. Values represent mean ± SEM (n=3). Statistical comparison was performed using paired t-test. Statistical differences are represented as * ($p < 0.05$); (B) TEM images of MDA-MB-231 treated with NEs and their negative control cells (CTRL). LDs are indicated by blue arrows and their consumption by orange arrows. Scale bars represent 2µm and augmented image at the bottom presents a scale bar of 1µm.

These results point towards the following mechanism for the NEs: firstly, NEs are taken up by breast cancer cells and activate the cell metabolism (part of the NEs are sent directly to mitochondria to be oxidized), as shown in **Figure 22** (it is observed an increase in cell viability after each NEs addition (black arrows)). Moreover, data are also in agreement with the initial hypothesis of cytoplasmatic accumulation of NEs (acting as LDs). In fact, as shown by flow cytometry (**Figure 25A, 4h**) and by TEM (**Figure 25B, 4h**) part of NEs are transformed as LDs. Then, cells start to consume the NEs in a similar trend as they do with LDs, in agreement with TEM images (**Figure 25B, 24h**).

1.4. Conclusions

In this chapter we have formulated nanoemulsions that can be conveniently modulated related to their size and composition. Their physico-chemical properties were analysed, and all the compounds used for preparation of NEs (OA, CH, and PC) were demonstrated to be indeed part of the final formulation.

Moreover, a concentration of NEs for cell culture conditions was chosen and the uptake was proved. Importantly, the ability to induce cell proliferation was not only validated using three different breast cancer cell lines (HCC1143, MDA-MB-231, and MCF-7) but also in the mCTCs (a model of CTCs generated in our own laboratory). In addition, a gene expression analysis was carried out in mCTCs to determine specific markers involved; higher expression of E2F4 and Ki67 were observed in case of cells treated with NEs compared to cells without treatment. Then, this data could be supporting the effect observed previously *in vitro*. Finally, we studied the mechanism of action that NEs presented in breast cancer cells and the results indicated that NEs were internalized into the cytoplasm, part being storage as LDs.

These results led us to believe that the addition of our NEs could result in a profitable tool for *ex vivo* CTC culture of metastatic breast cancer patients. Using an easy and simple protocol, we can stimulate cell viability,

promoting proliferation, and supporting the cell culture of breast cancer cells.

Chapter 2

Chapter 2.

Use of nanoemulsions in short-term *ex vivo* culture of CTCs from advance breast cancer patients: clinical implications

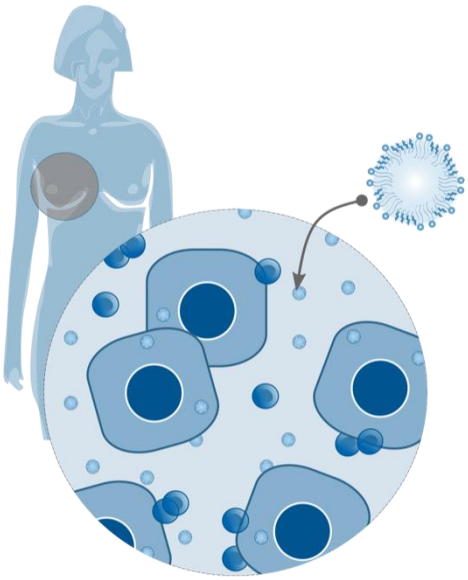

CHAPTER 2

Use of nanoemulsions in short-term *ex vivo* culture of CTCs from advance breast cancer patients: clinical implications.

The results from this chapter have been adapted/extracted from our previous published article[147]

Short-Term *Ex Vivo* Culture of CTCs from Advance Breast Cancer Patients: Clinical Implications.

Nuria Carmona-Ule[1], Miriam González-Conde[1,2], Carmen Abuín[1], Juan F. Cueva[2,3], Patricia Palacios[2,3], Rafael López-López[1,2,3], Clotilde Costa[1,2,] and Ana Belén Dávila-Ibáñez[1]

[1]Roche-Chus Joint Unit, Translational Medical Oncology Group (Oncomet), Health Research Institute of Santiago de Compostela (IDIS), Hospital Gil Casares, Travesía da Choupana, s/n Cp:15706 Santiago de Compostela, Spain.

[2]Cancer Network Research (CIBERONC), 28029 Madrid, Spain.

[3]Translational Medical Oncology Group (Oncomet), Health Research Institute of Santiago de Compostela (IDIS), Hospital Clínico Universitario de Santiago de Compostela (SERGAS); Travesía. Choupana s/n 15706, Santiago de Compostela, Spain.

Cancers. 13 (11). 2668. ISSN: 2072-6694
MDPI, 28/05/21.
Full-text available: https://doi.org/10.3390/cancers13112668

Abstract

CTCs have relevance as prognostic markers in breast cancer. However, the functional properties of CTCs or their molecular characterization have not been well-studied. Experimental models indicate that only a few cells can survive in the circulation and eventually metastasize. Thus, it is essential to identify these surviving cells capable of forming such metastases. In this study, we isolated viable CTCs from 50 peripheral blood samples obtained from 35 patients with advanced metastatic breast cancer using RosetteSep™ for *ex vivo* culture. The CTCs were seeded and monitored on plates under low adherence conditions and with media supplemented with growth factors and NEs, formulated and characterized from the previous chapter. Phenotypic analysis was performed by immunofluorescence and gene expression analysis using RT-qPCR and CTCs counting by the CellSearch® system. We found that in 75 % of samples the CTC cultures lasted more than 23 days, predicting a shorter PFS in these patients, independently of having ≥ 5 CTC by CellSearch®. We also observed that CTCs before and after culture showed a different gene expression profile. Altogether, these results suggest that the cultivability of CTCs is a predictive factor. Furthermore, the subset of cells capable of growing *ex vivo* show stem or mesenchymal features and may represent the CTC population with metastatic potential *in vivo*.

Graphical abstract

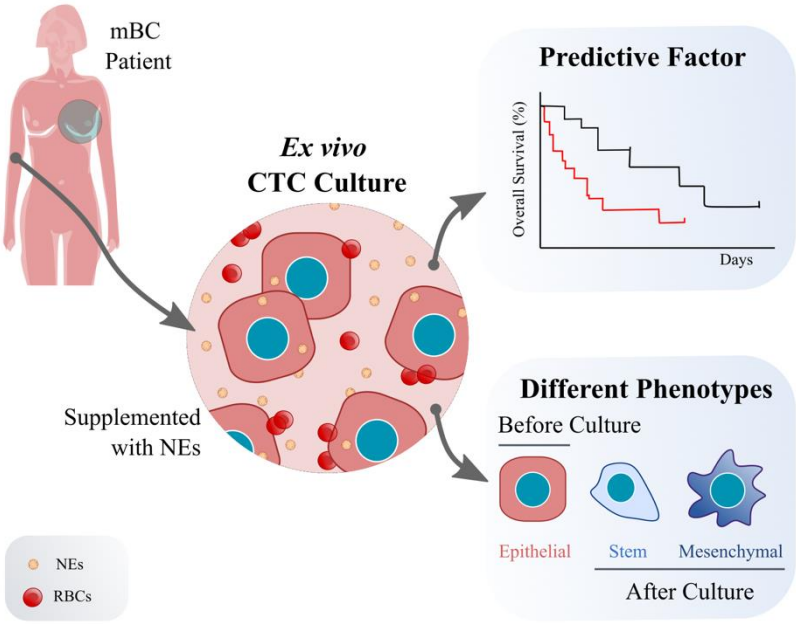

2.1. Introduction

The CTCs are those cells that abandon the primary tumour and circulate through the vascular system to eventually colonize distant organs and originate the formation of metastasis[148]. High CTC numbers have been linked with worse outcome in prostate, colon and breast cancer metastatic patients[80,149,150] and the CTC number increase over time indicates therapy failure[151]. However, nowadays CTC count does not allow therapeutic intervention. Therefore, CTC expansion *in vitro* would permit their downstream analysis, and evaluate personalized cancer therapies and drug sensitivity testing[152,153]. Even though CTCs are a highly valuable source of tumour material, their molecular analysis is still challenging due to their rarity, as they are as infrequent as < 20 CTCs from 10 mL of blood[154]. Additionally, most of the CTC population dies in the bloodstream due to shear stress or immune surveillance[155]. Moreover, isolated CTCs show reduced proliferation hindering their *ex vivo* expansion[100]. Due to all these reasons, CTC growth *ex vivo* is still one of the main challenges in the field.

Despite its obvious complexity (low-abundance, fragility, and phenotypic heterogeneity), different cultures of CTCs have already been established. Thus, the first CTCs primary culture was established in 2013 from advanced breast cancer patients using isolated EpCAM negative-CTCs[101]. Later, in 2015, Cayrefourcq *et al.* established different cultures and a permanent cell line from CTCs isolated from a metastatic colon cancer patient, who presented a high number of CTCs (≥ 300 CTC)[74]. Currently, it is established that for long-term CTC cultures success, a high number of CTCs is required[156]. Numerous attempts have been made to culture CTCs from patient blood samples, however, the success rates of *in vitro* CTC cultures is around 6–20 %[157]. To date, only a few short-term CTCs cultures, from 3 to 14 days but also up to 40 days, have been reported for different cancers[74,75,67,68,105,158–163], and specifically for breast cancer[73,104,157]. Nonetheless, the establishment of long-term CTC cultures has proven to be even more challenging for breast[73,101,164] and other tumour types[165–167], having much lower success.

When it comes to *ex vivo* tumour cell culture, historically they were performed in 2D cultures, however the cell morphology or cell-cell and spatial interactions are lost in this condition[168]. Since the importance of these interactions in different cellular functions as proliferation or cell differentiation has been demonstrated[169], 2D cultures show a considerable drawback. Furthermore, in 2D cultures nutrients or oxygen accessibility is unlimited[170], thus, this situation do not fully represents the setting in the tumour mass in reality[171]. To this end, 3D cultures appears as a solution to overcome these limitations, simulating the environment of tumour cells, in which cell-cell and cell-environment interactions are maintained, as well as cell polarity and morphology[160,172]. Precisely, a non-adhesive substrate is employed to culture cancer stem-like cells from primary tumours creating a multi-layered cell cluster[173,174]. Thus, for *ex vivo* CTC expansion, ultra-low attachment plates are frequently used[73,175–177]. Besides, hypoxic conditions (1–2 % O_2) can promote cellular reprogramming towards a cancer stem cell phenotype[178]. *In vivo*, tumour cells are supplied with growth factors, hormones, lipids and other metabolites from serum. Nonetheless, standard culture media are devoid of them, although they are essential for the CTC culture *ex vivo*[179]. Thus, the majority of protocols for CTC culture employ supplemented media to provide all the necessary nutrients for these rare cells[73,166].

However, there is still the need of knowledge to achieve the optimal conditions that influence the success of CTC cultures and to deeply analyse the CTCs populations capable of surviving *in vitro*. Therefore, to shed light on this, we carried out a functional study of CTCs isolated from patients with metastatic breast cancer, placing them in culture and monitoring them over time. As a novelty, we used a culture protocol in which, together with growth factors, we added NEs described in the Chapter 1 of this thesis. Therefore, NEs were included in the culture medium to stimulate the metabolism of isolated CTCs. The workflow followed in this study is represented in **Figure 26**.

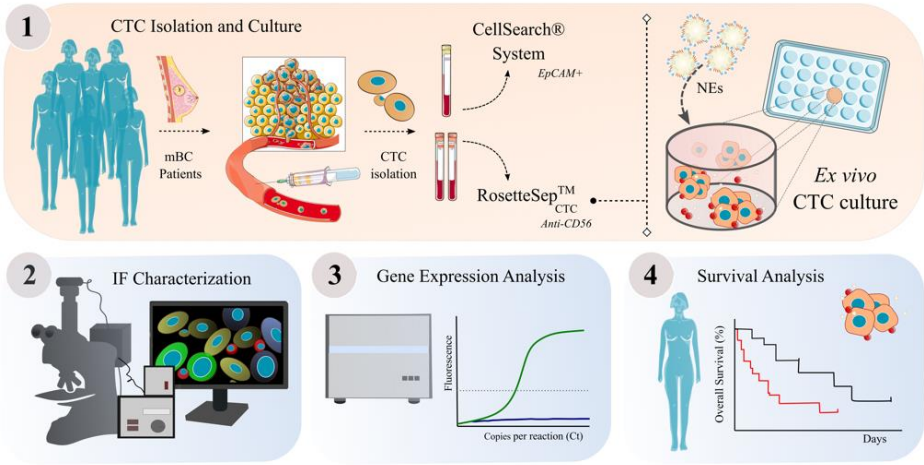

Figure 26. Schematic workflow of Circulating Tumour Cells (CTCs) samples isolation, cell culture and subsequent analyses. (1) Methodology followed for the isolation and *ex vivo* cell culture of CTCs from metastatic breast cancer (mBC) patients. Cells were isolated using: CellSearch®system (determination of $EpCAM^+$ cells) and RosetteSep™ (enrichment of CTCs for cell culture). Cells were cultured under ultra-low attachment plates to support 3D culture and every two days cells were supplemented with fresh supplemented medium and NEs; (2) Immunofluorescence characterization by Confocal microscopy and Fluorescence microscopy of cell cultures; (3) Gene Expression Analysis was performed using paired samples before and after cell culture; (4) Survival Analysis was carried out to determine the relation between time (days) of culture or presence of Red Blood Cells (RBCs) as a predictive factor in the patient's outcome.

2.2. Materials and methods

2.2.1. Materials

RosetteSep™ CTC Enrichment Cocktail Containing Anti-CD56, Lymphoprep™, SepMate™ tubes, heparin, hydrocortisone and MammoCult™ Human Medium Kit were obtained from STEMCELL Technologies. EDTA-coated vacutainer tubes were purchased from Becton Dickinson. RNAlater™ Solution and CK Pan Antibody (AlexaFluor-488 anti-human, Clone AE1/AE3) were obtained from Invitrogen, ThermoFisher Scientific. 4 % PFA, cDNA with SuperScript III, preamplified with Taqman Preamp Master Mix, and NucBlue™ (Hoechst 33342 dye) were obtained from ThermoFisher Scientific. Lipoid® S100 a soybean PC (18:0/18:1) (94%) was a gift from Lipoid GmbH. OA, CH, progesterone, ß-estradiol, and penicillin/streptomycin were purchased from Sigma-Aldrich. Ultra-Low-Attachment 96-well plate, ultra-low attachment 24-well plates, and ultra-low attachment 25 cm^2 Flasks were obtained from Corning. CellSave Preservative tubes and CellSearch® Epithelial Circulating Tumor Cell Kit were purchaed from Menarini, Silicon Biosystems Inc. dPBS was purchased from Lonza. MQ-water was purified by Millipore® Direct-Q® 3 with UV system. EpCAM Antibody (AlexaFluor-488 anti-human, Clone 9C4 and E-Cadherin Antibody (FITC anti-human CD324, Clone 67A4) were obtained from Biolegend. Vimentin Antibody (Alexa®-647 anti-human, Clone D21H3 was obtained from CellSignaling Technology. CD45 Antibody (PE anti-human, Clone MEM-28) was purchased from ExBio. InsidePerm Buffer (from Inside Stain Kit) was obtained from MiltenyiBiotec. AllPrep DNA/RNA Mini Kit was obtained from QIAGEN. UltraGRO™ was obtained from AventaCell BioMedical Co. Master Mix TaqMan was purchased from Applied Biosystems. B-27 Supplement (50X) and recombinant basic Fibroblast Growth Factor (bFGF) were obtained from Gibco. Recombinant EGF was purchased from Sino Biological.

2.2.2. Clinical samples: metastatic breast cancer patient cohort

This study was approved by the local ethics committee (Ethics Committee of Galicia approval reference number 2015/772) and all patients gave written informed consent. All samples were anonymized and encoded before the analysis.

Inclusion criteria: women, advanced breast cancer, any subtype, age ≥ 18 years. Exclusion criteria: known diagnosis of psychiatric illness that prevents the patient from understanding and accepting the conditions of the study, current of malignant tumour in the last 5 years, except for basal cell carcinoma, squamous cell carcinoma or carcinoma *in situ* of the cervix properly treated. The patient's characteristics are described in **Table 5** and in **2.3.1. Section from Results and discussion.**

Table 5. Clinic-pathologic characteristics of the cohort of metastatic breast cancer patients (*n* =35). ER = Estrogen Receptor, PR = Progesterone Receptor, HER2 = Human Epidermal Growth Factor Receptor 2, CDKi = Cyclin Dependent Kinase inhibitor, and ET = Endocrine Therapy.

Category	*n*	%
Age		
≤57	18	51.43
>57	17	48.57
Tumour stage		
IV	35	100
ER status		
Positive	21	60
Negative	12	34.29
PR status		
Positive	15	42.86
Negative	18	51.43
HER2 status		
Positive	8	22.86
Negative	26	74.29
Metastasis location		
Bone	26	74.29
Visceral	32	91.43
Bone & Visceral	23	65.71
Number of metastatic sites		
1	4	11.43
2	13	37.14
≥3	18	51.43
Therapy		
Chemotherapy	26	74.29
CDKi + ET	6	17.14
ET	2	5.71
Lines of therapy		
Basal	14	40
1 Line	7	20
≥2 Lines	14	40
Progression	31	88.57
Exitus	24	68.57

2.2.3. CTC isolation and *ex vivo* culture

Two EDTA-coated vacutainer tubes of 7.5 mL of peripheral blood were collected per patient at different time points. Blood samples were processed within two hours after withdrawal. CTC isolation was performed using the label-independent antibody cocktail RosetteSep™ CTC Enrichment Cocktail Containing Anti-CD56. Enriched cells isolated with RosetteSep™ from the 1st EDTA tube were used for CTC culture as described below. In some random samples, the 2nd EDTA tube was processed for CTC enrichment by RosetteSep™, placed in RNAlater™ Solution and kept at −80 ℃ until further gene expression analyses. Besides, the Peripheral Blood Mononuclear cells (PBMCs) of some patients were isolated from one 7.5 mL EDTA tube of peripheral blood by density gradient centrifugation protocol (Lymphoprep™) in SepMate™ tubes according to manufacturer's instructions, for *ex vivo* culture, RNAlater storage and subsequent gene expression analysis.

Cell pellet from the previous step was resuspended in 200 µL of supplemented MammoCult™ Human Medium Kit. This supplemented medium contained 0.4 µg/mL progesterone, 0.4 µg/mL ß-estradiol, 4 µg/mL heparin, 0.48 µg/mL hydrocortisone, 5 % (*v*/*v*) UltraGRO™, 4 % (*v*/*v*) B-27 Supplement (50X), 20 ng/mL recombinant basic Fibroblast Growth Factor (bFGF), 20 ng/mL recombinant EGF, and 1 % (*v*/*v*) penicillin/streptomycin. The cell suspension was seeded initially in one well of an ultra-low-attachment 96-well plate and cultured using hypoxic conditions (37 ℃, 1–2 % O_2) for 1 week. Cell cultures were supplemented with fresh medium every 2 days with minimal well disturbance to avoid cell loss. NEs were prepared as previously described[147], and were added to the media every two days at the same time as the fresh medium supplement. Before addition to the media, NEs were filtered using Acrodisc® PFS Syringe filters and mixed with cell medium (concentration ranges were within 6.7×10^8 NP/mL to 2.14×10^9 NP/mL). After 1 week of cell culture, cells were switched to standard cell culture conditions (37 ℃, 5 % CO_2). When 85 % confluence was reached, growing cells were transferred to an ultra-low attachment 24-well plate and subsequently to ultra-low attachment 25 cm^2 Flasks at 90 % of

confluence. Cultures were maintained up to the entrance to the decline phase (live cells declined as cell death predominated in the culture). Samples for immunofluorescence and RNA isolation were taken between 10 and 15 days after seeding.

2.2.4. CTC enumeration

In 34 samples, one 10 mL CellSave Preservative tube was collected in parallel to EDTA tubes and processed for CTC enumeration by the CellSearch® system, using CellSearch® Epithelial Circulating Tumour Cell Kit. CellSave™ (Menarini-Silicon Biosystem, Bologna, Italy) blood collection tubes have been designed to increase the preservation of CTCs[180]. EpCAM-positive enriched cells were labelled with phycoerythrin-conjugated anti-CKs (8, 18, and 19) antibodies, allophycocyanin-conjugated anti-CD45 antibodies, and 4,6-diamino-2-phenylindole (DAPI). The CellTracks Analyzer (Menarini-Silicon Biosystems) was used to acquire digital images of the 3 different fluorescent dyes, which were reviewed by trained operators to determine the CTCs count.

2.2.5. Immunofluorescence staining, fluorescence microscopy and confocal microscopy analyses

Cells from 3D culture were washed with dPBS (centrifugation at 500× *g*, 5 min, 20 ℃) and fixed with cold 4 % paraformaldehyde (PFA) for 15 min. Then, cells were washed with dPBS (centrifugation at 500 × *g*, 5 min, 20 ℃). Afterward, cell solutions were immunostained using a combination of epithelial antibodies: CK Pan Antibody (1:50, AlexaFluor-488 anti-human), EpCAM Antibody (1:25, AlexaFluor-488 anti-human), E-Cadherin Antibody (1:25, FITC anti-human CD324); Vimentin Antibody (1:200, Alexa®-647 anti-human), and CD45 Antibody (1:30, PE anti-human). NucBlue™ (Hoechst 33342 dye) was used to counterstain nuclei. InsidePerm Buffer was used as antibody diluent.

Stained solutions were examined by (i) confocal microscope (Leica TSC SP5 X, Leica Microsystems) and (ii) fluorescence microscope (Leica DMi8 automated Microscope, Leica Microsystems). In both microscopes, 63× oil

immersion objective was used. Images were used for the morphometric analysis using ImageJ software[181], following previously described parameters[182].

2.2.6. RNA extraction and gene expression analysis

AllPrep DNA/RNA Mini Kit was used for RNA extraction (CTCs and PBMCs), following the manufacturer's protocol. An amount of 11 µL of total RNA were retrotranscribed into cDNA with SuperScript III. Samples were preamplified with Taqman Preamp Master Mix. Gene expression analysis for a custom panel of 20 genes (**Table 6**) was performed with probes and Master Mix TaqMan on a LightCycler 480 II (Roche Diagnostics). This part was carried out by the line of liquid biopsy from the Roche-Chus join unit. The relative expression was calculated considering *B2M* as a reference gene. To clarify the visualization of the heatmap, relative expression was codified from 0 to 7 points, 0 being no gene amplification.

Table 6. Probes of the listed genes for Gene Expression Custom Panel and their functional gene grouping.

TaqMan Probes	Reference	Functional Gene Grouping
ALDH1A1	Hs00946916_m1	Stem cell-like phenotype
BCL11A1	Hs01093197_m1	Stem cell-like phenotype
CCND1	Hs00765553_m1	Proliferation/Cell cycle regulation
CD36	Hs00169627_m1	Cell metabolism
CD45	Hs04189704_m1	Leukocyte marker
CDH1	Hs00170423_m1	Epithelial
CTNNB1	Hs00355049_m1	Cell adhesion/Gene transcription
E2F4	Hs00608098_m1	Proliferation/Cell cycle regulation
EpCAM	Hs00158980_m1	Epithelial
ESR1	Hs01046816_m1	Breast cancer associated
GDF15	Hs00171132_m1	Proliferation/Cell cycle regulation
Ki67	Hs00171132_m1	Proliferation/Cell cycle regulation
KRT5	Hs00361185_m1	Epithelial
MYCL	Hs00420495_m1	Oncogene
PALB2	Hs00226617_m1	Breast cancer associated
PROM1	Hs01009257_m1	Stem cell-like phenotype
SNAI1	Hs00195591_m1	EMT
TWIST	Hs01675818_s1	EMT
VIM	Hs01675818_s1	EMT
B2M	Hs00187842_m1	Housekeeping gene

2.2.7. Statistical Analysis

Statistical analysis was performed using GraphPad Prism 6.01 software (GraphPad Software Inc.) and R Studio Version R-3.6.3. ClustVis tool was used for heatmap and Principal Component Analysis (PCA) performance. Fisher exact test and Chi-square test were used for association analysis. We used the Wilcoxon signed-rank test for media comparisons (CTC enumeration between groups and gene expression comparison before and after culture using paired test). PFS and OS were visualized using Kaplan-Meier plots and tested by the log-rank test and by univariate and multivariate Cox proportional hazards models. Progression was calculated from the moment the sample was taken until disease progression was detected, either by biochemistry or by imaging. Only p values < 0.05 were considered statistically significant.

2.3. Results and discussion

2.3.1. Patients and samples characteristics

A total of 50 blood samples from 35 metastatic breast cancer patients were analysed in this study. All patients were stage IV and 88.57% had ≥ 2 metastatic locations. Moreover, 23 out of 35 had bone and visceral metastasis alone.

Considering the time of sample collection as the starting point, median PFS was 6.3 months and median OS was 10 months. All longitudinal samples were collected at different time points through the disease. Hence, 32 samples out of 50 (64%) were collected after the start of therapy and 36 % were collected at baseline (diagnosis of metastasis). Of the treated patient samples, 14 were first-line and 18 had ≥ 2 lines of treatment (**Supporting Figure S4-Scheme Cohort**). In relation to patient's treatments: 35 patients received chemotherapy (71.43 %), endocrine therapy plus CDK4/6 inhibitors (17.14 %) or others as endocrine therapy alone or anti-Her2 therapies.

2.3.2. Short-term CTC culture establishment

CTCs were enriched using the negative isolation technique RosetteSep™. Cells isolated were plated under non-adherent conditions, using MammoCult cell medium supplemented with growth factors plus NEs. During first seven days, cells were under hypoxic conditions (1-2 % CO_2, 37 ºC), then cells were culture using standard parameters (5 % CO_2, 37 ºC).

Of the initial 50 samples, the follow-up was carried out in 48 of them; the mean time was 56.35 days (range of 8-291 days). To consider the endpoint of cultures, parameters as reduction of cell density and observation of apoptotic cells were used. It was established a criterion to discriminate between a successful culture (culture (+)) and non-successful culture (culture (–)). Considering the median progression time (100 days) and days of culture of CTCs, it was performed a ROC curve analysis. The best threshold able to discriminate both groups was 23.5 days (AUC = 0.65). As a result, it was considered the cut-off of 23 days as a successful CTC culture

(Culture (+)). Using this criterion, short-term cultures were successfully propagated in 36 samples (75 %). In 6 of them, follow-up was stopped due to presence of contamination in culture. Samples that contamination occurred before the 23rd day (n = 2), were considered failed cultures.

Figure 27 shows representative images of the short-term culture of CTCs. Since cells were grown on ultra-low attachment plates, most of them grow in suspension. Curiously, some samples presented cells growing both, in suspension and adherence.

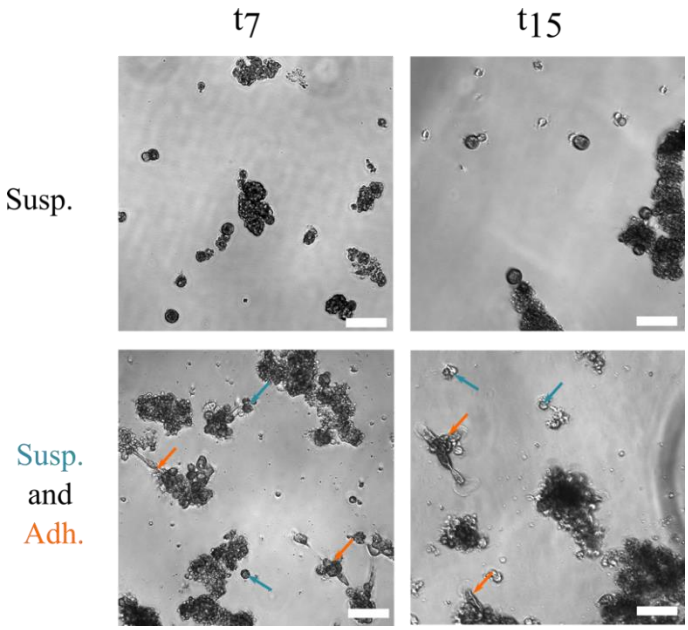

Figure 27. Representative image of cultured CTCs in ultra-low attachment 96-well plates at 7 and 15 days (t7, t15), left and right panel, respectively. Two growth behaviours were observed: (i) cells that grow in suspension (Susp.) (upper panel); (ii) cells growing in suspension (Susp.) co-existing with adherent cells (Adh.) (bottom panel). Blue arrows represent cells in suspension while orange arrows point to cells growing in adherence. Both samples had not received treatment (basal). Scale bars represent 75 µm.

In 34 samples from 28 patients, paired CTC enumeration was performed by CellSearch® system at the starting point of culture. In 53 % of samples, it was observed ≥ 5 CTCs (range of 0-1,000 CTCs), although only

4 of them had ≥ 350 CTCs. Interestingly, as **Figure 28** shows, no association was observed between culture successes and the fact of having ≥ 5 CTCs (the pre-established cut-off in metastatic breast cancer). Despite this, the highest CTCs count was detected in the successful culture group (culture (+)), but there were no significant differences in the mean of CTCs numbers between both groups.

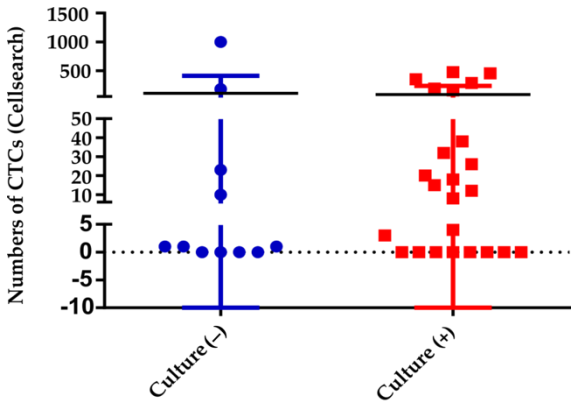

Figure 28. Association study between having ≥ 5 CTCs and groups of culture (–) and culture (+). Number of CTCs measured by CellSearch® with respect to their ability to establish a successful culture in 34 metastatic breast cancer samples. Negative culture, in blue (*n* = 11) and positive culture in red (n = 25).

Altogether, these data suggest that by employing the aforementioned protocol with NEs addition, CTCs can grow *ex vivo* for weeks (mean 8 weeks). It was observed a positive culture in 75 % of the analysed samples, implying more than 23 days with proliferative and survival features, which is a higher percentage than previously published works which reported 13 or 28 % of success[183,184].

2.3.3. CTC culture characterization by immunofluorescence

It was performed a phenotypic characterization in some random samples after ~ 2 weeks of culture. Specifically, a triple immunofluorescence assay was carried out for epithelial (E-Cadherin, EpCAM and Pancitokeratin (PanCK)), mesenchymal (Vimentin) and white

blood cells marker (CD45), (**Figure 29**). As a result, epithelial features were observed in low percentage of samples (18.18 %, n = 22), compared to vimentin^{+} cells (47 %, n = 17). This is in agreement with different published studies that indicate that after 14 days in culture, CTCs lost their epithelial features[104,185] and exhibited mesenchymal markers[162,186]. Furthermore, it was detected no marker but nucleus in scarce samples.

Of the analysed samples by immunofluorescence, only 4 did not result in a culture (+) and none of them showed positive marker expression by immunofluorescence. Likewise, CD45^{+} cells were detected co-inhabiting in the most of cultures. In contrast, CellSearch® data (before culture) did not associate with the expression of epithelial markers after culture process.

In recent years, the standard CTC condition has included morphological criteria based on cytopathological identification[187–191]. Even though, there is not a standardized protocol, different research groups had reported a larger nucleus size (> 9 µm) and nucleus/cytoplasm ratio (> 0.8) in CTCs compared to blood cells [182]. Due to some cells did not meet the standardized CTC criterions (CK^{+}, CD45^{-}, and DAPI^{+}), morphometric analysis of some immunofluorescence images (n = 82 from 18 patients) were performed. In our study, it was observed that nucleus from cells with epithelial^{+}, vimentin^{+}, or with absence of any marker, were larger than those cells CD45^{+} (mean of 12.97 µm vs 10.27 µm, p = 0.008). In addition, it was observed for both parameters (nucleus size (> 9 µm) and the nucleus/cytoplasm ratio > 0.8), that CD45^{-} cells met the criterion preferentially (p = 0.02). Therefore, we have seen that cells in culture with epithelial characteristics or absence of CD45 meet the morphometric criteria of CTC described by other authors [182]. It is known that there are distinct subpopulations of CTCs with differential expressions and morphological data. Besides, the conditions in which these parameters are obtained (before or after suspension culture; suspension or adherence; immunofluorescence or immunocytochemistry assay, CTC-isolation approach) can lead to a variety of results. Therefore, there is no universal criterion, although it is clear that cytometric analyses discriminate CTCs from blood cells (monocytes, granulocytes or tumour-associated macrophages) [192].

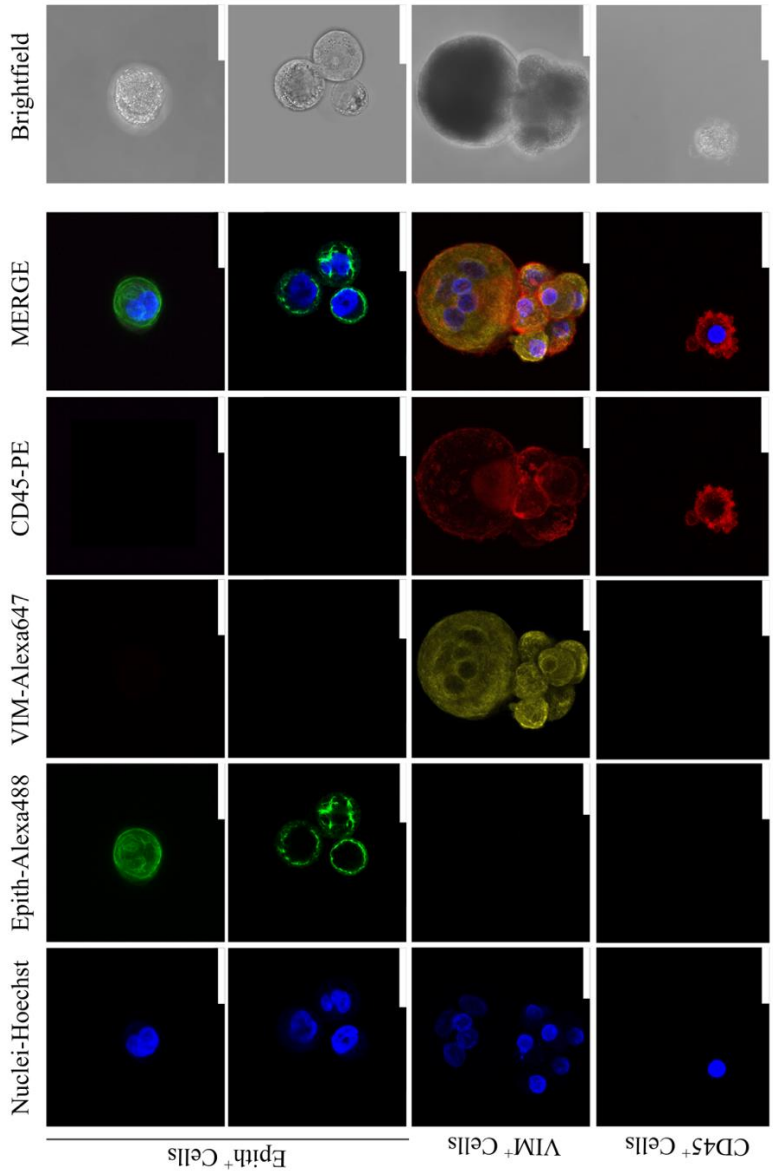

Figure 29. Representative images by confocal microscopy of Immunofluorescence characterization of CTCs after culture. Immunofluorescent staining was performed using a combination of anti-human Epithelial markers (Epith: EpCAM, E-Cadherin, and PanCK) (in green), anti-Vimentin (anti-VIM) (in yellow), and anti-CD45 (in red). Scale bars represent 25 µm.

It was observed in 70.9 % of samples a contamination with RBCs that eventually disappeared during cell culture. However, the success of cultures did not present an association with the following parameters: molecular type, age of the patient, therapy received, visit in which sample was collected (before or after treatment start; first line or ≥ 2 lines of treatments), and presence of RBCs.

2.3.4. Gene expression analysis of CTC culture samples

An expression analysis study with a customised panel of 20 selected genes was performed in samples collected before and after culture (~ 2 weeks), (described in **Table 6 from Materials and Methods section**). Selected genes included epithelial (*EpCAM*, *KRT5*, and *CDH*), mesenchymal (*SNAI1*, *TWIST*, and *VIM*), stem (*PROM1* and *ALDH1A1*), breast specific (*PALB2* and *ESR1*), and other genes related to cell cycle/cancer pathways (*Ki67*, *CCND1*, and *CTNNB1*).

Remarkably, we observed that epithelial markers were expressed preferentially in the CTCs freshly isolated from the blood, which have not been culture (**Figure 30A and B**). The Hierarchical clustering (**Figure 30B**) and the PCA (**Figure 30C**) diagrams concluded that CTCs before and after culture presented a differential gene expression pattern. Breast specific markers such as *PALB2* and *ESR1* were expressed independently of being cultured or not; despite both genes presented a higher relative expression in CTCs from cell culture ($p = 0.03$ and 0.06, respectively). This observation suggested that mammary tumour cells were proliferating in cell cultures. Besides, *PALB2* expression in CTCs was already described and linked with worse outcome in advanced breast cancer patients by our group[193]. Related to mesenchymal features, it was observed that *TWIST* expression appeared only after cell culture in 2 out of 6 samples and that *SNAI1* expression disappeared after culture in 5 out of 6 samples. Significantly, *VIM* was presented in all the samples both before and after culture, and it was overexpressed in 4 out of 6 samples after culture. Moreover, one of the cultured samples, showed less *VIM* expression and an increase in *CDH1*, which indicated a maintenance of epithelial phenotype in this case.

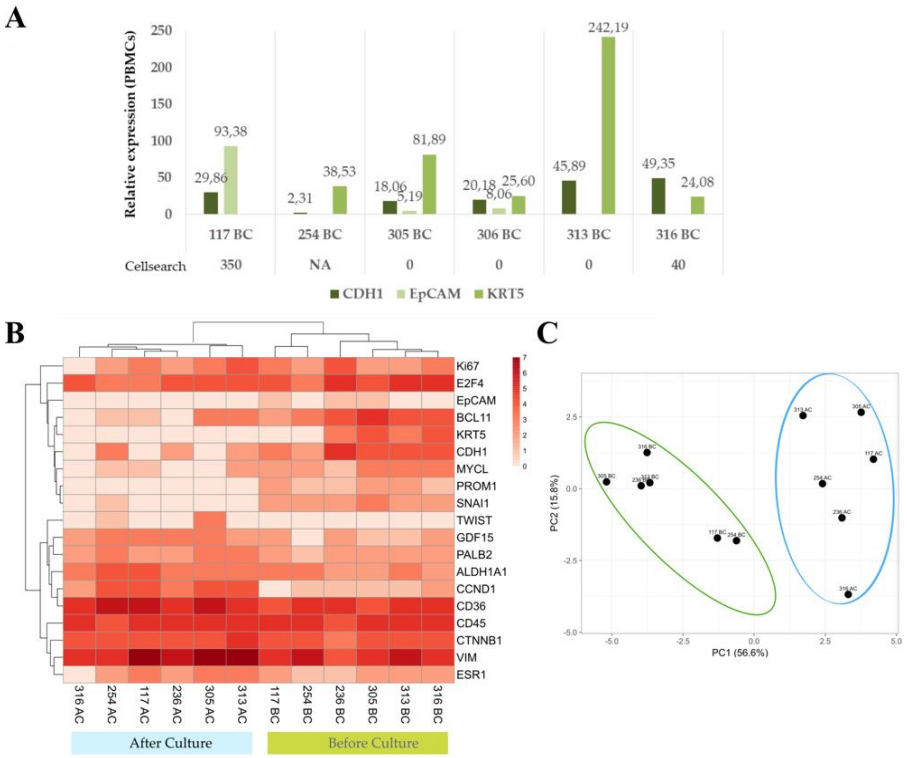

Figure 30. CTC gene expression analysis of six samples. Of these samples, four of them were not included in the previous immunofluorescence characterization. Five samples were collected after therapy initiation. (**A**) Relative gene expression for epithelial markers (*E-Cadh*, *EpCAM* and *KRT5*) of CTC-fraction isolated by Rosettesep and normalized with paired Peripheral Blood Mononuclear Cells (PBMCs) (before culture). Comparison with Cellsearch® data is shown; (**B**) Clustered heatmap depicting CTCs gene expression levels of the listed genes. Light red indicates no expression. Relative gene expression (to *B2M*) was ranged and coded from 1 to 7 (dark red); (**C**) PCA using gene expression of the listed genes (see Heatmap).

To establish whether blood cells contaminations were influencing the genetic expression analysis, in 4 of the 6 samples we analysed the expression of PBMCs before and after culture (isolated PBMCs were cultured under same conditions as CTC enriched fraction, **2.2.3 Section from Materials and Methods**).

Within cell culture process, representative differential expression profile was observed; ruling out that gene expression was influenced by non-specific cells that are present in the culture of CTCs (**Figure 31A and B**). CTCs before culture seem to show higher contamination of $CD45^+$ cells, as supported by the hierarchical clustering which groups these samples interspersed with PBMCs while CTCs after culture sited together (**Figure 31B**). Even though, in the majority of cultured samples, we detect associated $CD45^+$ cells, similarly to other related publications[104] which reported the benefit of $CD45^+$ (leukocytes) to support CTCs survival[194].

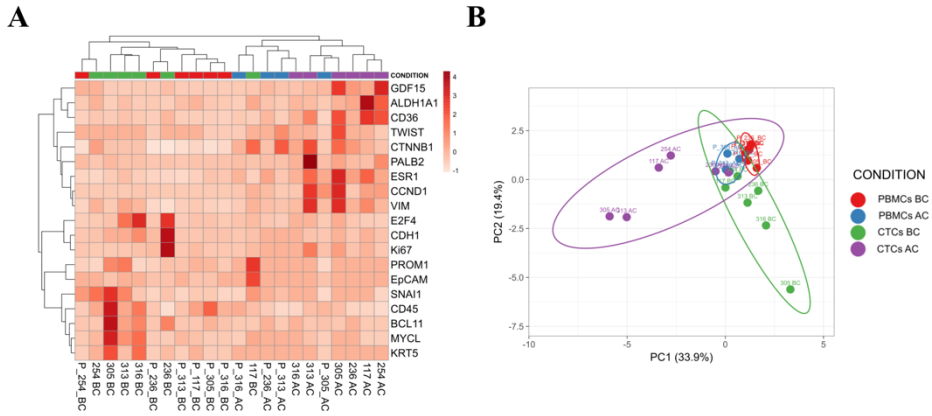

Figure 31. Gene expression analysis of PBMCs Before Culture (BC, red) and After Culture (AC, blue) and paired CTCs Before Culture (BC, green) and After culture (AC, purple) of 6 patients. PBMCs after culture we only evaluated in 4 out of 6 samples. (A) Clustered heatmap depicting CTCs and PBMCs relative gene expression (to *B2M*) levels of listed genes. Light red indicates no expression; (B) PCA using gene expression of listed genes (see Heatmap). CTCs after culture grouped together while CTCs before culture exhibited more similarity to PBMCs, probably due to unspecific isolated cells.

In regards to the presence of $CD45^+$ cells that we observed in culture, Xiao *et al.* have described that cells concomitant with $CD45^+$ cell in short-term culture (30 days) of metastatic breast cancer samples displayed higher growth potential[157]. In future studies, it would be relevant to characterize in-depth the population of contaminating $CD45^+$ cells to know if they present specific characteristics and to determine if their nature is indeed capable of conditioning the achievement of the culture. However, we had no data

regarding concomitant expression of stem cell markers and CD45 after culture since gene expression analysis was performed in a pool of CTCs. It has also been published that the fusion of myeloid cells with cancer stem cells promotes metastasis in lung cancer. These hybrid cells escape the immune system and are capable of colonizing distal organs[195]. This phenomenon could be favouring the presence of $CD45^+$ cells in the CTC enriched samples, which would explain its contribution to culture success.

As well as the previous genes, other EMT related genes were analysed. Specifically, *GDF15* and *CTNNB1* showed higher relative gene expression after culture ($p = 0.06$ and $p = 0.03$, respectively), (**Figure 30B)**. Importantly, both genes are related to EMT and stemness. On one hand, *GDF15*, a member of the TGF-β superfamily, has been linked with macrophages, adipocytes, and several carcinomas including breast cancer. *GDF15* plays a dual role in the evolution of cancer[196]. Thus, under normal physiological conditions, it inhibits early tumour promotion. However, its abnormal expression in advanced cancers causes proliferation, angiogenesis, invasion, metastasis, drug resistance, stemness or immune escape[197]. On the other hand, *CTNNB1*, which encodes beta-catenin, has been linked to the EMT process, cancer stem cell pluripotency, and cancer signalling[198]. Regarding proliferation/cell cycle regulation-associated genes, *CCND1* presented an increase, despite it did not result significant.

As **Figure 30B** shows, expression of *ALDH1A1* and CD36 was observed in all samples (before and after culture), resulting significantly elevated in samples after culture ($p = 0.03$). ALDH1A1 is a stem cell marker linked with mammary stemness[186]. This result is in agreement with Zhang and colleagues who established long-term culture from CTCs $ALDH1A1^+$; $EpCAM^-$ in breast cancer suggesting that this CTC population was able to form brain metastasis[101]. Related to the CD36 fatty acids transporter, it is known that its expression can be associated with the addition of OA to the CTC cultures. Previous work showed that after exogenous addition of OA to breast cancer samples, CD36 expression increased, followed by accumulation of cytoplasmic LDs only in CD36-expressing cells[199]. These findings are in agreement with our previous work where we observed an

accumulation of cytoplasmic LDs in breast cancer cells after the addition of NEs, which lead to increased cell viability[95].

Due to CD36 is a marker that has been associated with certain myeloid cells, we decided to check whether *CD36* expression could come from PBMCs co-habiting in the culture. To this end, we compared the relative expression of CTCs and PBMCs before and after culture. **Figure 32** presents that we detected a notable overexpression in cultures of CTCs ($p = 0.002$) while PBMCs after culture just showed a slight increase ($p = 0.64$).

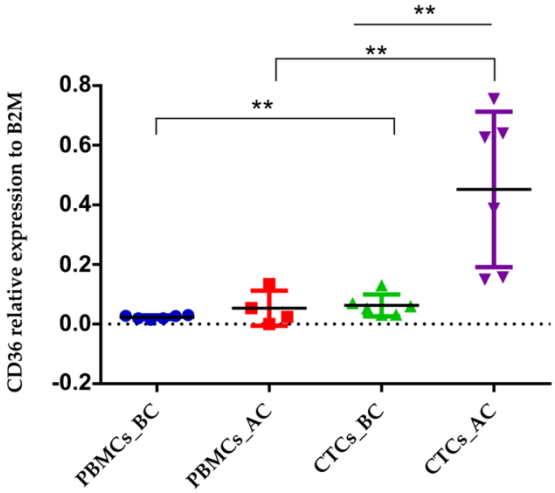

Figure 32. Relative gene expression of *CD36* gene. Relative gene expression is related to *B2M*. Analysis was performed for PBMCs Before Culture (BC, red) and After Culture (AC, blue) and paired CTCs before culture (BC, green) and After culture (AC, purple).

Therefore, we found that cultures of CTCs showed mesenchymal and stem features, together with breast specific markers. Furthermore, their genetic profiles differ from paired cultures of PBMCs, reinforcing the tumoural origin of cells from the short-term culture.

Accordingly, it has been reported that EMT induction leads to stem markers expression and increased tumorigenic capacity in mouse models[200,201] and that the EMT program led to a spectrum of cell states with mixed epithelial and mesenchymal characteristics. Importantly, only those cells with the intermediate phenotype and stem feature associate with

metastatic spread[202]. This agrees with our data since we saw that the cells that survive in culture show mainly stem or mesenchymal features. Regarding EMT, previous works have reported how CTCs in the blood circulation suffered from fluid shear stress, promoting EMT phenotype and maintained pre-existing mesenchymal cells[203]. Hence, most tumour cells released into circulation can be eliminated by fluid shear stress and if so, those CTCs capable of surviving and resisting fluid shear stress should be the subpopulations capable of generating metastatic tumours *in vivo* or cultures of CTCs *in vitro*.

In this study, there is a limitation due to the lack of pheno- and genotypic characterization of samples. Through immunofluorescence, we can evaluate the co-expression of markers, but we have limited the number of genes explored. This is something that we have tried to replace with the gene expression analysis, although it does not offer exhaustive information on how the co-expression of genes takes place. It is necessary to consider that once the cells are plated, the manipulation and removal of small amounts for analysis on many occasions conditions its culture continuity. Therefore, characterization was not carried out in each sample included in the study.

2.3.5. CTC cultivability and RBCs presence in culture samples predict patient progression

To identify markers with prognostic value, we next performed a survival analysis. To this end, two parameters were observed: (i) the cultivability of CTCs and (ii) presence of RBCs at the beginning of the cell culture.

First, considering (i) the cultivability of CTCs cultures (+ or – based on being > 23 days), (**Figure 33A**), we assessed if this parameter could predict the PFS and the OS. **Figure 33B** shows that patients whose samples established cultures (+), had shorter times to progression ($p = 0.008$, log-rank test, 354 vs 84 days; n = 48). Likewise, if only samples that have paired CellSearch® data are considered, cultures (+) also predicted shorter PFS ($p = 0.002$, log-rank test, 365 vs 84 days; n = 32), (**Supporting Figure S5A**). In

contrast, presenting ≥ 5 CTCs (measured by CellSearch®) did not predict patients PFS in this study (p = 0.2, log-rank test, 147 vs 85.8 days; n = 32), (**Figure 33C**). It is important to highlight that only 53 % of samples were positive for CTCs by Cellsearch® (cut-off of ≥5 CTCs) compared with 75 % of cultivability in this cohort. Therefore, it should be influencing that the enumeration of CTCs was performed using an epitope-dependent technology (Cellsearch®) that bases its isolation on $EpCAM^+$ cells, missing stem/mesenchymal cells-like phenotype. In contrast, for *in vitro* culture we use a negative enrichment approach that isolates all populations of CTC^{168}. For this reason, the comparison of both systems might be biased, and the lack of association may be precisely due to the different subpopulations that could be contributing to the cultivation and its success.

Furthermore, considering only 1 sample per patient a culture (+) was also predictive (p = 0.05, log-rank test, n = 34), (**Supporting Figure S5B**). For this last sample's cohort, the culture success was 76.47 %.

Regarding OS, **Figure 33D** shows that culture (+) was not a predictive factor in these samples (p = 0.3, log-rank test, 596 vs 317 days; n = 48). Still, the mean OS times of both groups were significantly different (592.5 vs 158 days, p = 0.01). Conversely to PFS analysis, having ≥ 5 CTCs was linked with shorter OS (p = 0.01, log-rank test, 749 vs 167 days; n = 34), (**Figure 33E**).

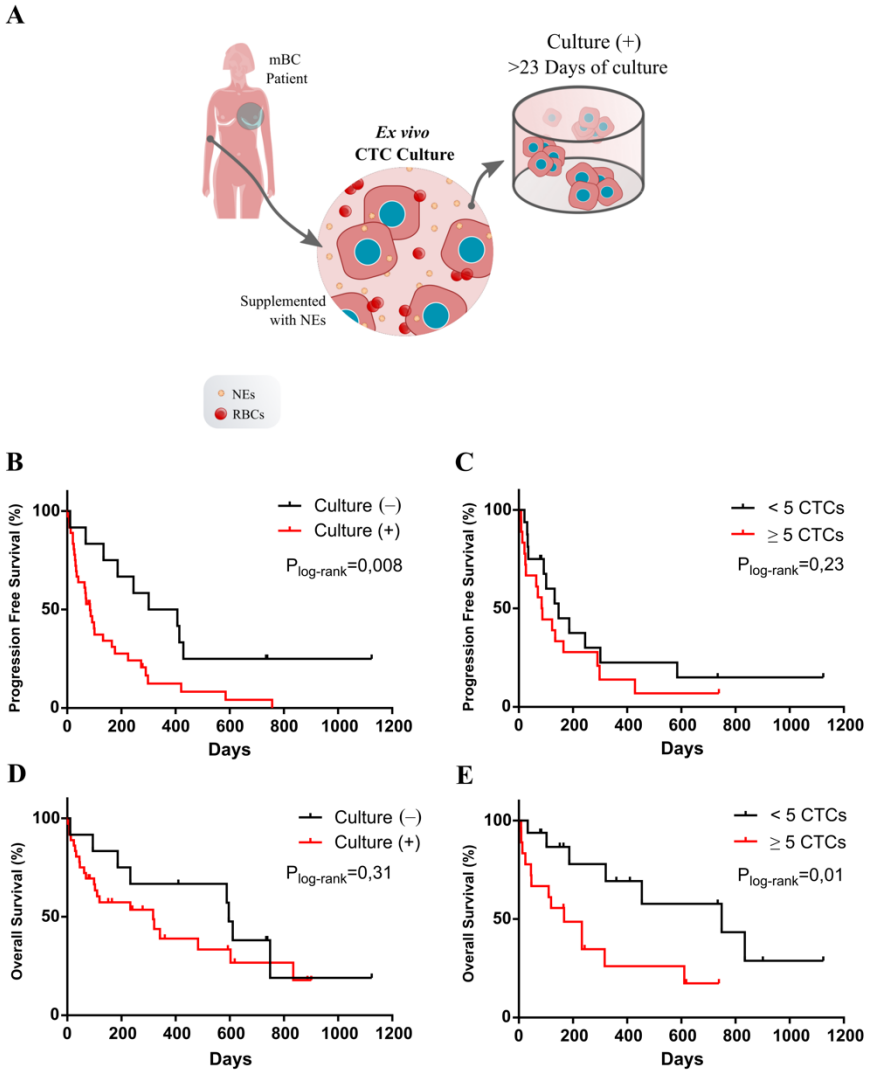

Figure 33. Scheme of CTC cultivability and Kaplan–Meier plots for CTC cultivability and for CTCs enumeration by CellSearch® system. (A) Scheme of culture of CTCs from metastatic breast cancer patients and their observation of culture (+), > 23 days in culture; (B,D) Kaplan-Meier plots for Progression-Free Survival (PFS) and Overall Survival (OS) for cultivability (culture negative (black) or positive (red))**;** (C,E) Kaplan-Meier plots for CTCs enumeration by CellSearch® system (≥5 CTCs (red) or < 5 CTCs (black). *p*-values were calculated using the log-rank test.

Second, we considered (ii) the presence of RBCs in the culture (**Figure 34A**) establishing the criterion of RBCs (+) or RBCs (–) based on the amount of RBCs in culture (**Figure 34B**). We observed that RBCs (+) cultures were linked to a worse patient outcome: PFS ($p = 0.03$, log-rank test, 443 vs 99 days, n = 31), (**Figure 34C**) and OS ($p = 0.04$, log-rank test, 834 vs 454, n = 31), (**Figure 34D**). Likewise, considering the other two cohorts: only those samples with paired CellSearch® data (**Supporting Figure S5C**) and the one with just one sample per patient (**Supporting Figure S5D**), we observed that RBCs presence was also a predictive factor for PFS ($p = 0.01$ and $p = 0.05$, respectively). More in detail, the amount of RBCs observed in culture correlated with shorter both PFS and OS ($p = 0.05$ and 0.03, respectively), (**Supporting Figure S5E and F**). These results indicate that the presence of RBCs, evaluated at the beginning of culture, is linked with a worse patient's outcome although it does not influence the success of the culture. Unspecific RBCs isolated in the CTC-enriched fraction were mainly seen in patients with advanced disease, but not in patients in early stages or healthy donors (data not shown). It has been described that oncologic patients display anaemia and coagulation issues[204–206] but as far as we know, the causes are unknown. The non-specific isolation of RBCs in patients with breast cancer could reflect these imbalances in hematopoietic homeostasis due to bone marrow affectation or other alterations derived from the therapy or the general state of these patients.

Altogether, our results suggest that the short-term culture of CTCs, as well as the presence of RBCs, could be useful tools in the clinic, due to their predictive value of patient's outcome. Since the results are rapid (on day 23 or immediately, respectively), those patients with positive cultures or the presence of RBCs may require more exhaustive follow-up.

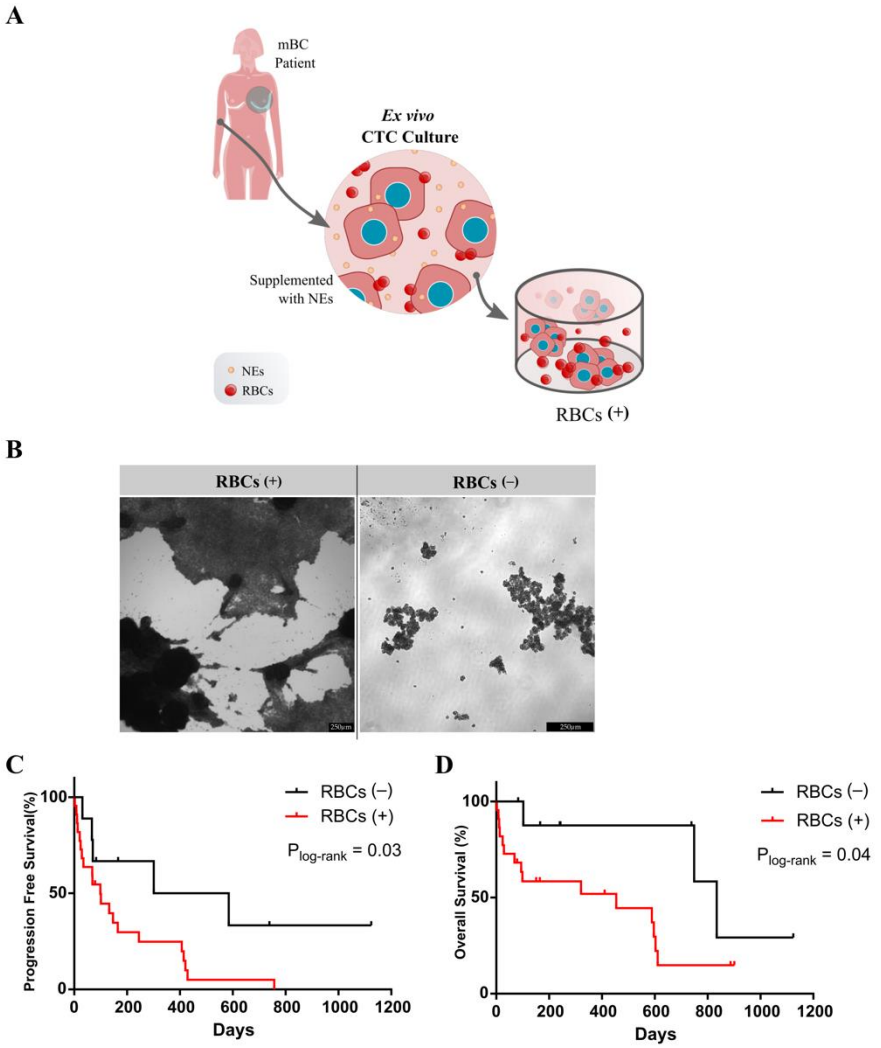

Figure 34. RBCs presence in CTC cultures images and Kaplan–Meier plots for Progression-Free survival (PFS) and Overall Survival (OS). (A) Scheme of presence of RBCs in cultures of metastatic breast cancer patients; (B) Representative images of RBCs in co-culture with CTCs. In the left panel, the number of RBCs is high, forming a network among them and with the cells (RBCs (+)). In the right panel, RBCs are present in low density in the culture (RBCs (–)); (C) Kaplan-Meier plot for PFS; (D) Kaplan-Meier plot for OS. Kaplan-Meir plots are for presence of RBCs (red) or absence (black) observed in the culture. *p*-values were calculated using the log-rank test.

2.4. Conclusions

In the present section of the thesis, we have described for first time the use of NEs to support short-term cultures of CTCs from metastatic breast cancer patients. Interestingly, samples included in this work represent real patients CTCs, adding more value to the study. Moreover, to our knowledge this is also the first time that shelf-life culture of CTCs is a predictive factor in metastatic breast cancer. The analysis of CTCs in culture has also allowed us to study the precursor cells, characterized by presenting mesenchymal and stem features. In addition to culture capacity, the presence of RBCs in culture is also of great relevance to predict patient outcome.

Therefore, once validated the benefit effect of NEs in cultures of CTCs isolated from patients, our formulation could represent an opportunity to use them as the base of an isolation device. To achieve that, NEs could be functionalized with ligands that recognize cell membrane proteins on the CTCs.

Chapter 3

Chapter 3.

Peptide-functionalized nanoemulsions for their immobilization on chip surfaces: a tool for isolation and support *ex vivo* culture of CTCs

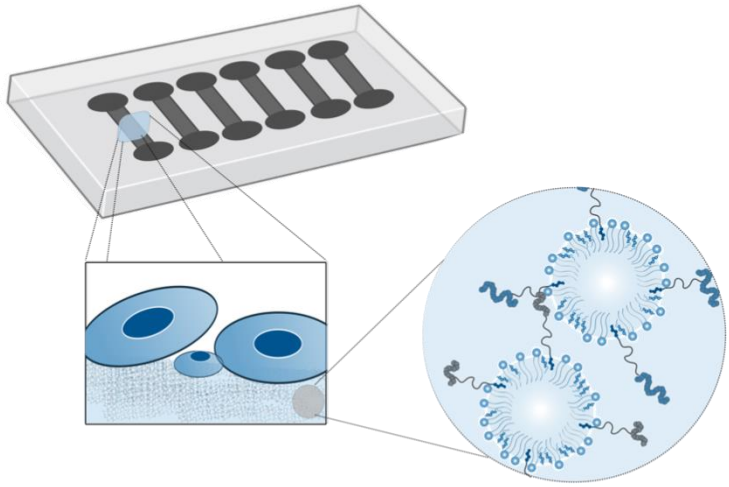

CHAPTER 3

Peptide-functionalized nanoemulsions for their immobilization on chip surfaces: a tool for isolation and support *ex vivo* culture of CTCs

This chapter has been partially developed at the Laboratory for Cell Mimicry (Dr. Brigitte Städler), in the Interdisciplinary Nanoscience Center (iNANO) at Aarhus University (Denmark).

Abstract

From liquid biopsy, CTCs represents a useful tool to understand the biology of metastasis in cancer disease. However, there is a lack of standardized protocols to isolate and to culture them. In the two previous chapters of this thesis, we reported the development and validation of our NEs to support CTC cultures from metastatic breast cancer patients. On this line, in the present work Peptide-Functionalized Nanoemulsions (Pept-NEs) were formulated to develop a tool for CTC isolation, with the final aim to use them immobilized on the surface of microfluidic devices.

The idea was to develop a versatile platform for the isolation of different populations of CTCs. To achieve that, the approach was to functionalize our NEs with peptides against specific cell membrane proteins. Accordingly, we performed a proof of concept of this system by using two different peptides: Pep10 and GE11, that targets EpCAM and EGFR, respectively. Once Pept-NEs were formulated and characterized, it was demonstrated by Quartz Crystal Microbalance with Dissipation Monitoring (QCM-D) that they could be immobilized on the surface device using a layer of polylysine (PLL). Moreover, using QCM-D, it was also confirmed their ligand-binding specificity. Additionally, a cell viability study was performed to determine that Pept-NEs immobilized on the surface of plates allowed culture along 9 days.

Graphical abstract

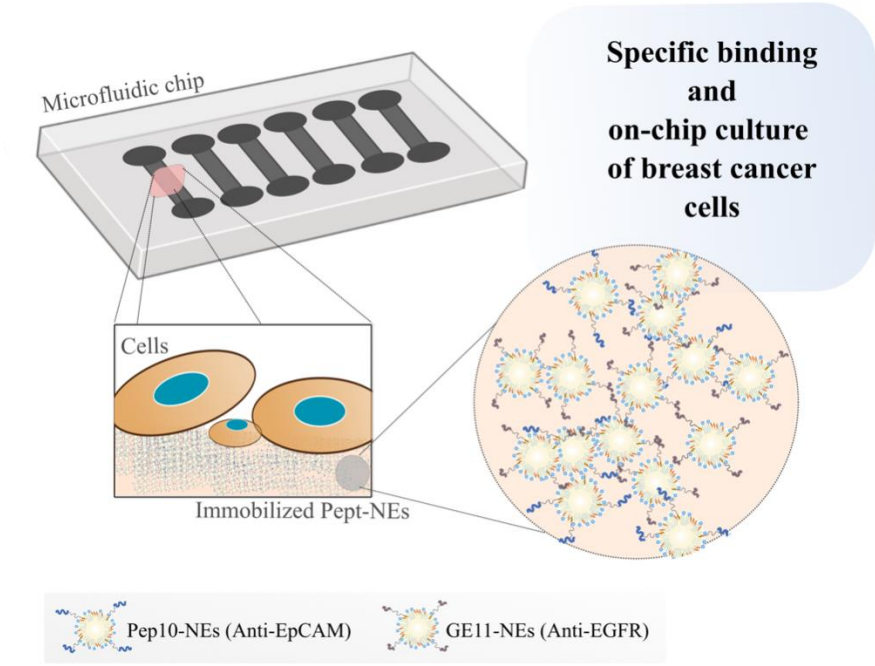

3.1. Introduction

Metastasis is one of the main causes of cancer death, that consists in a dynamic succession of events involving the dissemination of tumour cells[207]. These cells, called CTCs, are shed from primary tumour and travel through the blood to finally colonize distant organs generating a new metastatic niche[208]. Liquid biopsy refers to any technique that detects and analyses circulating biomarkers in body fluids, most notably blood. For their characteristics, liquid biopsy is revolutionizing the early detection of cancer by allowing physicians to monitor the blood, instead of taking a tissue sample (conventional solid biopsy), providing patient information in real time in a less invasive manner. Regarding liquid biopsy in cancer disease, various circulating biomarkers have been studied such as exosomes, ctDNA, functional mRNA, CTCs, etc. However, among all these biomarkers, CTCs are a powerful tool in research and clinics, mainly because CTCs allow to analyse the whole genetic material and they can be used in different functional downstream analyses. Therefore, these cells give an in-depth knowledge about the disease and its evolution[209,210]. Accordingly, molecular analysis of CTCs has become an outcome predictor in several types of cancer, including breast[211–214], prostate[215], colon[74,216], liver[217], and bladder[218] cancers. However, CTCs isolation remains a challenge for clinical use because of the rarity and heterogeneity of these cells, in part due to the continuous evolution in their biomarkers through EMT or MET[219,220].

When it comes to CTC enrichment, there are mainly two strategies used for their capture: (i) based on their biological features (or label-dependent enrichment) and (ii) on their physical properties (or label-independent enrichment)[221,222]. Relatedto their biological properties, the most relevant tool in this field is the CellSearch® system (Menarini Silicon Biosystems, Inc.). This system is the only device approved by the US FDA for clinical application. It is used to make a prognosis of tumour recurrence of metastasis in breast, prostate, or colorectal cancer[223]. This is an EpCAM-based detecting system. It consists in EpCAM antibodies conjugated to magnetic beads; presenting a powerful system for clinicians, although it is not able to distinguish between heterogenic tumour subpopulations and not

capture low EpCAM-expressing cells. Related to their physical properties, there are several different strategies including size-based (Parsortix® device, Angle) or density-based approaches (OncoQuick®, Greiner Bio-One). Despite the advances in new technologies marketed in recent years, it does not exist a technology either based on their biological or physical properties that can be applied as a standard method for CTCs isolation and culture. To solve this, the exploitation of combining both, biological and physical characteristics, has gained importance using microfluic devices such as Target Selector™ (Biocept, Inc.) platform, IsoFlux (Fluxion Bioscience, Inc.) or ^{HB}CTC-Chip[224]. Microfluidic chips attract more attention than other systems due to their inner features such as easily integration multifunction, continuous sample processing, reduction of sample consumption and changeable chip design; allowing high-speed, high specificity, high-throughput, and easy for operation[225].

To promote clinical application of CTCs, smart biomaterials in combination with microfluidics might be develop. Based on that, to address current limitations of CTCs isolation technologies, we have developed a bottom-up methodology to formulate Peptide-Functionalized Nanoemulsions (Pept-NEs), which in combination with a microfluidic device could isolate target cancer cells. The workflow for this study is represented in the **Figure 35**. As showed in the Chapter 1 of this thesis, we developed NEs that showed a supporting effect on culture of breast tumoural cells[95]. Being NEs biodegradable and biocompatible, we decided to use this formulation as the basis of our isolation nano-platform. Due to CTCs exhibit some specific biomarkers, such as EpCAM and EGFR, we propose the use of immune recognition to specifically isolate cells expressing these specific antigens with higher specificity. To obtain the Pept-NEs, NHS ester was chosen as reactive chemical group to directly conjugate the two synthetic peptides: GE11 and Pep10. Specifically, EGFR is targeted with GE11 peptide and EpCAM is targeted with Pep10 peptide. Hence, using two different Pept-NEs: GE11-NEs and Pep10-NEs, we are able of targeting the different cancer populations by immobilizing these Pept-NEs on microfluidic chips, affording gentle and efficient isolation of CTCs.

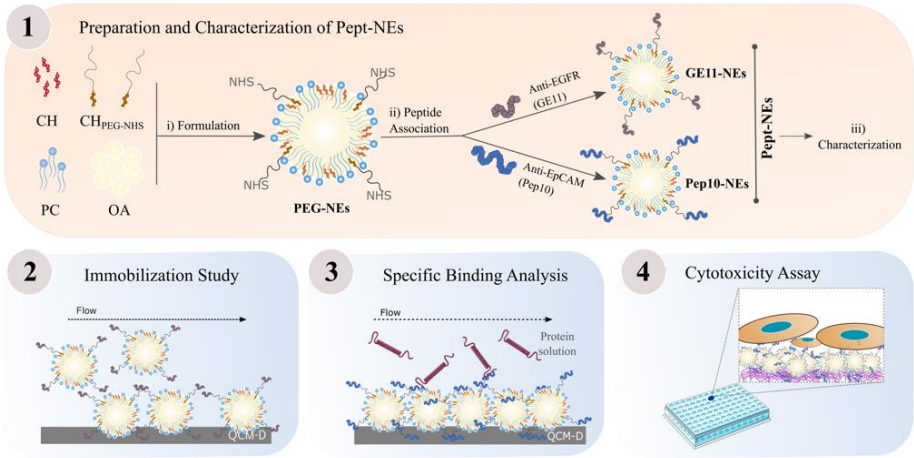

Fig. 35. Workflow for the Development and Characterization of Peptide-functionalized Nanoemulsions (Pept-NEs). (1) First, preparation and characterization of Pept-NEs: i) formulation of PEG-NEs, ii) association with two peptides (GE11 and Pep10) to obtain: GE11-NEs and Pep10-NEs, and iii) characterization; (2) Second, study of the immobilization of Pept-NEs on surfaces by Quartz Crystal Microbalance with Dissipation Monitoring (QCM-D); (3) Third, study of their specific binding ability to their targeted protein by QCM-D; (4) Forth, study of the cell viability after a culture of 9 days on Pept-NEs functionalized plates.

3.2. Materials and methods

3.2.1. Materials

Lipoid® S100 PC (18:0/18:1) from soybean (94%) was a gift from Lipoid GmbH. Cholesterol Polyethylene glycol N-Hydroxysuccinimide (CH PEG NHS) (MW:2 kDa was purchased from NANOCS. OA, CH, TopFluor® PC, Dymethil Sulfoxide (DMSO), Polylysine (PLL, MW 30-70 kDa), Cell Counting Kit-8 (CKK-8), trypsin with EDTA solution, Acetic Acid Solution, FBS, BSA, and penicillin-streptomycin, were purchased from Sigma-Aldrich. Ethanol absolute was purchased from Scharlau. Amicon®, Ultra-4 100K centrifugal filters were provided by Merk Millipore. MQ-water was purified by Millipore® Direct-Q® 3 with UV system. dPBS, and DMEM High glucose was purchased from Biowest. Tissue culture dishes (100mm) were provided by VWR. Black 96-well plates and ultra-low-attachment 24-well plates were purchased from Corning. Paraformaldehyde solution (PFA) 4% in PBS and NucBlue™ Hoechst 33342 dye were purchased from Thermo Fisher Scientific. Human EGFR protein (His Tag-Biotinylated) (630 aa, MW: 69.8 kDa), Human EpCAM protein (His Tag-Biotinylated) (253 aa, MW: 29 kDa) were provided by Sino Biological. All peptides were purchased from GenScript:GE11 (12aa: YHWYGYTPQNVI), fluorescent GE11 (13aa; sequence: YHWYGYTPQNVI{K(TMR)}, Pep10 (23aa; sequence: VRRDAPRFSMQGLDACGGNNCNN) and fluorescent Pep10 (24aa; sequence VRRDAPRFSMQGLDACGGNNCNN{K(TMR)}).

3.2.2. Cell cultures

All the cell lines used in this paper were purchased from Sigma-Aldrich. The human breast cancer MCF-7 and MDA-MB-231 cell lines were cultured in DMEM-High glucose medium. Cell culture media was supplemented with 10 % fetal bovine serum and 1 % penicillin-streptomycin. The cells were cultured at 37 °C in a humidified atmosphere containing 5 % CO_2. At 85 % confluence, cells were harvested using 0.05 % Trypsin-EDTA (5 min, 37 °C).

3.2.3. Preparation of peptide-functionalized nanoemulsions (Pept-NEs): GE11-NEs and Pep10-NEs

3.2.3.1. Formulation of PEGylated nanoemulsions (PEG-NEs)

PEG-NEs with the crosslinking reagent (NHS ester) on the surface were formulated at 1mL scale by low-energy self-emulsification oil in water (O/W) method. Briefly, stock solution of lipids PC (10 mg/mL), CH (10 mg/ml), CH linked to a polyethylene glycol chain-terminated N-Hydroxysuccinimide (CH PEG NHS) (10 mg/mL), and OA (100 mg/mL), were prepared in ethanol. The concentration of the stock solution of CH PEG NHS used in the formulation was calculated following protocol recommendations for NHS ester reactions. In case of fluorescently labelled formulations a stock solution of TopFluor® PC (1 mg/mL) was additionally used. Then, lipids were mixed to obtain an organic phase at final molar percent: 3.45% PC, 3.38% CH, 0.65% CH PEG NHS, 92.48% OA, and 0.05% TopFluor® PC. The organic phase (100 μL) was quickly injected into the deionized water (900 μL), under magnetic stirring at room temperature. After 15 minutes, stirring was stopped and the PEG-NEs with the NHS ester surface ending were obtained. PEG-NEs formulation was concentrated and purified using one Amicon® Ultra-4 100K filter at 3,234 xg, 29 min at room temperature (**Figure 36**).

3.2.3.2. Conjugation of GE11 and Pep10 peptides on the surface of PEG-NEs

To endow PEG-NEs with active targeting capability to CTCs, two peptides (GE11 and Pep10) were conjugated to obtain the Pept-NEs: GE11-NEs and Pep10-NEs, respectively. First, peptides stocks were prepared at 0.5 mg/mL, for Pep10, the solvent used was MQ-water and for GE11 a solution of ratio 1:1 of MQ-water and 10 % acetic acid was used. In brief, concentrated previously synthesized PEG-NEs, were incubated with Pep10 (0.0195 mg/mL) or with GE11 (0.0163 mg/mL) in 1mL of dPBS (pH 7.4) for 30 min at room temperature under magnetic stirring (**Figure 36**).

Resulting GE11-NEs and Pep10-NEs were isolated from non-conjugated peptides using Amicon® Ultra-4 100K filters by centrifuged them at 3,234 xg, 20 min (room temperature conditions). The filters allow to retain components bigger than 100,000 Da, as PEG-NEs, while components with lower sizes, like peptides (GE11 (1,377 Da) and Pep10 (2,496 Da)) and free lipids passes though the filter. Then, both formulations were washed with MQ-Water twice, using the same Amicon® Ultra-4 100K filters and centrifugation at 3,234 xg, 20 min at room temperature. Finally, samples were re-suspended in MQ-water for its storage in a final volume 1 mL (**Figure 36**).

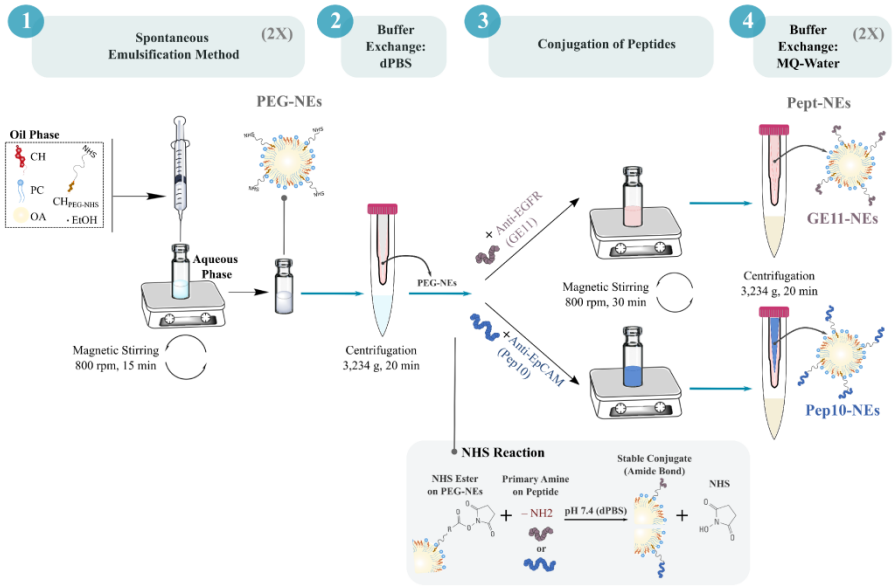

Fig. 36. Schematic representation of the formulation procedure to obtain the Pept-NEs (GE11-NEs and Pep10-NEs). The four main steps in the procedure are: (1) spontaneous emulsification (performed twice (2X) to obtain 2 mL of PEG-NEs), (2) buffer exchange (from MQ-Water to dPBS), (3) Conjugation of peptides using 1 mL of PEG-NEs for each peptide (the chemical reaction is represented in the grey box), and the last step (4) is performing a second buffer exchange (from dPBS to MQ-Water) to storage. This buffer exchange is carried out twice to ensure that buffer exchange is completely achieved.

3.2.4. Characterization of Pept-NEs

3.2.4.1. DLS, surface charge analysis and NTA

Mean average size (z-average) and their PdI were determined by DLS at room temperature using Malvern® Zetasizer® (Nano ZS90, Malvern). ζ-Potential was determined using electrophoretic cells (Malvern). Concentrations of GE11-NEs and Pep10-NEs were determined by NTA using the NanoSight instrument (Malvern). All measurements were taken using a 1:100 v/v dilution ratio in MQ-water. The stability of Pept-NEs stored at 4 ºC was measured (size, PdI and ζ-Potential data were acquired once a month for a period of 3 months).

3.2.4.2. TEM analysis

25 µL of GE11-NEs and Pep10-NEs were mixed separately with 25 µL of 2 % sodium phosphotungstate. Once were negatively stained, were dropped on carbon support films for 2 min. After washing with MQ-Water and drying overnight (vacuum conditions), the samples were observed by TEM (JEOL 2010 TEM).

3.2.4.3. Determination of peptide concentration of Pept-NEs formulations

Fluorescently labelled peptides ($GE11^{(TMR)}$ and $Pep10^{(TMR)}$) were used to prepare standard curves of peptides for GE11 and Pep10, respectively. Hence, fluorescently labelled peptides were used also in the formulation of the Pept-NEs to obtain $Pept^{(TMR)}$-NEs to calculate the association efficiency of the peptide onto PEG-NEs. Firstly, fluorescence intensities of peptides ($GE11^{(TMR)}$ or $Pep10^{(TMR)}$) at increasing known-concentrations were read on FLUOstar OPTIMA (BMG LABTECH) multimode plate reader in the presence of a constant concentration of PEG-NEs to prepare the standard curve. This constant concentration of PEG-NEs was used due to the scattering influence of nanoemulsions. Secondly, intensity of the $Pept^{(TMR)}$-NEs samples ($GE11^{(TMR)}$-NEs and $Pep10^{(TMR)}$-NEs) at the same NP

concentration were also read to determine peptide concentration in the two formulation. Finally, the unknown-concentration of peptide on Pept$^{(TMR)}$-NEs samples were determined using the previous standard curves. The measurement condition was fluorescent excitation wavelength, 544 nm, and fluorescent emission wavelength, 590nm.

3.2.5. Quartz crystal microbalance with dissipation monitoring (QCM-D) experiments

QCM-D experiments (Q-Sense E4, Sweden) were performed to analyse the adsorption behaviour of the PEG-NEs onto surfaces (immobilization) and to study the specific binding of the Pept-NEs for their receptors. Before starting any experiment, QCM-D crystals were cleaned by immersion in a 2 % sodium dodecyl sulphate solution overnight and rising with MQ-water. Then, crystals were blow-dried with N_2, followed by exposure to UV for 20 min. For all experiments, the frequency changes (ΔF) and dissipation changes (ΔD) were monitored at 24 ± 0.02 ºC.

First, to determine the optimal surface and buffer required for the immobilization, three different surfaces were required: (1) gold-coated crystals (QSX301, Q-sense), (2) silica-coated crystals (QSX300, Q-sense), and (3) PLL precoated silica crystals (QSX300, Q-sense). Furthermore, three different buffers were used: (A) MQ-Water, (B) dPBS and (C) HEPES2 (10 mM HEPES, 150 nM NaCl, pH 7.4). In the particular condition of the PLL precoated silica crystal, when a stable baseline in buffer solutions were achieved, the polymer solution (1 mg/mL of PLL, in the corresponding buffer) was introduced into the measurement chamber and left to adsorb onto the silica crystal. In this case, after the surface was saturated, the chamber was rising with buffer solutions to remove the excess polymer. Once precoated with PLL, this surface and the other two (Au and silica crystals) were exposed to negatively charged PEG-NEs and incubated until surfaces were saturated. The PEG-NEs were introduced in the chambers using a 1:2 v/v dilution ratio in the corresponding running buffer. Then, corresponding buffer solution for each condition was introduced for

washing. After that, PEG-NEs layer stabilities were analysed in the different conditions.

Second, to study the specific binding ability of the Pept-NEs against their targets, only PLL precoated silica crystals and MQ-Water (as running buffer) were used. Once achieved the polymer coated surface (1 mg/mL PLL, MQ-Water), solutions of GE11-NEs and Pep10-NEs were exposed separately to the PLL layer and let to incubate until surfaces were saturated (both formulations were introduced using a 1:2 v/v dilution ratio in MQ-water). The Pept-NEs solutions introduced into the chambers were replaced with MQ-water and the experiment continued by introducing EpCAM or EGFR protein solutions at a concentration of 0.8 µg/mL (MQ-Water). All experiments were carried out in duplicates, under a continuous flow (150 µL/min). The third overtone was used to present normalized frequencies. The increase of mass on the surface (adsorption effect) is reflected by a negative ΔF (bars point upwards). Desorption effect or any phenomenon leading to mass loss results in a positive ΔF (bars point downwards).

3.2.6. Fluorescence microscopy

For imaging the specific binding for their targeted cells, fluorescently labelled Pept-NEs and the bare PEG-NEs were formulated using TopFluor® PC. MCF-7 and MDA-MB-231 were seeded at a final concentration of 30,000 cells/mL in 0.2 mL per well (ibidi 8-wells plates) and let to attach overnight. Then cells were fixed using 4 % cold PFA in PBS (15 min, room temperature) and washed 3 times. Once fixed, they were let to interact with PEG-NEs, GE11-NEs or Pep10-NEs during 30 min at room temperature. In cases of negative control (PBS was used instead). After that, samples were washed 3 times with PBS and NucBlue™ (Hoechst 33342 dye) was added for nucleus staining. Leica DMi8 automated Microscope (Leica Microsystems) was used equipped with corresponding filters to take the images. The 63X oil immersion objective was used.

3.2.7. Cell viability analysis

CKK-8 kit was used to analyse the viability of the cells incubated with the immobilized formulations (PEG-NEs, GE11-NEs and Pep10-NEs); PLL and the wells without adding any extra layer (Ø) were used as controls. First, 1 mg/mL of PLL solution in MQ-water was add to each well (only in case of the conditions: PLL, PEG-NEs, GE11-NEs and Pep10-NEs). This PLL solution was incubated during 5 min and washed 2 times using MQ-water. Second, stock formulations (PEG-NEs, GE11-NEs and Pep10-NEs) were added in the wells using a 1:2 v/v dilution ratio in MQ-Water (50 µL/well). In the same way, conditions Ø and PLL were only treated with 50 µL/well of water. After 1 hour of incubation, wells were washed twice with MQ-Water and lastly washed with DMEM-HG. Then, MCF-7 and MDA-MB-231 in DMEM-HG were seeded in these pre-treated plates (1,000 cells/well in 100 µL). Times measured were: 0, 1, 3, 6 and 9 days (t0, t1, t3, t6 and t9, respectively). Media was refreshed every 3 days. For all time measurements, 10 µL CCK-8 were added to each well and cells were incubated for 2 h at 37 ºC, 5 % CO_2. Finally, 100 µL of the solution from each well was transferred to a new plate and measured by multimode plate reader (Infinite M1000, Tekan) at 450 nm. Three independent repeats were performed for all conditions.

3.2.8. Statistical analysis

Statistical analysis was performed using GraphPad Prism 6.01 software (GraphPad Software Inc., La Jolla, CA, USA). Student's t-test was used for the comparison of two group analyses. In cases of *p* values less than 0.05 the result was considered statistically significant.

3.3. Results and discussion

3.3.1. Formulation and characterization of Pept-NEs

The capability of NEs to support proliferation in CTC culture was proved in Chapter 1[95]. In the present chapter, the aim was to endow NEs to specifically recognize breast cancer CTCs. Accordingly, the final goal is to develop a nanotechnology-assisted isolation chip, for CTC capture and culture. This approach is based on the idea of providing a versatile platform, where different peptides are used to functionalize NEs. The selection of the peptide would be influenced by the CTC population that want to be isolated. In this respect, two proteins were chosen for being one of the most commonly used biomarkers of breast cancer cells: EGFR and EpCAM[226,227]. In case of EGFR was previously reported to be overexpressed in triple-negative breast cancer cells[228] and EpCAM is overexpressed in breast cancer cells. Consequently, we carried out a proof of concept of the potential platform using two peptides: GE11 and Pep10, since their recognize EGFR and EpCAM, respectively.

These peptides have been used in other studies for the functionalization of NPs, but they are mostly applied in nanotechnology to assist therapy. For example, GE11 peptide-modified reversibly cross-linked polymersomal doxorubicin was designed for ovarian cancer treatment. Their good results in *in vivo* studies using SKOV3 human ovarian tumours, which overexpress EGFR, are mainly because of the efficient targeting of the peptide. As a result, this approach has emerged as an advanced alternative to currently Lipo-Dox for treatment of EGFR-overexpressing ovarian cancers[229]. Moreover, this peptide was used to capture liver CTCs using lipid bilayers with higher CTC capture for hepatic carcinoma cells than CellSearch®[230]. Regarding Pep10, this peptide has been used for the isolation of $EpCAM^+$ CTCs. Wang's identified this peptide by cell-based selection and functionalized 200 nm magnetic NPs for spiked breast, prostate, and liver cancer cells from human blood[231].

In this context, to functionalize NEs formulation with these peptides, the original formulation was modified by the addition of a CH-PEG with N-

Hydroxy Succinimide ester (NHS) ending group, into the standard formulation (PEG-NEs). The modification of NEs allowed the binding of GE11 and Pep10 peptides on the PEG-NEs surface, obtaining GE11-NEs and Pep10-NEs, respectively (**Figure 37A**). The NHS ester was chosen as crosslinker reactive group because, is one of the most commonly crosslinkers used to obtain a strong covalent chemical attachment between peptides and primary amines ($-NH_2$)[232]. Therefore, the NHS ending group onto NEs surface, allowed the covalent reaction between the ester (NHS) and the amino tail groups from the peptides, in basic conditions (pH 7.4), after a short time incubation (30 min). Nowadays, most of the CTC isolation technologies are based on nanomaterial surfaces decorated with antibodies, but here we used peptides as novel approach, since compared with antibodies, peptides are stable, small, and easy to synthesize in large amounts[233]. Moreover, EpCAM recognition peptide was described to presents better binding affinity than EpCAM antibody (Pep10 K_D is 1.98 x 10^{-9} mol/L and EpCAM antibody K_D is 2.69 x 10^{-10} mol/L) in a previous study[231].

Formulations were characterized in terms of hydrodynamic sizes for PEG-NEs, GE11-NEs and Pep10-NEs (**Figure 37B**). NTA was performed for Pept-NEs (**Figure 37C**). All formulations were less than 200 nm. PdI was lower than 0.2, suggesting good monodispersity for the three formulations (**Figure 37B**). Furthermore, ζ-Potentials were measured, and results suggested effective peptide functionalization; GE11-NEs, that contains GE11 peptide (positive overall charge peptide) presented a more positive ζ-Potential value than PEG-NEs while Pep10-NEs, that have Pep10 (negative overall charge peptide) showed more negative ζ-Potential than the initial PEG-NEs formulation (**Figure 37B**). In addition, TEM images showed that the two Pept-NEs present spherical shape (**Figure 37D**). At the same time, Pept-NEs concentrations (NPs/mL) were determined by NTA, proving the reproducibility of the synthesis process to obtain Pep-NEs (**Figure 37E**). The final concentrations of peptides were determined using a standard curve of fluorescently labelled peptides (**Figure 37D and Supporting Figure S6**). Furthermore, it was evaluated that formulations were stable at least three months (**Supporting Figure S7**).

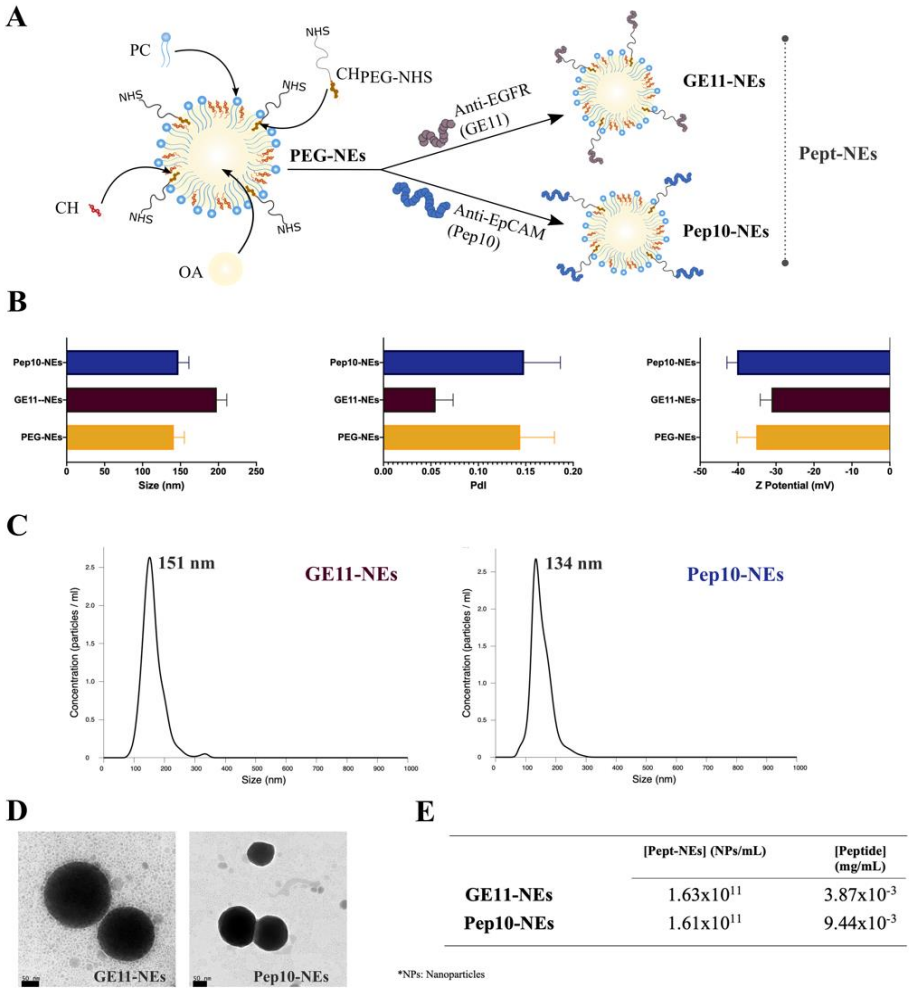

Figure 37. Characterization of PEG-NEs, GE11-NEs and Pep10-NEs. (A) Scheme for the formulation of PEG-NEs (made of Phosphatidylcholine (PC), Cholesterol (CH), Oleic Acid (OA) and cholesterol-PEG with N-HydroxySuccinimide ester-PEG modification ($CH_{PEG-NHS}$)) and the association of peptides to obtain Pept-NEs (GE11-NEs and Pep10-NEs); (B) Hydrodynamic size (nm), Polydispersity index (PdI), and ζ-Potential (mV) measurements. Values represent mean ± SD (n = 10); (C) Sizes of Pept-NEs by Nanoparticle Tracking Analysis (NTA); (D) TEM images of GE11-NEs and Pep10-NEs; (E) Pept-NEs concentrations (NPs/mL) and concentrations of the peptides at 1 mL formulation (mg/mL).

3.3.2. Immobilization on surfaces of PEG-NEs and Specific binding analysis by QCM-D

3.3.2.1. PEG-NEs immobilization analysis

To determine the optimal surface to immobilize bare PEG-NEs, their adsorption behaviours were analysed by a label-free methodology, the QCM-D[234]. The crystals used were: gold-crystals, silica-coated crystals, and PLL precoated silica crystals. To optimize and quantify the concentration of bare PEG-NEs incorporated on the Q-sensors, we monitored the frequency changes of these different QCM crystals upon the addition of PEG-NEs using three buffers: MQ-Water, dPBS and HEPES2. In case of PLL precoated silica crystals, when stable baseline was achieved, a PLL solution (1 mg/mL, in one of the three buffers) was introduced into the measurement chamber. Then, PLL solution was left to adsorb onto the crystal to form a polymer precursor layer. After the surface was saturated with PLL, the chamber was rinsed with the specific buffer solution (to remove the excess polymer). Once surface was precoated with PLL, all surfaces employed (gold-crystals, silica-coated crystals, and PLL precoated silica crystals) were exposed to the negatively charged PEG-NEs and left to flow incubate until the surface was saturated. Frequencies using the third overtone are presented in **Figure 38**. The increase of mass on the surface (adsorption of polymer/PEG-NEs) was reflected by a negative ΔF (the bar points upwards). By contrast, PEG-NEs desorption or other phenomenon leading to mass loss results in a positive ΔF (the bar points downwards). The adsorption onto the positively charged surface, PPL precursor layer, in MQ-water produces a stable monolayer of PEG-NEs, while other surfaces (gold-crystals and silica coated-crystals) and buffers (dPBS and HEPES2) do not support stable adsorption over time, as error bars indicate in **Figure 38**. For this reason, PLL precoated silica crystals and MQ-Water as buffer, were chosen as the conditions for the following experiments and for the final immobilization on chips.

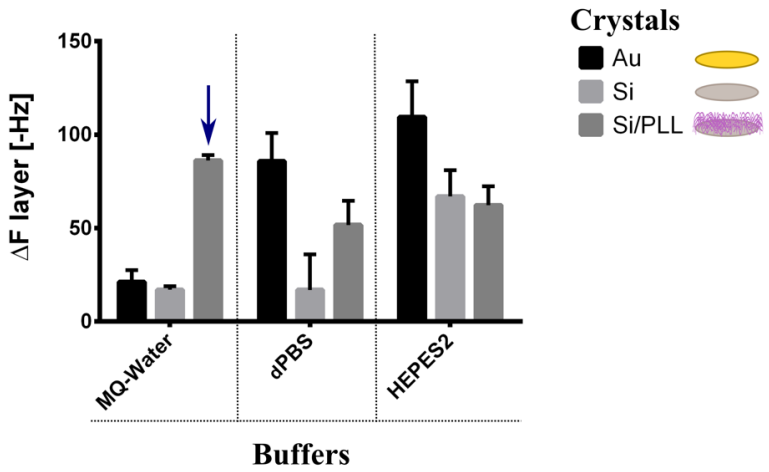

Figure 38. Immobilization analysis on surfaces of PEG-NEs. QCM-D frequency changes upon binding of PEG-NEs to different surfaces (Crystals used: gold (Au), silica (Si), and silica/polylysine (Si/PLL)) using different buffers (MQ-Water, dPBS and HEPES2). Values represent mean ± SD (n = 2). Blue arrow indicates the condition chosen.

3.3.2.2. Specific binding analysis of Pept-NEs under continuous flow

The final aim is to immobilize GE11-NEs and Pep10-NEs on chips surfaces to recognize and isolate breast cancer cells. Hence, to validate the specific recognition of these Pept-NEs for their targeted proteins, QCM-D technique was used. As previously mentioned, GE11 recognition peptide targets EGFR and Pep10 targets EpCAM (**Figure 39A**). This time, once Pept-NEs were immobilized on PLL-coated silica-crystals, protein solutions in MQ-water (EGFR or EpCAM) were introduced separately into the chambers. Then, we studied the biding affinity under continuous flow (150 µL/min). As shown in **Figure 39B**, Pep10-NEs showed the highest binding ability to EpCAM recombinant protein, while GE11-NEs presented very low binding capacity under the same conditions. This result proves that, Pep10-NEs can selectively bind to EpCAM. Surprisingly, related to EGFR, in **Figure 39B** it is possible to observe desorption or other phenomenon leading to mass loss in both cases (Pep10-NEs and GE11-NEs). On

explanation might be that due to EGFR protein has a MW of 69.8 kDa, which is much bigger than EpCAM (MW: 29 kDa), could be influencing desorption under the flow conditions chosen. Another explanation could be regarding instability of electrostatic charges, due to the cationic PLL is what immobilize the anionic Pept-NEs, EGFR solution could be breaking the electrostatic forces between PLL and Pept-NEs, losing the attachment of the Pept-NEs. In any case, GE11-NEs presents the higher desorption effect, suggesting a strong behaviour in front of its targeted protein (EGFR). Therefore, both Pep10-NEs and GE11-NEs can recognize specifically their targets: EpCAM and EGFR proteins, respectively.

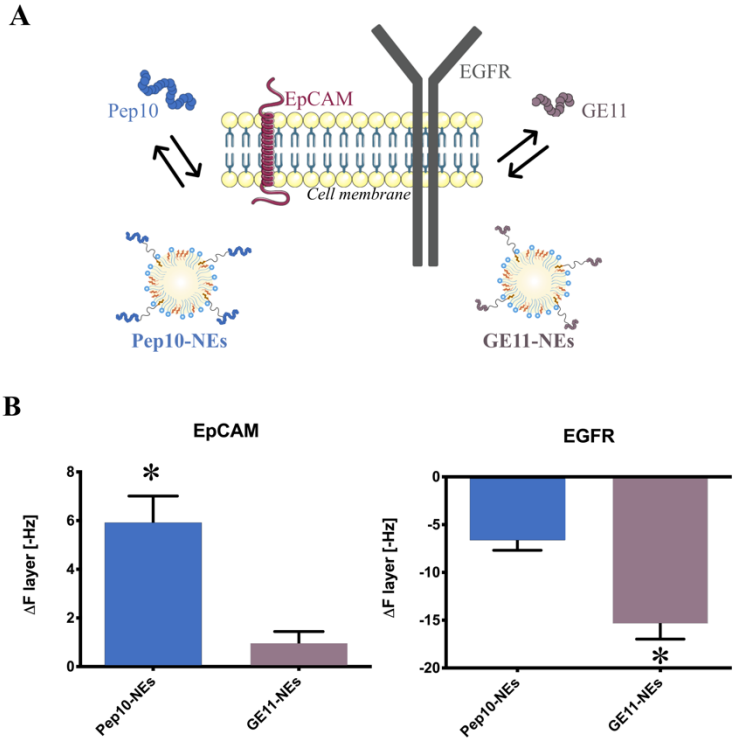

Figure 39. Specific binding analysis of Pept-NEs at protein level. (A) Diagram of targeting abilities of Pept-NEs (Pep10-NEs and GE11-NEs): ligands (GE11 and Pep10 peptides) and their receptors (EGFR and EpCAM), respectively; (B) QCM-D frequency changes upon binding of proteins (EpCAM and EGFR) to Pept-NEs (Pep10-NEs and GE11-NEs). Values represent mean ± SD (n = 2).

3.3.3. Specific binding analysis with cells by fluorescent microscopy

To determine the specific recognition of Pept-NEs for different breast cancer cells, fluorescently labelled Pept-NEs (using TopFluor® PC) were formulated to analyse by fluorescence microscopy. Additionally, fluorescently labelled PEG-NEs were formulated as negative control. Selection of the cell lines used was based on reported by Vila *et al.*, who indicated that MCF-7 and MDA-MB-231 cell lines expressed different percentage of EGFR an EpCAM. Specifically, MCF-7 cells expressed 94.25 % EpCAM and 2.79 %, EGFR, whereas MDA-MB-231 expressed 5.47 % EpCAM and 92.57 % EGFR[227]. Both cell lines were chosen to confirm the specific binding ability between the Pept-NEs and the specific cells population. The Pept-NEs showed selective binding to their cell targets. As shown in **Figure 40**, Pep10-NEs present selective biding to $EpCAM^+$ MCF-7 cells but not MDA-MB-231. Likewise, GE11-NEs demonstrated specific biding to $EGFR^+$MDA-MB-231 but not MCF-7, proving the ability of the Pept-NEs to target their specific receptors.

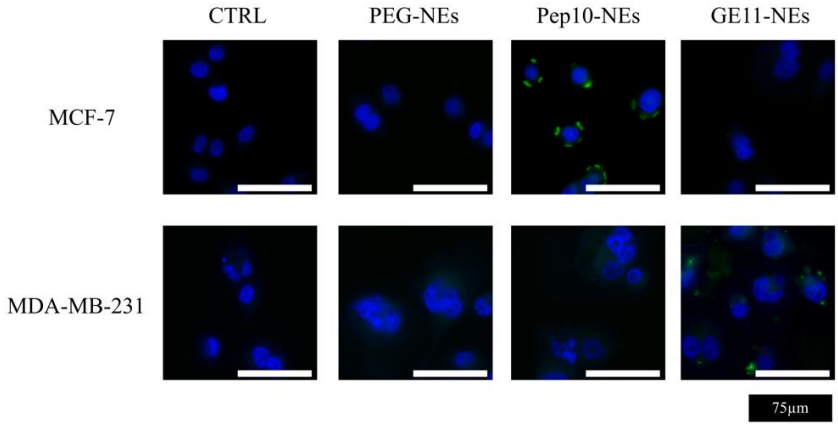

Figure 40. Specific binding analysis of Pept-NEs at cellular level. Binding analysis by fluorescence microscopy of PEG-NEs and Pept-NEs to MDA-MB-231 and MCF-7. Negative controls (CTRL) show cells without PEG-NEs or Pept-NEs incubation. Scale bar represents 75 µm.

3.3.4. Cell viability study of immobilized Pept-NEs

Once confirmed that Pept-NEs can be immobilized onto the surfaces by using an initial layer of PLL, viability assay was performed to determine that there was not cytotoxicity associated to the immobilized Pept-NEs. The experimental set-up is represented in **Figure 41A** and the concentration employed was the one used in QCM-D experiments. To mimic the situation of CTCs in a blood sample from patients, the smallest number of cells that the CCK-8 can detect were seeded (1,000 cells/well). As is shown in **Figure 41B**, non-toxicity was observed in any of the conditions during 9 days of culture. Therefore, it has been proved that Pept-NEs immobilized on the surface of chips at this concentration allowed on-chip culture. This result is very relevant, due to one of the most common challenges after the isolation of CTCs from patient's blood is their release from the capturing substrate at the end of the process. Furthermore, the possibility of an initial on-chip culture reduces the risk of cell loss, along with that maintains cell viability for establishing short-term cultures. Moreover, our Pept-NEs system could allow to harvest cell using enzymatic release such as trypsin, resulting in a less invasive method of detachment compare with other systems[92].

Initially, we hypothesize that Pept-NEs would have the same effect described for NEs, but it seems that immobilized at that concentration they do not present the positive effect in viability. Despite this, Pept-NEs were not toxic, so they still represent a good option for the base of an isolation device. Therefore, a future protocol might be: first, CTCs are captured by Pept-NEs immobilized on microfluidic devices and then, the on-chip culture of these cells is supported by adding our proliferative NEs.

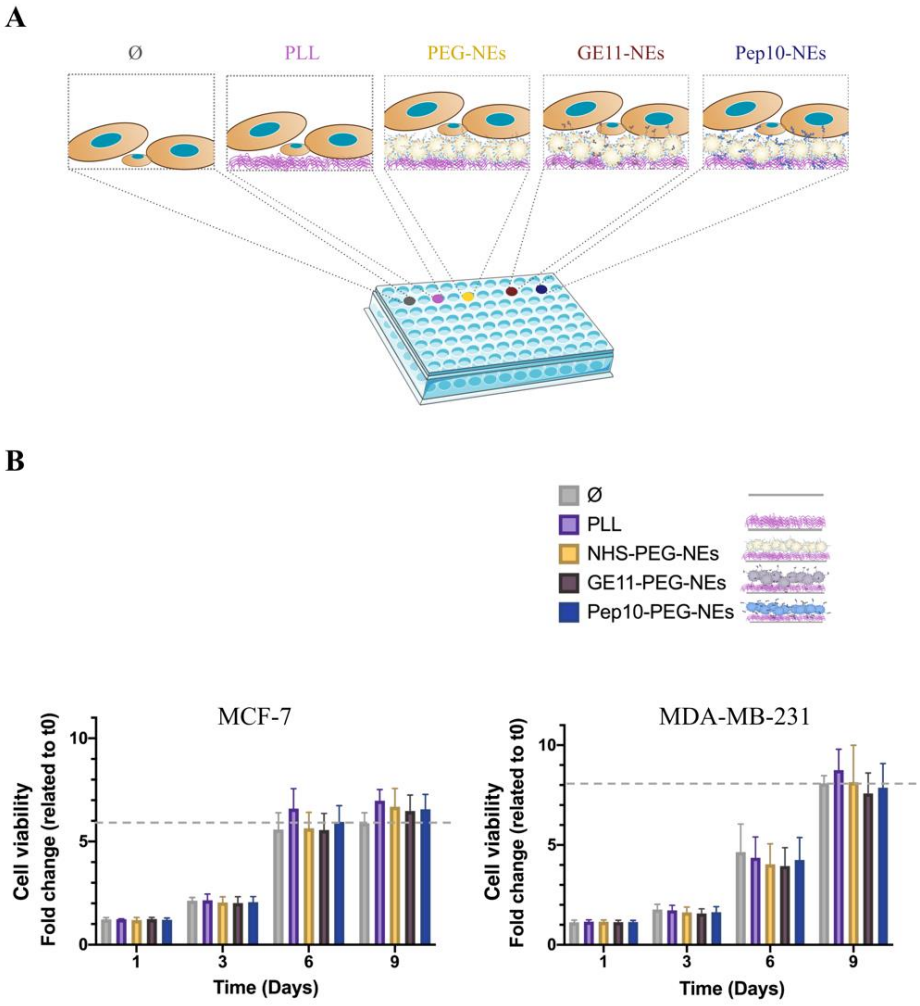

Figure 41.Cytotoxicity Assay. (A) Scheme of the experimental setup. Breast cancer cells were in contact with different surfaces during 9 days of culture in a 96-well plate. Ø shows cell culture in wells without pre-treatment, the rest were pre-treated with PLL. In case of PEG-NEs and Pept-NEs conditions formulations were added after PLL pre-treatment; (B) Viability results of MCF-7 and MDA-MB-231 cells incubated with PLL, PEG-NEs and Pept-NEs (GE11-NEs and Pept10-NEs) immobilized on plates. The results are expressed in fold change values relative to the corresponding control (Ø). Values represent mean ± SD (n = 3).

Furthermore, we propose for future work using devices with micropillars instead of flat surface-chips, due to the advantages associated[90]. Formerly, it has been demonstrated that the capture efficiencies are strongly influenced by the functional components of their devices. For example, in one study for different types of pancreatic cancer cells, a microfluidic device with nanowires was functionalized with a cocktail of peptides and compared the same cocktail of peptides but immobilized on a flat surface device. The combination of nanowires and the cocktail of peptides realized highest capture efficiency, compared with the flat surface device[235]. Moreover, the advantage of using Pept-NEs immobilized on chip-surfaces in this 3D structures, respect using only immobilized peptides, is that they act as a cushion layer[236]. That is, reducing impact force during the isolation process. There are other works that performed on-chip culture after isolation, but this would be the first time using immobilized nanoemulsions decorated with peptides[237,238].

3.4. Conclusions

Taken together, we have successfully designed and characterized Pept-NEs for breast cancer CTC isolation. We have studied their immobilization on chip surfaces and their specific binding to cell membrane proteins by QCM-D. The cytotoxicity analysis showed that immobilized Pept-NEs did not present toxicity associated. Therefore, Pept-NEs results in a good option for a potential isolation technology due to the possibility of on-chip culture reduces the risk of cell loss. This part is related to the fact that our technique would avoid multi-strep procedures of off-chip re-culturing.

Furthermore, we chose a technology that allows cells release by enzymatic degradation, and low impact on cell viability could be achieved after their retrieval. However, further work must be carried out to optimize the use of Pet-NEs-functionalized for CTC isolation.

Overall discussion

OVERALL DISCUSSION

Comprehensive characterization of CTCs in transcriptomic, genomic, and functional terms is difficult mainly due to their low frequency in blood, heterogeneity, poor survivability, and challenging methods of CTC isolation[239]. In this thesis, based on the improvements that nanotechnology provides, we wanted to develop nanotechnology-assisted tools for their use in translational oncology. Most specifically, we propose the use of nanoemulsions to face two of the most challenging elements in the field of liquid biopsy: *ex vivo* culture and isolation of CTCs.

Regarding the former, we developed NEs, as a controlled lipid and fatty acids delivery to boost CTC cultures. We determined that NEs represent a valuable tool for CTC culture of metastatic breast cancer, allowing new strategies to support the study of these cells. In respect of the latter, due to NEs are biocompatible and biodegradable, we thought that it would be convenient using them as the base of an isolation approach for CTCs. Therefore, we functionalized NEs to obtain Pept-NEs that can recognize breast cancer cells. It is important to highlight the versatility of Pept-NEs, we used two peptides as a proof of concept, but they could be designed with others. The idea for the future would be to use our nanoemulsions as part of a system where both approaches (expansion of CTCs and isolation) were covered (**Figure 42**).

As a result of this thesis, we achieved the efficient delivery of lipid components for supporting breast cancer cell cultures. Nanoemulsions have been designed previously to develop new treatments for breast cancer[240,241]. However, as far as we know, the CTC *ex vivo* expansion has not been addressed employing nanoemulsions for protocol improvements. After we established the protocol for proliferative NEs, we used them for supporting the culture of CTCs from metastatic breast cancer patients to further characterize these cells. We observed that following this protocol, CTCs grew *ex vivo* for weeks (mean 8 weeks). A positive culture was achieved in 75 % of the analysed samples, implying more than 23 days with proliferative

and survival features, which is a higher percentage than previously published works which reported 13 or 28 % of success[183,184].

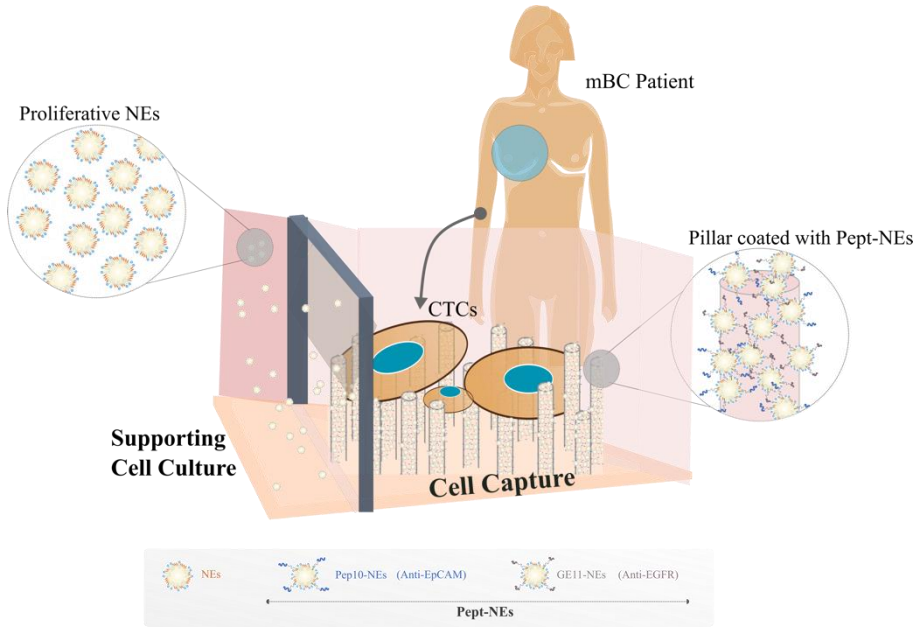

Figure 42. Nanoemulsions for the isolation and on-chip culture of CTCs. First, cells are captured by Pept-NEs immobilized on micropillars and then on-chip culture is supported by adding proliferative NEs. These NEs are made of lipids and fatty acids that interfere in cancer metabolism.

We also proposed a mechanism of action of NEs, where part of them could be directly transferred to the mitochondria to be oxidized (effect observed at 3 h of incubation) and the other part could be stored as LDs (effect observed at t24 h). In relation to the latter point, Cruz *et al.* related the function of LDs to the deregulating cellular energetic hallmark of cancer and also to other categories such as sustaining proliferative signalling (cell cycle progression)[242]. In fact, LDs may have an essential role during two process: i) initial tumour promotion and ii) during more advanced stages (boosting a more aggressive phenotype of metastatic cells)[242].

Regarding the effect in lipid metabolism due to the use of proliferative NEs, we detected an overexpression of CD36 in the CTCs after culture. CD36 was already linked with metastatic potential in breast and melanoma

cancer metastasis[44] and as a key element of survival in resistant breast cancer cells[243]. However, when we analysed mCTCs (the model generated in our laboratory) the relative expression level of CD36 remained the same after NEs addition. This could be explained by the dependency based on different metabolism. In fact, it has been determined that MDA-MB-321 (the parental cell line of mCTCs) presents a reduced expression of CD36[244], so it could be possible that in the cell line generated this expression have not been modified.

Consequently, studies such as the one we performed support the observation that lipid metabolism represent a key element to understand the complexity in breast cancer. This field is under deeply research, because lipid metabolism might be suitable candidates for next generation therapies in oncology. Moreover, metabolic hallmarks of early events of metastasis could be translated to biomarkers predicting metastasis formation risk. Therefore, a versatile tool such as nanoemulsions provides the possibility to prepare different mixes of lipids and fatty acids, making possible to study the effect of different compounds in cancer cells. They could help to unravel the roles for inhibitors of lipid droplet as target for cancer therapy. An excellent example of developing a solution to the impact of lipid metabolism in metastasis process would be the ONA Therapeutics company. This start-up, formed in 2019, took their research about CD36[44] further and now is developing an advance humanized version of the CD36-targeted antibody.

Interestingly, in this thesis we also observed that following our protocol using NEs in CTC cultures could be used as a predictive factor in the clinic. It was proved that the ability of CTCs to grow *ex vivo* predicts patient outcome, in terms of PFS (**Figure 43**). Having biomarkers for PFS prediction can be very useful to evaluate the response to therapy in short times. Thus, the CTC population prone to survive and proliferate *in vitro* could reflect the malignancy of CTCs and the patient's state. Furthermore, we observed that the presence of RBCs in these CTC cultures could predict PFS and OS, and in this case the information can be obtained as soon as the isolation process (negative enrichment) is finished, (**Figure 43**). Notwithstanding, the clinical significance of these observations in *ex vivo*

CTC culture should be elucidated in further research with larger patient cohorts.

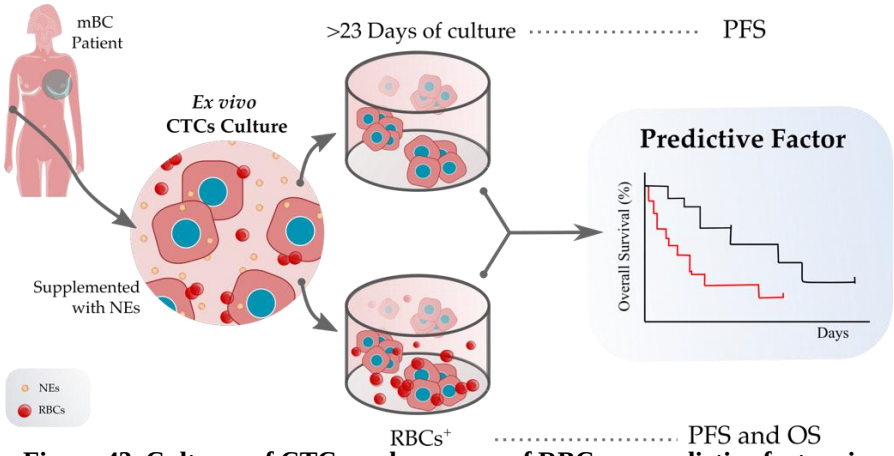

Figure 43. Cultures of CTCs and presence of RBCs as predictive factors in metastatic breast cancer (mBC). Schematic representation of what was observed in cultures of CTCs treated with NEs.

All in all, this technology offers a significant opportunity for further work. Here we only try in this type of cancer, but the importance relays on the fact that this technology could be designed in the future for other types of cancer.

Regarding the Pept-NEs developed in this thesis, it was demonstrated that it is possible to functionalize NEs using different peptides to target specific surface proteins of CTCs. Since the isolation of CTCs using microfluidics occurs in flow, the validation of the specific recognition of immobilized Pept-NEs under protein flow reflects a good starting point for a potential biodegradable capture system.

Therefore, it might be convenient to develop a platform based on NEs and Pept-NEs. The relevance of our approach is that, by using the same technology it is possible to produce different products (NEs, Pept-NEs, and labelled-Pept-NEs), as schematically represented in **Figure 44**. Using this platform, it might be possible to isolate CTCs using biocompatible Pept-NEs immobilized on micropillars of a microfluidic device. Then, it would allow

to perform different downstream processes such as expansion using (i) proliferative NEs and detection of specific subtypes by using (ii) labelled Pept-NEs. Regarding the first point mentioned, (i) our *in vitro* CTC culture protocol is simple and less time-consuming compared to *in vivo* models. Moreover, a key aspect to explore in the future is that these cultures, in their proliferative phase, could be potentially used for drug-testing and molecular characterization for personalized oncology. Referred to the second point, (ii) Pept-NEs are versatile nanosystems that can be designed to recognized different cells that result helpful in terms of cell plasticity of CTCs.

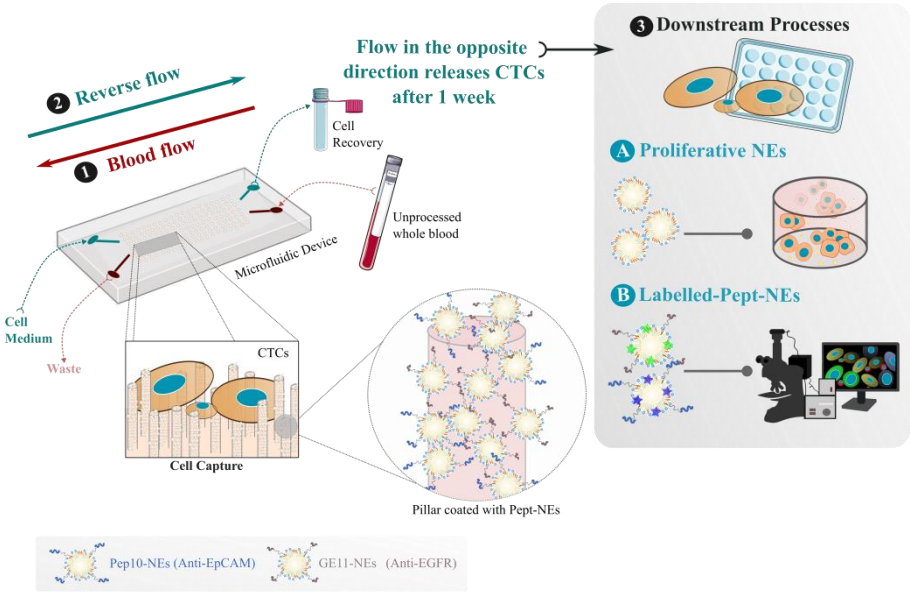

Figure 44. Nanoemulsions platform for the isolation and on-chip culture of CTCs. The first step it would be the isolation by Pept-NEs immobilized on the micropillars. Then, different downstream processes could be performed.

As a conclusion of this thesis project, we demonstrated that NEs are useful to favour the establishment of short-term CTC cultures from metastatic breast cancer patients. Moreover, the analysis of these cells in culture not only showed that the precursor cells had mesenchymal and stem

features but also it was determined that the capability of CTCs to grow *ex vivo* using the established protocol is a predictive factor. Finally, the NEs were functionalized with peptides (Pept-NEs) to endow them with specific recognition capabilities, and it was confirmed that Pept-NEs can be immobilized on surfaces for their use as a potential isolation system. Therefore, this platform could represent a valuable tool in liquid biopsy, supporting the isolation and culture of CTCs to advance precision medicine in cancer.

Conclusions

CONCLUSIONS

The experimental work conducted in this thesis allowed us to conclude:

1. NEs composed by a combination of lipids with potential to impact cell viability can be formulated using the spontaneous emulsification method. The resulting NEs present adequate properties and it is confirmed that all the compounds used are part of the final formulation.
2. It was validated that the addition of NEs to breast cancer cells and to the mCTC cell line enhances proliferation. This effect is related to the specific combination of lipids used, and to the fact of lipids formulated into NEs.
3. The use of proliferative NEs was successfully translated to *ex vivo* CTC cultures from metastatic breast cancer patients to expand these cells for their characterization. The analysis of CTCs in culture from metastatic breast cancer patients allowed us to study the precursor cells, characterized by presenting mesenchymal and stem features.
4. It was demonstrated for the first time that the capability of CTCs to grow *ex vivo* using the established NEs protocol is a predictive factor in metastatic breast cancer. In addition to culture capacity, the presence of RBCs in culture is also of great relevance to predict patient outcome.
5. NEs can be opportunely functionalized with peptides (Pept-NEs) to endow them with specific recognition capabilities. Pept-NEs can be immobilized on surfaces for their use as a potential isolation system of breast cancer cells. Moreover, the flow system used, which included the targeted cell membrane proteins, determined the specific recognition capabilities of immobilized Pept-NEs.

Supplementary material

SUPPLEMENTARY MATERIAL

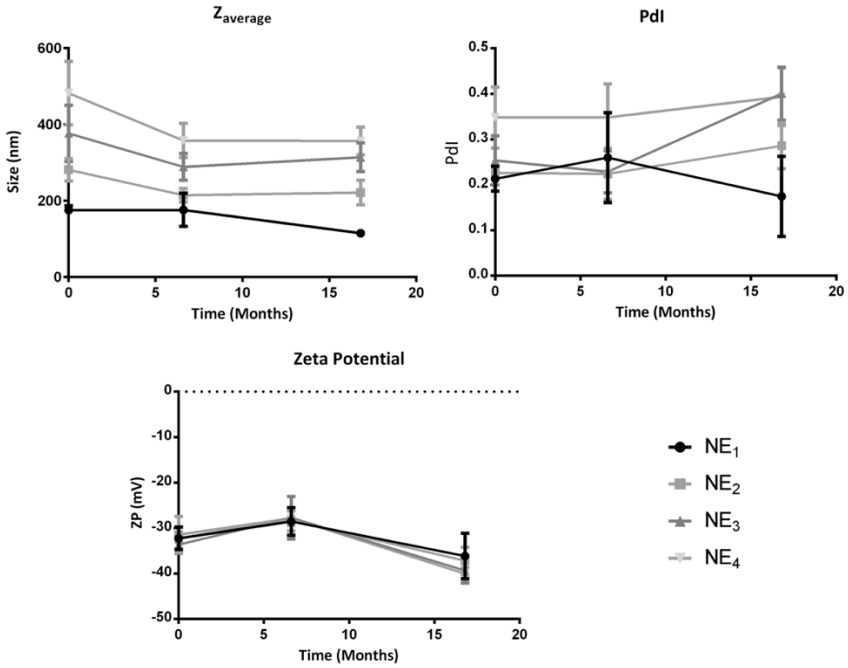

Supporting Figure S1. Analysis of the stability of the NEs. Stability after storage for one year and 4 months at 4 °C, according to the size ($Z_{average}$), polydispersity index (PdI) and ζ-Potential values (ZP).

NMR signal(ppm)	D (m2 s-1)
Integral(0.888432,0.782335)	4.00E-12
Integral(1.616252,1.469839)	4.00E-12
Integral(2.072466,1.858151)	3.60E-12
Integral(2.314365,2.159465)	3.72E-12
Integral(5.312646,5.206549)	3.49E-12

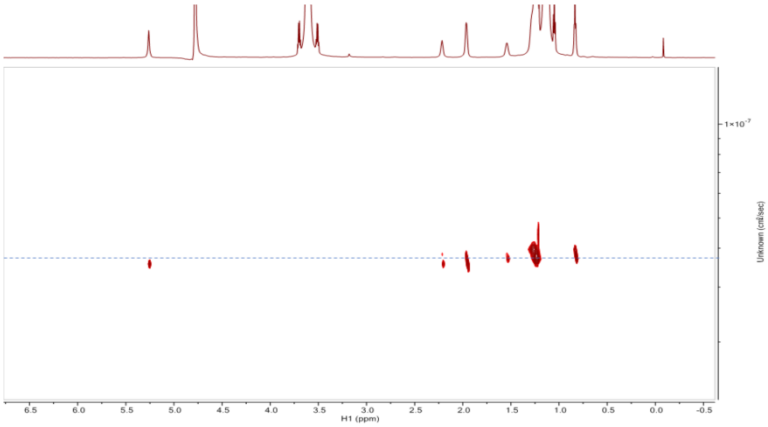

Supporting Figure S2. DOSY spectrum of NEs. Table indicates the peaks selected after Fourier transformation in the ^{1}H dimension and self-diffusion coefficient (D) values.

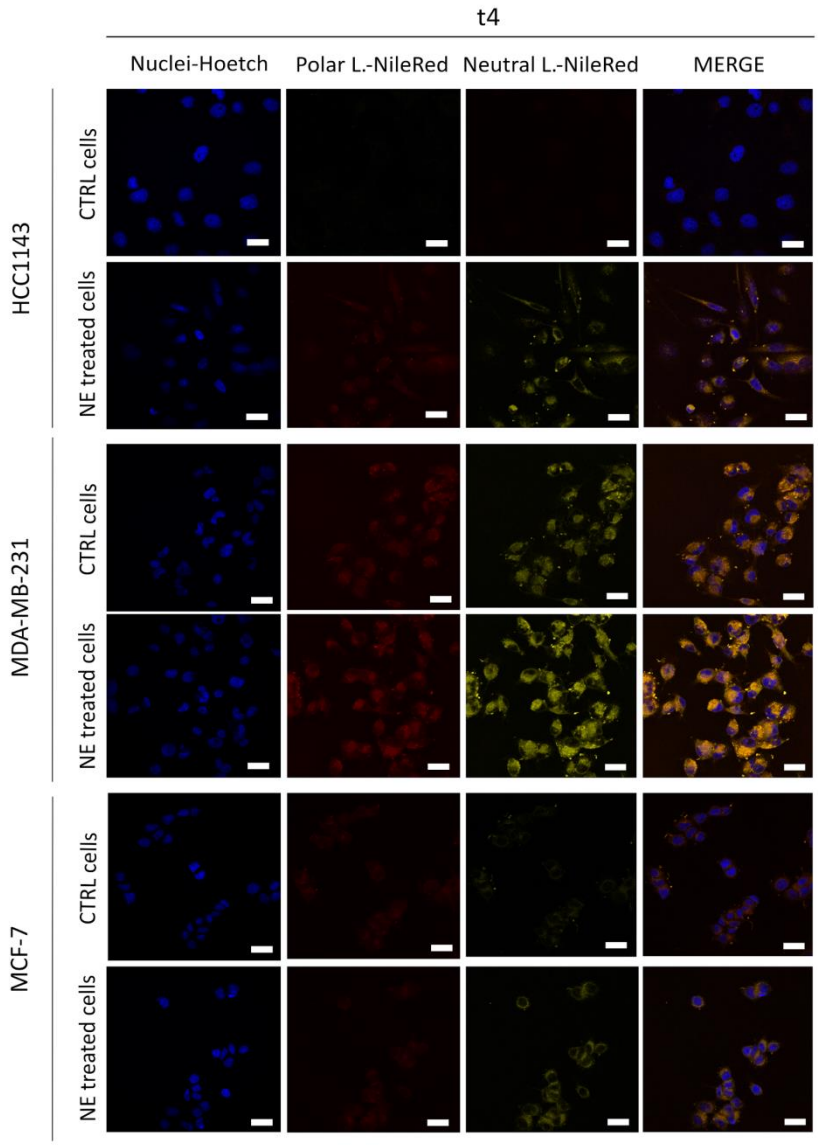

Supporting Figure S3. Analysis of lipid storage after treatment of breast cancer cells with the NEs. Confocal microscopy images of lipids and fatty acid stained with Nile Red in control cells and after the addition of the NEs, in relation to the untreated control cells, for three cell lines: HCC1143, MDA-MB-231, and MCF-7; scale bar is 25 μm. Neutral lipids staining is represented in yellow, polar lipids staining is represented in red, and the cell nuclei is represented in blue.

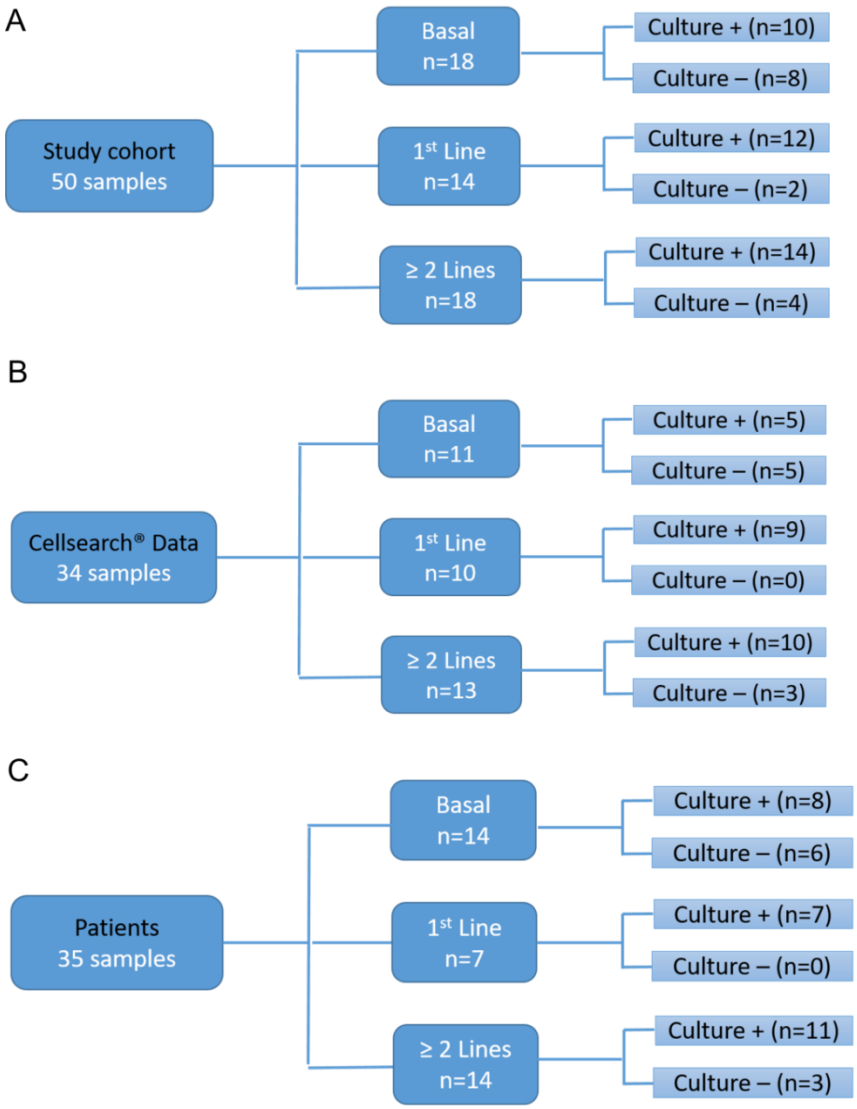

Supporting Figure S4. Diagram of the samples used in the analyses, which describes the number of samples included in each cohort, the treatment at the time of sample collection, and their distribution + or – culture. (A) The study cohort includes 50 samples from 35 patients; (B) Those samples in which there are paired data of enumeration of CTCs by CellSearch®; (C) Those samples in which only one sample per patient is considered. In patients with different samples collected, the basal sample was selected preferentially. In 9 patients ≥ 2 samples were collected at different times of the disease (range 2-4 visits).

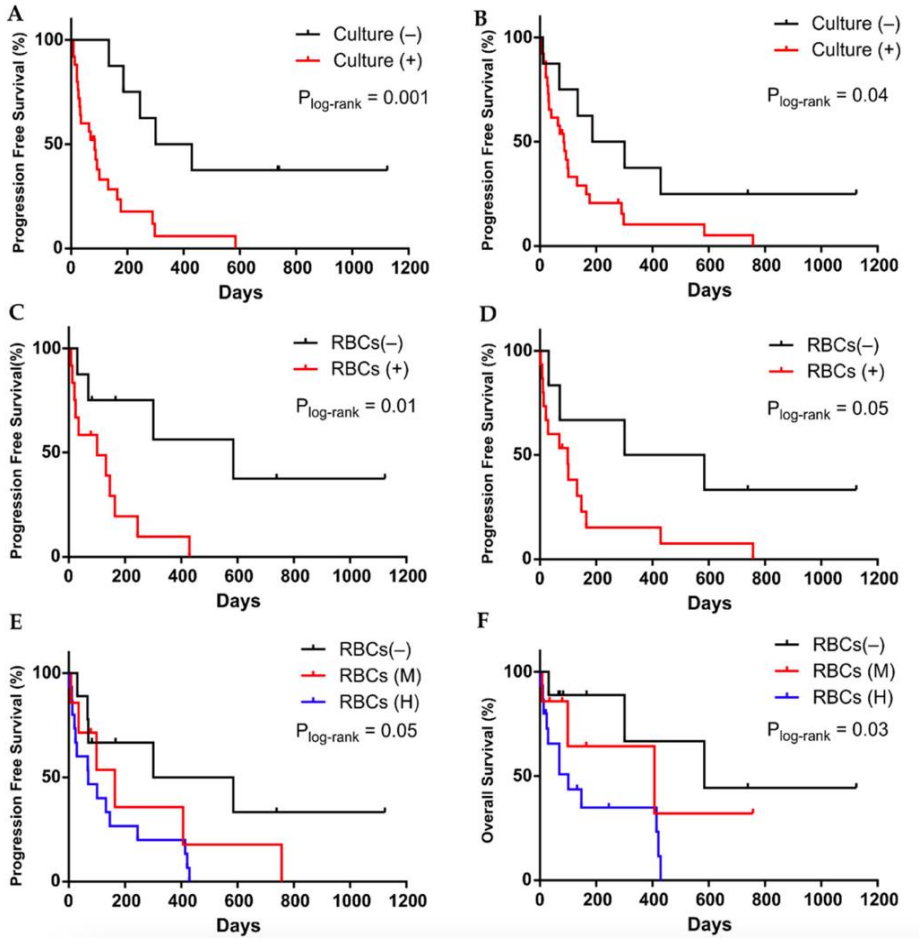

Supporting Figure S5. Survival analysis of alternative samples cohorts. (A-B) Kaplan–Meier plots for PFS for cultivability (culture (–) (black) or (+) (red)) in samples with paired CTC enumeration by CellSearch® data. (A) or considering only 1 sample per patient (B); (C-D) Kaplan–Meier plots for PFS for presence (red) or absence (black) of RBCs in culture in samples with paired CTCs enumeration by CellSearch® data (C) or considering only 1 sample per patient (D); (E-F) Kaplan–Meier plots for PFS and OS for the amount of RBCs in the culture: low or absence (black), medium (red) and high (blue). *p*-values were calculated using the log-rank test.

A

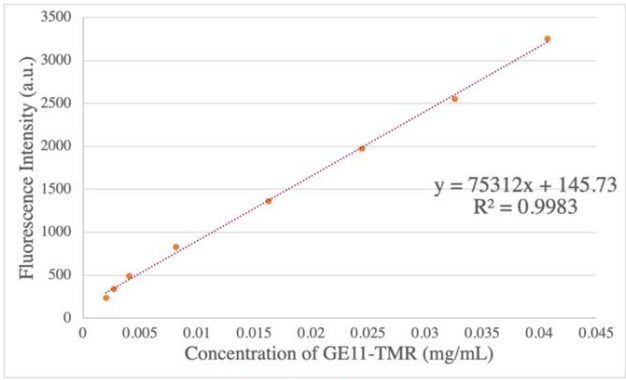

GE11(TMR) in 1mL formulation				
Concentration added GE11 (mg/mL)				
0.0163				
	n1	n2	n3	n4
Concentration1	0.005208599	0.003376222	0.003522281	0.004265854
Concentration2	0.005248433	0.003442612	0.00373473	0.004199464
Concentration3	0.004929759	0.003137216	0.003588671	0.003880789
Average	0.00512893	0.003318683	0.003615227	0.004115369
	0.004044552			

B

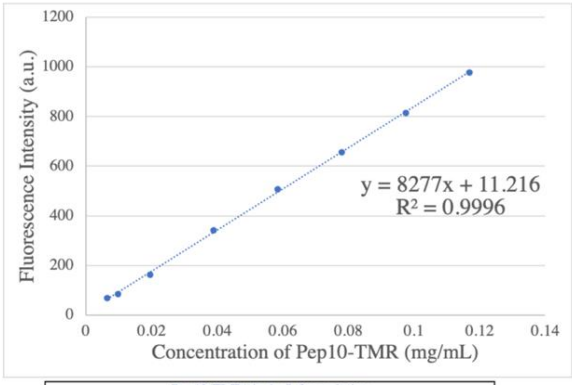

Pep10(TMR) in 1mL formulation				
Concentration added Pep10 (mg/mL)				
0.0195				
	n1	n2	n3	n4
Concentration1	0.008793524	0.009518425	0.009880875	0.009155974
Concentration2	0.008914341	0.009035158	0.010243325	0.008914341
Concentration3	0.009397608	0.009155974	0.009397608	0.009035158
Average	0.009035158	0.009236519	0.009840602	0.009035158
	0.009286859			

Supporting Figure S6. Analysis of final concentration in Pep10-NEs and GE11-NEs formulations.

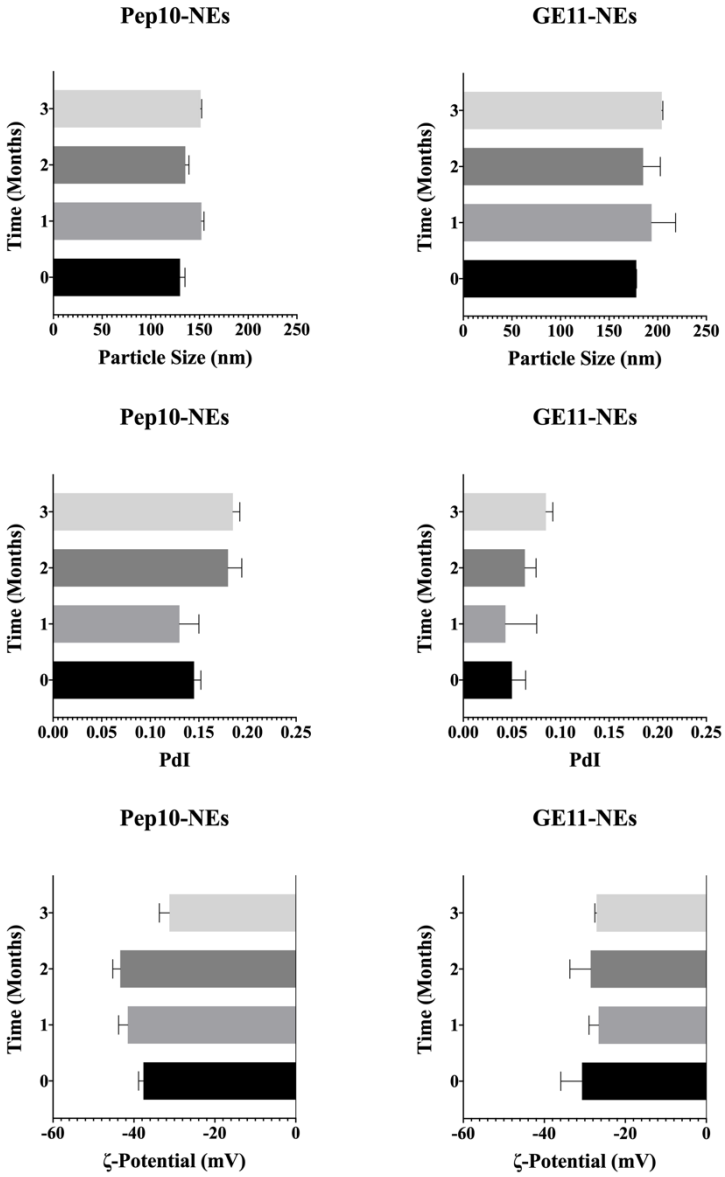

Supporting Figure S7. Analysis of the stability after storage for 3 months at 4 °C, particle size, PdI and ζ-Potential values for Pep10-NEs and GE11.

Appendix

APPENDIX

LIST OF PUBLICATIONS

N. Carmona-Ule, C. Abuín-Redondo, C. Costa, R. Piñeiro, T. Pereira-Veiga, I. Martínez-Pena, P. Hurtado, R. López-López, M. de la Fuente, A.B. Dávila-Ibáñez, Nanoemulsions to support *ex vivo* cell culture of breast cancer circulating tumor cells, Mater. Today Chem. 16 (2020).

ISSN: 2468-5194
Elsevier Ltd, 03/04/2020.
Full-text available: https://doi.org/10.1016/j.mtchem.2020.100265

Journal Citation Reports (JCR) category rank: Q1: Biomaterials
IF: 8.301 (2020)
Contribution to this work: I, Nuria Carmona Ule, was involved in the methodology, validation, investigation, visualization, writing, review and editing of the manuscript.

N. Carmona-Ule, M. González-Conde, C. Abuín, J.F. Cueva, P. Palacios, R. López-López, C. Costa, A.B. Dávila-Ibáñez, Short-Term *Ex Vivo* Culture of CTCs from Advance Breast Cancer Patients : Clinical Implications, Cancers. 13 (2021) 2668.

ISSN: 2072-6694
MDPI, 28/05/21.
Full-text available: https://doi.org/10.3390/cancers13112668

JCR category rank: Q1: Oncology
IF: 6.639 (2020)
5-year IF: 6.999

Contribution to this work: I, Nuria Carmona Ule, was involved in the methodology, formal analysis, investigation, writing of the original draft preparation, writing, review and editing of the manuscript.

Ethical considerations and permissions

ETHICAL CONSIDERATIONS AND PERMISSION

Favourable report animal experimentation ethical committee of the University of Santiago de Compostela (CEEA)

VICERREITORADO DE INVESTIGACIÓN
E INNOVACIÓN
Oficina de Investigación e Tecnoloxía

Edificio CACTUS – Campus universitario sur
15782 Santiago de Compostela
Tel. 981 547 040 - Fax 981 547 077
Correo electrónico
http://imaisd.usc.es

Informe del Comité de Ética de Experimentación Animal (CEEA) de los centros usuarios de animales de experimentación de la USC en el Campus de Santiago

El CEEA de los centros usuarios de animales de experimentación de la USC en el Campus de Santiago, tras evaluar el Proyecto titulado "Desarrollo de xenotrasplantes derivados de Células Tumorales Circulantes (CTC) de pacientes metastásicos en modelos murinos" del que es Investigadora Responsable Dña. Clotilde Costa Nogueira, acordó con fecha 1 de Octubre de 2018 emitir

INFORME FAVORABLE

para la realización de dicho proyecto, así como los procedimientos que incluye, en las instalaciones del establecimiento usuario Animalario del CIMUS, con número de registro ES150780275701, siempre que, en cumplimiento del RD 53/2013, se obtenga la correspondiente autorización administrativa.

En Santiago, a 3 de Octubre de 2018

Fdo. El secretario

Fdo. El presidente

Responsable administrativo:	Nombre: Raúl Vieira Miguel Cargo: Director de la RIAIDT de la USC	V.º B.º Firma y sello

Favourable report (Clinical research ethics committee of Galicia, CEIC)

XUNTA DE GALICIA
CONSELLERÍA DE SANIDADE
Secretaría Xeral Técnica

Edificio Administrativo San Lázaro
15703 SANTIAGO DE COMPOSTELA
Teléfono: 881546425
ceic@sergas.es

galicia

DICTAMEN DEL COMITÉ AUTONÓMICO DE ÉTICA DE LA INVESTIGACIÓN DE GALICIA

Paula M. López Vázquez, Secretaria del Comité Autonómico de Ética de la Investigación de Galicia

CERTIFICA:

Que este Comité evaluó en su reunión del día 22/12/15 :

Título: Biopsia líquida para oncología de precisión
Promotor*:* Rafael López López
Tipo de estudio:EPA-SP
Version: versión 30 de noviembre de 2015 y HIP/CI (cultivo, control biopsia, y biopsia líquida) de la misma fecha
Código del Promotor:RLL-BL-2015_01
Código de Registro: 2015/772

Y, tomando en consideración las siguientes cuestiones:

- La pertinencia del estudio, teniendo en cuenta el conocimiento disponible, así como los requisitos legales aplicables, y en particular la Ley 14/2007, de investigación biomédica, el Real Decreto 1716/2011, de 18 de noviembre, por el que se establecen los requisitos básicos de autorización y funcionamiento de los biobancos con fines de investigación biomédica y del tratamiento de las muestras biológicas de origen humano, y se regula el funcionamiento y organización del Registro Nacional de Biobancos para investigación biomédica, la ORDEN SAS/3470/2009, de 16 de diciembre, por la que se publican las Directrices sobre estudios Posautorización de Tipo Observacional para medicamentos de uso humano, y la Circular nº 07 / 2004, investigaciones clínicas con productos sanitarios.
- La idoneidad del protocolo en relación con los objetivos del estudio, justificación de los riesgos y molestias previsibles para el sujeto, así como los beneficios esperados.
- Los principios éticos de la Declaración de Helsinki vigente.
- Los Procedimientos Normalizados de Trabajo del CEIC de Galicia

Emite un **INFORME FAVORABLE** para la realización del estudio por el/la investigador/a del centro:

Centros	Investigadores Principales
C.H. Universitario de Santiago	Clotilde Costa Nogueira

XUNTA DE GALICIA
CONSELLERÍA DE SANIDADE
Secretaría Xeral Técnica

Edificio Administrativo San Lázaro
15703 SANTIAGO DE COMPOSTELA
Teléfono: 881546425
ceic@sergas.es

galicia

Y HACE CONSTAR QUE:

1 El CAEIG cumple los requisitos legales vigentes (R.D 223/2004 por el que se regulan los ensayos clínicos con medicamentos, y la Ley 14/2007 de Investigación Biomédica).
2 El CAEIG tanto en su composición como en sus PNTs cumple las Normas de Buena Práctica Clínica (CPMP/ICH/135/95).
3 La composición actual del CAEIG es:

Manuel Portela Romero. (Presidente). Médico Especialista en Medicina Familiar y Comunitaria.
Irene Zarra Ferro. (Vicepresidenta). Farmacéutica de Atención Especializada.
Paula Mª López Vázquez, (Secretaria). Médico Especialista en Farmacología Clínica.
Juan Vázquez Lago (Secretario Suplente). Médico Especialista en Medicina Preventiva y Salud Pública.
Jesús Alberdi Sudupe. Médico especialista en Psiquiatría.
Rosendo Bugarín González. Médico Especialista en Medicina Familiar y Comunitaria.
Juan Casariego Rosón. Médico Especialista en Cardiología.
Xoán X. Casas Rodríguez. Médico Especialista en Medicina Familiar y Comunitaria.
Juana Mª Cruz del Río. Trabajadora Social.
Juan Fernando Cueva Bañuelos. Médico Especialista en Oncología Médica.
José Álvaro Fernández Rial. Médico Especialista en Medicina Interna.
José Luis Fernández Trisac. Médico Especialista en Pediatría.
Mª José Ferreira Díaz. Diplomada Universitaria de Enfermería
Pablo Nimo Ríos. Licenciado en Derecho. Miembro externo
Pilar Gayoso Diz. Médico Especialista en Medicina Familiar y Comunitaria.
Agustín Pía Morandeira. Farmacéutico de Atención Primaria
Salvador Pita Fernández. Médico Especialista en Medicina Familiar y Comunitaria.
Carmen Rodríguez-Tenreiro Sánchez. Licenciada en Farmacia.
Susana María Romero Yuste. Médico Especialista en Reumatología.
Mª Asunción Verdejo González. Médico Especialista en Farmacología Clínica.

En Santiago de Compostela, a 05 de enero de 2015

Firmado digitalmente por LOPEZ VAZQUEZ PAULA MARIA - DNI 46900339G
Nombre de reconocimiento (DN): c=ES, o=XUNTA DE GALICIA, ou=certificado electrónico de empleado público, serialNumber=46900339G, sn=LOPEZ VAZQUEZ, givenName=PAULA MARIA, cn=LOPEZ VAZQUEZ PAULA MARIA - DNI 46900339G
Fecha: 2016.01.05 13:55:23 +01'00'

Attributions to figures employed in the manuscript

To construct Figures: 7, 9, 26, and 44 some images were taken from Medical Art website. Servier Medical Art by Servier is licensed under a Creative Commons Attribution 3.0Unported License.
(smart.servier.com)

Agradecimientos

AGRADECIMIENTOS

Quiero aprovechar este espacio para agradecer a mucha de la gente que ha formado parte de este viaje que es la tesis. Han sido unos años de aprendizaje constante en los que me he sentido acompañada por muchas grandes personas.

En primer lugar, quería agradecer a mis dos directores de tesis, el Dr. Rafael López y la Dra. Ana Belén Dávila, por su dedicación a lo largo de estos años y por haberme dado la oportunidad de vivir esta aventura.

Gracias a todos los integrantes de la Unidad mixta Roche-Chus, que sin ellos esta tesis no sería posible: Dra. Clotilde Costa, Dr. Roberto Piñeiro, Gloria García, Carmen Abuín, Sandra Alijas, Pablo Hurtado, Miriam González, Celso Yañez, y José Antonio Trillo. Y a las compañeras que formaron parte de ella: Dra. Thais Pereira, Dra. Inés Martínez y Virginia Rodríguez.
De igual forma, quiero agradecer al gran equipo que es el grupo Oncomet, los conocimientos y experiencias compartidas, gracias a: Carolina Herrero, Carlos Casas, Patricia Mondelo, Aida Bao, Aitor Rodríguez, Manuel Mosquera, Oscar Rapado, Ramón Lago, Dr. Jorge Barbazán, Dra. Laura Muinelo, Dr. Miguel Abal, Dra. Alba Ferreirós, Dra. Lorena Alonso, Alicia Abalo y Dr. Roberto Díaz. Gracias también al equipo de Nano-Oncología, por todos los consejos que me han dado a lo largo de estos años, en especial gracias a: la Dra. María de la Fuente, Sandra Díez, Saínza Lores, Marce Abal y María Cascallar.

Agradecer también a Roche Farma, que sin su iniciativa de invertir en la creación de la unidad mixta esta tesis y todo su trabajo no existiría. Gracias también al Hospital Universitario de Santiago, a la Universidad de Santiago (USC) y al iNANO por la oportunidad de hacer uso de sus instalaciones y equipos.

Very kind acknowledgements to Dr. Brigitte Städler for letting me work with your team at iNANO in Aarhus. Thanks for bringing me the opportunity to learn a lot of new technologies as well as discover how incredible Denmark is. También me gustaría agradecer a los que fueron mi familia allí, la "cuadrilla increíble": Leire, David y Víctor.

Del mismo modo, quería aprovechar este espacio para agradecer a todos los que han hecho, a lo largo de mi vida científica, que llegara hasta el punto de escribir una tesis. En especial gracias: Dr. Hugo Cabedo (Insituto de Neurociencias CSIC-UMH), Dra. Marisa García (Universitat de Barcelona), Dra. Elena Sánchez (Universitat de Barcelona), Dr. Francesc Mitjans (Centro tecnológico Leitat), Dra. Lourdes Roque (Centro tecnológico Leitat) y Toni Coll (Centro tecnológico Leitat).

En un lugar muy especial, no puedo dejar de agradecer a todos los amigos que me han apoyado continuamente a lo largo de los años: Carmen, María, Enri, Mar, Miriam, María Ca., Marchena, Sandra, Mere, Mima, Robe, Marta, Miguel, Lidoy, Xabo, Helena, Irati y Martín.

Agradecer a mi familia su apoyo constante a lo largo de esta experiencia. Gracias Mamá y Papá por apostar siempre por mi formación y por vuestro apoyo incondicional. Gracias por venir a verme allá donde estuviera y trasladar "casa" a cualquier lugar. Gracias a mi hermana, Ana, ya sabes lo importante que eres para mi, mi gran apoyo, confidente y amiga. Eres la gran suerte de mi vida y estoy muy orgullosa de ti.

A mis tías, tíos, primas y primos que siempre han sido un gran apoyo, fuentes de momentos muy felices y de sentirme muy querida. Gracias en especial a mi Tío Javi y mi Tía Carmen, con los que disfruto tanto cada vez que nos vemos. A mi Abu, por transmitirme desde siempre que "disfrute, pero con cabeza".

En un lugar muy destacado, gracias a ti Marc, por tantos momentos especiales que hemos creado juntos. Por transmitirme tranquilidad y seguridad en los momentos de duda. En esta etapa de la tesis hemos tenido

que aprender a vivir a distancia, pero eso nos ha permitido viajar mucho y ha hecho de cada encuentro mágico. Estoy segura de que nuestra nueva etapa va a ser insuperable. Te quiero.

Por último, no quiero acabar este espacio sin transmitir mi más profundo agradecimiento a todos los pacientes y a sus familiares.

¡Muchísimas gracias a todos de corazón!

References

REFERENCES

1. Feynman, R. P. There is plenty of room at the bottom. California Institute of Technology. *J. Eng. Sci.***4**, 23–36 (1960).
2. Jain, K. K. Introduction. In *The Handbook of Nanomedicine* (ed. Jain, K. K.) 1–9 (Humana Press, Totowa, NJ 2017).
3. Kaur, K. & Thombre, R. Chapter 1. In Nanobiotechnology: methods, applications, and future prospects. *Nanobiotechnology* (eds. Ghosh, S. & Webster, T. J.) 1–20 (Elsevier Inc., 2021).
4. Anselmo, A. C. & Mitragotri, S. Nanoparticles in the clinic: An update. *Bioeng. Transl. Med.***4**, 1–16 (2019).
5. Fenton, O. S., Olafson, K. N., Pillai, P. S., Mitchell, M. J. & Langer, R. Advances in Biomaterials for Drug Delivery. *Adv. Mater.***30**, 1–29 (2018).
6. Singh, Y. *et al.* Nanoemulsion: Concepts, development and applications in drug delivery. *J. Control. Release* **252**, 28–49 (2017).
7. McClements, D. J. & Jafari, S. M. General Aspects of Nanoemulsions and Their Formulation. In *Nanoemulsions: Formulation, Applications, and Characterization* (ed. McClements, D. J. & Jafari, S.) 3–20 (Elsevier Inc., 2018).
8. Isailović, T. M., Todosijević, M. N., Dordević, S. M. & Savić, S. D. Chapter 7 Natural Surfactants-Based Micro/Nanoemulsion Systems for NSAIDs- Practical Formulation Approach, Physicochemical and Biopharmaceutical Characteristics/Performances. In *Microsized and Nanosized Carriers for Nonsteroidal Anti-Inflammatory Drugs: Formulation Challenges and Potential Benefits* (ed. Čalija, B.) 179–217 (Elsevier Inc., 2017).
9. McClements, D. J. & Gumus, C. E. Natural emulsifiers — Biosurfactants, phospholipids, biopolymers, and colloidal particles: Molecular and physicochemical basis of functional performance. *Adv. Colloid Interface Sci.***234**, 3–26 (2016).
10. Zhang, Y. *et al.* Nanoemulsion for solubilization, stabilization, and in vitro release of pterostilbene for oral delivery. *AAPS PharmSciTech* **15**, 1000–1008 (2014).
11. Sánchez-López, E. *et al.* Current Applications of Nanoemulsions in

Cancer Therapeutics. *Nanomaterials* **9**, 821 (2019).
12. Ugelstad, J., El-Aasser, M. S. & Vanderhoff, J. W. Emulsion polymerization: Initiation of polymerization in monomer droplets. *J. Polym. Sci. Polym. Lett. Ed.***11**, 503–513 (1973).
13. Ganta, S., Talekar, M., Singh, A., Coleman, T. P. & Amiji, M. M. Nanoemulsions in Translational Research—Opportunities and Challenges in Targeted Cancer Therapy. *AAPS PharmSciTech* **15**, 694–708 (2014).
14. Fernández, M., Javaid, F. & Chudasama, V. Advances in targeting the folate receptor in the treatment/imaging of cancers. *Chem. Sci.* **9**, 790–810 (2018).
15. Chemical Reactivity of Crosslinkers and Modification Reagents. In *Crosslinking Technical Handbook.* 3–9. (Thermo Scientific, 2012).
16. Wani, T. A., Masoodi, F. A., Jafari, S. M. & McClements, D. J. Safety of Nanoemulsions and Their Regulatory Status. In *Nanoemulsions: Formulation, Applications, and Characterization* (ed. McClements, D. J. & Jafari, S.) 613–628 (Elsevier Inc., 2018).
17. Bourbon, A. I., Gonçalves, R. F. S., Vicente, A. A. & Pinheiro, A. C. Characterization of Particle Properties in Nanoemulsions. In *Nanoemulsions: Formulation, Applications, and Characterization* (ed. McClements, D. J. & Jafari, S.) 519–546 (Elsevier Inc., 2018).
18. Lifshitz, I. M. & Slyozov, V. V. The kinetics of precipitation from supersaturated solid solutions. *J. Phys. Chem. Solids* **19**, 35–50 (1961).
19. Taylor, P. Ostwald ripening in emulsions. *Colloids Surfaces A Physicochem. Eng. Asp.***99**, 175–185 (1995).
20. Zhang, Z. & McClements, D. J. Overview of Nanoemulsion Properties: Stability, Rheology, and Appearance. In *Nanoemulsions: Formulation, Applications, and Characterization* (ed. McClements, D. J. & Jafari, S.) 21–49 (Elsevier Inc., 2018).
21. Chung, C. & McClements, D. J. Characterization of Physicochemical Properties of Nanoemulsions: Appearance, Stability, and Rheology. In *Nanoemulsions: Formulation, Applications, and Characterization.* 547–576 (Elsevier Inc., 2018).
22. Sung, H. *et al.* Global cancer statistics 2020: GLOBOCAN estimates

of incidence and mortality worldwide for 36 cancers in 185 countries. *CA. Cancer J. Clin.***3**, 209–249 (2021).

23. Loibl, S., Poortmans, P., Morrow, M., Denkert, C. & Curigliano, G. Breast cancer. *Lancet* **397**, 1750–1769 (2021).
24. Poloz, Y., Dowling, R. J. O. & Stambolic, V. Fundamental Pathways in Breast Cancer : Signaling from the Membrane. In *Breast Cancer: Innovations in Research and Management* (eds. Veronesi, U., Goldhirsch, A., Veronesi, P., Gentilini, O. D. & Leonardi, M. C.) 3–12 (Springer New York, 2017).
25. Turashvili, G. & Brogi, E. Tumor heterogeneity in breast cancer. *Front. Med.***4**, (2017).
26. Baliu-Piqué, M., Pandiella, A. & Ocana, A. Breast Cancer Heterogeneity and Response to Novel Therapeutics. *Cancers (Basel).***12**, (2020).
27. G., C. Effects of chemotherapy and hormonal therapy for early breast cancer on recurrence and 15-year survival: an overview of the randomised trials. *Lancet* **365**, 1687–1717 (2005).
28. Alix-Panabières, C. & Pantel, K. Challenges in circulating tumour cell research. *Nat. Rev. Cancer* **14**, 623–631 (2014).
29. Algire, G. H. *et al.* Vascular Reactions of Normal and Malignant Tissues in vivo. III. Vascular Reactions of Mice to Fibroblasts Treated in vitro with Methylcholanthrene. *JNCI J. Natl. Cancer Inst.***11**, 555–579 (1950).
30. Ferrara, N. & Kerbel, R. S. Angiogenesis as a therapeutic target. *Nature* **438**, 967–974 (2005).
31. McDonald, D. M. & Baluk, P. Significance of blood vessel leakiness in cancer. *Cancer Res.***62**, 5381–5385 (2002).
32. Aceto, N., Toner, M., Maheswaran, S. & Haber, D. A. En Route to Metastasis: Circulating Tumor Cell Clusters and Epithelial-to-Mesenchymal Transition. *Trends in Cancer* **1**, 44–52 (2015).
33. Sflomos, G. & Brisken, C. Breast Cancer Microenvironment and the Metastatic Process. In *Breast Cancer: Innovations in Research and Management* (eds. Veronesi, U., Goldhirsch, A., Veronesi, P., Gentilini, O. D. & Leonardi, M. C.). 39–48 (Springer New York, 2017).

34. Mani, S. A. *et al.*The Epithelial-Mesenchymal Transition Generates Cells with Properties of Stem Cells. *Cell* **133**, 704–715 (2008).
35. Polyak, K. & Weinberg, R. A. Transitions between epithelial and mesenchymal states: acquisition of malignant and stem cell traits. *Nat. Rev. Cancer* **9**, 265–273 (2009).
36. Francart, M. E. *et al.* Epithelial–mesenchymal plasticity and circulating tumor cells: Travel companions to metastases. *Dev. Dyn.* **247**, 432–450 (2018).
37. Genna, A. *et al.* Emt-associated heterogeneity in circulating tumor cells: Sticky friends on the road to metastasis. *Cancers (Basel).***12**, 1–38 (2020).
38. Hanahan, D. & Weinberg, R. A. The Hallmarks of Cancer. *Cell* **100**, 57–70 (2000).
39. Hanahan, D. & Weinberg, R. A. Hallmarks of cancer: The next generation. *Cell* **144**, 646–674 (2011).
40. Warburg, O. On the Origin of Cancer Cells. *Science.***123**, 309 – 314 (1956).
41. Antalis, C. J., Uchida, A., Buhman, K. K. & Siddiqui, R. A. Migration of MDA-MB-231 breast cancer cells depends on the availability of exogenous lipids and cholesterol esterification. *Clin. Exp. Metastasis* **28**, 733–741 (2011).
42. Nath, A. & Chan, C. Genetic alterations in fatty acid transport and metabolism genes are associated with metastatic progression and poor prognosis of human cancers. *Sci. Rep.***6**, 18669 (2016).
43. Balaban, S. *et al.* Adipocyte lipolysis links obesity to breast cancer growth: adipocyte-derived fatty acids drive breast cancer cell proliferation and migration. *Cancer Metab.***5**, 1–14 (2017).
44. Pascual, G. *et al.* Targeting metastasis-initiating cells through the fatty acid receptor CD36. *Nature* **541**, 41–45 (2017).
45. Chen, S. *et al.* Obesity or overweight is associated with worse pathological response to neoadjuvant chemotherapy among Chinese women with breast cancer. *PLoS One* **7**, 1–7 (2012).
46. Broadfield, L. A., Pane, A. A., Talebi, A., Swinnen, J. V. & Fendt, S. M. Lipid metabolism in cancer: New perspectives and emerging mechanisms. *Dev. Cell* **56**, 1363–1393 (2021).

47. Pascual, G. *et al.* Targeting metastasis-initiating cells through the fatty acid receptor CD36. *Nature* **541**, 41–45 (2017).
48. Petan, T., Jarc, E. & Jusović, M. Lipid Droplets in Cancer: Guardians of Fat in a Stressful World. *Molecules* **23**, 1941 (2018).
49. Ubellacker, J. M. *et al.* Lymph protects metastasizing melanoma cells from ferroptosis. *Nature* **585**, 113–118 (2020).
50. Wang, Y. Y. *et al.* Mammary adipocytes stimulate breast cancer invasion through metabolic remodeling of tumor cells. *JCI Insight* **2**, (2017).
51. Attané, C. & Muller, C. Drilling for Oil: Tumor-Surrounding Adipocytes Fueling Cancer. *Trends in Cancer* **6**, 593–604 (2020).
52. Sivanand, S., Viney, I. & Wellen, K. E. Spatiotemporal Control of Acetyl-CoA Metabolism in Chromatin Regulation. *Trends Biochem. Sci.***43**, 61–74 (2018).
53. McDonnell, E. *et al.* Lipids Reprogram Metabolism to Become a Major Carbon Source for Histone Acetylation. *Cell Rep.***17**, 1463–1472 (2016).
54. Woolthuis, C. M. *et al.* Leukemic Stem Cells Evade Chemotherapy by Metabolic Adaptation to an Adipose Tissue Niche. *Cell Stem Cell* **19**, 23–37 (2016).
55. Wen, Y. A. *et al.* Adipocytes activate mitochondrial fatty acid oxidation and autophagy to promote tumor growth in colon cancer. *Cell Death Dis.***8**, 1–12 (2017).
56. Pietrocola, F., Galluzzi, L., Bravo-San Pedro, J. M., Madeo, F. & Kroemer, G. Acetyl coenzyme A: A central metabolite and second messenger. *Cell Metab.***21**, 805–821 (2015).
57. Carracedo, A., Cantley, L. C. & Pandolfi, P. P. Cancer metabolism: fatty acid oxidation in the limelight. *Nat. Rev. Cancer* **13**, 227–232 (2013).
58. Pantel, K. & Alix-Panabières, C. Real-time liquid biopsy in cancer patients: Fact or fiction? *Cancer Res.***73**, 6384–6388 (2013).
59. Pantel, K. & Alix-Panabières, C. Liquid biopsy and minimal residual disease — latest advances and implications for cure. *Nat. Rev. Clin. Oncol.***16**, 409–424 (2019).
60. Kanikarla-Marie, P., Lam, M., Menter, D. G. & Kopetz, S. Platelets,

circulating tumor cells, and the circulome. *Cancer Metastasis Rev.***36**, 235–248 (2017).

61. De Rubis, G., Rajeev Krishnan, S. & Bebawy, M. Liquid Biopsies in Cancer Diagnosis, Monitoring, and Prognosis. *Trends Pharmacol. Sci.***40**, 172–186 (2019).
62. Ashworth, T.R. A case of cancer in which cells similar to those in the tumours were seen in the blood after death. *Aust Med J.***5**, 146–147 (1869).
63. Alix-Panabières, C., Schwarzenbach, H. & Pantel, K. Circulating Tumor Cells and Circulating Tumor DNA. *Annu. Rev. Med.***63**, 199–215 (2012).
64. Ramirez, J. M. *et al.* Prognostic relevance of viable circulating tumor cells detected by EPISPOT in metastatic breast cancer patients. *Clin. Chem.***60**, 214–221 (2014).
65. Lim, S. Bin, Lim, C. T. & Lim, W. T. Single-cell analysis of circulating tumor cells: Why heterogeneity matters. *Cancers (Basel).***11**, 1–22 (2019).
66. Bobek, V., Gurlich, R., Eliasova, P. & Kolostova, K. Circulating tumor cells in pancreatic cancer patients: Enrichment and cultivation. *World J. Gastroenterol.***20**, 17163–17170 (2014).
67. Bobek, V. *et al.* Cultivation of circulating tumor cells in esophageal cancer. *Folia Histochem. Cytobiol.***52**, 171–177 (2014).
68. Cegan, M. *et al.* In vitro culturing of viable circulating tumor cells of urinary bladder cancer. *Int. J. Clin. Exp. Pathol.***7**, 7164–7171 (2014).
69. Malara, N. *et al.* Ex-vivo characterization of circulating colon cancer cells distinguished in stem and differentiated subset provides useful biomarker for personalized metastatic risk assessment. *J. Transl. Med.***14**, (2016).
70. Sheng, W. *et al.* Capture, release and culture of circulating tumor cells from pancreatic cancer patients using an enhanced mixing chip. *Lab Chip* **14**, 89–98 (2014).
71. Chen, J. Y. *et al.* Sensitive and specific biomimetic lipid coated microfluidics to isolate viable circulating tumor cells and microemboli for cancer detection. *PLoS One***11**, 1–21 (2016).
72. Zhang, Z. *et al.* Expansion of CTCs from early stage lung cancer

patients using a microfluidic co-culture model. *Oncotarget* **5**, 12383-22397 (2014).

73. Yu, M. *et al.* Ex vivo culture of circulating breast tumor cells for individualized testing of drug susceptibility. *Science* **345**, 216–220 (2014).
74. Cayrefourcq, L. *et al.* Establishment and characterization of a cell line from human Circulating colon cancer cells. *Cancer Res.***75**, 892–901 (2015).
75. Gao, D. *et al.* Organoid cultures derived from patients with advanced prostate cancer. *Cell* **159**, 176–187 (2014).
76. Hamilton, G., Burghuber, O. & Zeillinger, R. Circulating Tumor Cells in Small Cell Lung Cancer: Ex Vivo Expansion. *Lung* **193**, 451–452 (2015).
77. Krebs, M. G., Hou, J. M., Ward, T. H., Blackhall, F. H. & Dive, C. Circulating tumour cells: Their utility in cancer management and predicting outcomes. *Ther. Adv. Med. Oncol.* **2**, 351–365 (2010).
78. Lucci, A. *et al.* Circulating tumour cells in non-metastatic breast cancer: a prospective study. *Lancet Oncol.* **13**, 688–695 (2012).
79. Stopeck, A. *et al.* Circulating Tumor Cells, Disease Progression, and Survival in Metastatic Breast Cancer. *N. Engl. J. Med.* **351**, 781–791 (2004).
80. Bidard, F. C. *et al.* Clinical validity of circulating tumour cells in patients with metastatic breast cancer: A pooled analysis of individual patient data. *Lancet Oncol.* **15,** 406–414 (2014).
81. Dianat-Moghadam, H. *et al.* The role of circulating tumor cells in the metastatic cascade: Biology, technical challenges, and clinical relevance. *Cancers (Basel).***12**, (2020).
82. Amin M. B. *et al*. AJCC Cancer Staging Manual. 8th ed. (Springer New York, 2017).
83. Piñeiro, R. Introduction - Biology of Breast Cancer Metastasis and Importance of the Analysis of CTCs. In *Circulating Tumor Cells in Breast Cancer Metastatic Disease* (ed. Piñeiro, R.) 1–10 (Springer Switzerland AG, 2020).
84. Chinen, L. T. D. *et al.*Cytokeratin-based CTC counting unrelated to clinical follow up. *J. Thorac. Dis.* **5**, 593–599 (2013).

85. Müller, V. *et al.* Prognostic impact of circulating tumor cells assessed with the CellSearch System™ and AdnaTest Breast™ in metastatic breast cancer patients: The DETECT study. *Breast Cancer Res.***14**, R118 (2012).
86. Neurauter, A. A. *et al.* Cell isolation and expansion using dynabeads. in *Advances in Biochemical Engineering/Biotechnology* **106**, 41–73 (Springer Berlin, Heidelberg, 2007).
87. Lapin, M. *et al.* MINDEC-An Enhanced Negative Depletion Strategy for Circulating Tumour Cell Enrichment. *Sci. Rep.***6**, 1–10 (2016).
88. Bailey, P. & Martin, S. Insights on CTC Biology and Clinical Impact Emerging from Advances in Capture Technology. *Cells* **8**, 553 (2019).
89. Resch-Genger, U., Grabolle, M., Cavaliere-Jaricot, S., Nitschke, R. & Nann, T. Quantum dots versus organic dyes as fluorescent labels. *Nat. Methods* **5**, 763–775 (2008).
90. Dong, J. *et al.* Nanostructured Substrates for Detection and Characterization of Circulating Rare Cells : From Materials Research to Clinical Applications. **32**, e1903663 (2020).
91. Habli, Z., Alchamaa, W., Saab, R., Kadara, H. & Khraiche, M. L. Circulating tumor cell detection technologies and clinical utility: Challenges and opportunities. *Cancers (Basel).* **12**, 1–30 (2020).
92. Cheng, J. *et al.* Nanotechnology-assisted isolation and analysis of circulating tumor cells on microfluidic devices. *Micromachines* **11**, 774 (2020).
93. Zheng, Q., Iqbal, S. M. & Wan, Y. Cell detachment: Post-isolation challenges. *Biotechnol. Adv.***31**, 1664–1675 (2013).
94. Wu, L. L. *et al.* Chip-Assisted Single-Cell Biomarker Profiling of Heterogeneous Circulating Tumor Cells Using Multifunctional Nanospheres. *Anal. Chem.***90**, 10518–10526 (2018).
95. Carmona-Ule, N. *et al.* Nanoemulsions to support ex vivo cell culture of breast cancer circulating tumor cells. *Mater. Today Chem.***16**, 100265 (2020).
96. Torre, L. A., Bray, F., Siegel, R. L. & Ferlay, J. Global Cancer Statistics , 2012. **65**, 87–108 (2015).
97. Bray, F. *et al.* Global cancer statistics 2018: GLOBOCAN estimates

of incidence and mortality worldwide for 36 cancers in 185 countries. *CA. Cancer J. Clin.* **68,** 394-424 (2018).

98. Bray, F. *et al.* Cancer Incidence in Five Continents: Inclusion criteria, highlights from Volume X and the global status of cancer registration. *Int. J. Cancer* **137**, 2060–2071 (2015).
99. Harbeck, N. & Gnant, M. Breast cancer. *The Lancet* **389,** 1134–1150 (2017).
100. van der Toom, E. E., Verdone, J. E., Gorin, M. A. & Pienta, K. J. Technical challenges in the isolation and analysis of circulating tumor cells. *Oncotarget* **7,** 62754–62766 (2016).
101. Zhang, L. *et al.* The Identification and Characterization of Breast Cancer CTCs Competent for Brain Metastasis. *Sci. Transl. Med.* **5**, 180ra48 (2013).
102. Grenci, G. *et al.* Liquid biopsy and therapeutic response: Circulating tumor cell cultures for evaluation of anticancer treatment. *Sci. Adv.* **2**, e1600274 (2016).
103. Grillet, F. *et al.* Circulating tumour cells from patients with colorectal cancer have cancer stem cell hallmarks in ex vivo culture. *Gut* **66**, 1802–1810 (2017).
104. Khoo, B. L. *et al.* Short-term expansion of breast circulating cancer cells predicts response to anti-cancer therapy. *Oncotarget***6**, (2015).
105. Que, Z. *et al.* Establishment and characterization of a patient-derived circulating lung tumor cell line in vitro and in vivo. *Cancer Cell Int.* **19**, 21 (2019).
106. Gangoiti, P., Granado, M. H., Alonso, A., Goñi, F. M. & Gómez-Muñoz, A. Implication of ceramide, ceramide 1-phosphate and sphingosine 1-phosphate in tumorigenesis. *Transl. Oncogenomics* **2008**, 81–98 (2008).
107. Ratajczak, M. Z., Suszynska, M., Borkowska, S., Ratajczak, J. & Schneider, G. The role of sphingosine-1 phosphate and ceramide-1 phosphate in trafficking of normal stem cells and cancer cells. *Expert Opin. Ther. Targets* **18**, 95–107 (2014).
108. DeBerardinis, R. J. & Chandel, N. S. Fundamentals of cancer metabolism. *Sci. Adv.* **2**, e1600200 (2016).
109. Beloribi-Djefaflia, S., Vasseur, S. & Guillaumond, F. Lipid

metabolic reprogramming in cancer cells. *Oncogenesis* **5**, e189 (2016).
110. Bensinger, S. J. *et al.* LXR Signaling Couples Sterol Metabolism to Proliferation in the Acquired Immune Response. *Cell* **134**, 97–111 (2008).
111. Lo Sasso, G. *et al.* Down-regulation of the lxr transcriptome provides the requisite cholesterol levels to proliferating hepatocytes. *Hepatology* **51**, 1334–1344 (2010).
112. Clendening, J. W. *et al.* Dysregulation of the mevalonate pathway promotes transformation. *Proc. Natl. Acad. Sci.***107**, 15051–15056 (2010).
113. Dang, C. V. Links between metabolism and cancer. *Genes Dev.* **26**, 877–890 (2012).
114. Hilvo, M. *et al.*Novel theranostic opportunities offered by characterization of altered membrane lipid metabolism in breast cancer progression. *Cancer Res.***71**, 3236–3245 (2011).
115. Vanni, S. Intracellular lipid droplets: From structure to function. *Lipid Insights* **10**, 14–16 (2017).
116. Mazza, M., Alonso-Sande, M., Jones, M. C. & De La Fuente, M. The potential of nanoemulsions in biomedicine. In *Fundamentals of Pharmaceutical Nanoscience* (eds. Uchegbu, I., Schatzlein, A., Cheng, W. & Lalatsa, A.), 1–10 (Springer New York, 2013).
117. McClements, D. J. Emulsion Design to Improve the Delivery of Functional Lipophilic Components. *Annu. Rev. Food Sci. Technol.***1**, 241–269 (2010).
118. Segredo-Morales, E. *et al.* Mobility of Water and Polymer Species and Rheological Properties of Supramolecular Polypseudorotaxane Gels Suitable for Bone Regeneration. *Bioconjug. Chem.* **29**, 503–516 (2018).
119. Das, D. K. *et al.* Isolation and propagation of circulating tumor cells from a mouse cancer model. *J. Vis. Exp.* **104**, 52861 (2015).
120. Iorns, E. *et al.* A New Mouse Model for the Study of Human Breast Cancer Metastasis. **7**, e47995 (2012).
121. Brindley, D. N. Lipid phosphate phosphatases and related proteins: Signaling functions in development, cell division, and cancer. *J. Cell.*

Biochem. **92**, 900–912 (2004).

122. Baenke, F., Peck, B., Miess, H. & Schulze, A. Hooked on fat: the role of lipid synthesis in cancer metabolism and tumour development. *Dis. Model. Mech.* **6**, 1353–1363 (2013).
123. Zhao, J., Zhi, Z., Wang, C., Xing, H. & Song, G. Exogenous lipids promote the growth of breast cancer cells via CD36. *Oncol Rep.* **38**, 2105–2115 (2017).
124. Yang, P. *et al.* Dietary oleic acid-induced CD36 promotes cervical cancer cell growth and metastasis via up-regulation Src/ERK pathway. *Cancer Lett.***438**, 76–85 (2018).
125. Li, S. *et al.* High metastaticgastric and breast cancer cells consume oleic acid in an AMPK dependent manner. *PLoS One* **9**, e97330 (2014).
126. Navarro-Tito, N., Soto-Guzman, A., Castro-Sanchez, L., Martinez-Orozco, R. & Salazar, E. P. Oleic acid promotes migration on MDA-MB-231 breast cancer cells through an arachidonic acid-dependent pathway. *Int. J. Biochem. Cell Biol.* **42,** 306– 317 (2010).
127. Gándola, Y. B. *et al.*Mitogenic Effects of Phosphatidylcholine Nanoparticles on MCF-7 Breast Cancer Cells. *Biomed Res. Int.* **2014**, 687037 (2014).
128. Ridgway, N. D. The role of phosphatidylcholine and choline metabolites to cell proliferation and survival. *Crit. Rev. Biochem. Mol. Biol.***48**, 20–38 (2013).
129. Raza, S. *et al.* The cholesterol metabolite 27-hydroxycholesterol stimulates cell proliferation via ERβ in prostate cancer cells. *Cancer Cell Int.* **17**, 52 (2017).
130. Mcarthur, M. J. *et al.* Cellular uptake and intracellular trafficking of long chain fatty acids. **40**, 1371–1383 (1999).
131. Bruce, J. S. & Salter, A. M. Metabolic fate of oleic acid, palmitic acid and stearic acid in cultured hamster hepatocytes. *Biochem. J.* **316**, 847–852 (1996).
132. Bouchemal, K., Briançon, S., Perrier, E. & Fessi, H. Nano-emulsion formulation using spontaneous emulsification: Solvent, oil and surfactant optimisation. *Int. J. Pharm.* **280**, 241–251 (2004).
133. Thiam, A. R., Farese, R. V & Walther, T. C. The biophysics and cell

biology of lipid droplets. *Nat. Rev. Mol. Cell Biol.***14**, 775–86 (2013).
134. D'Arrigo, J. Stable Nanoemulsions: Self-Assembly in Nature and Nanomedicine. *Studies in Interface Science* **25**, 2–415 (2011).
135. Jacobsen, C. Chapter 8 - Oxidative Stability and Shelf Life of Food Emulsions. In *Oxidative Stability and Shelf Life of Foods Containing Oils and Fats* (eds. Hu, M. & Jacobsen, C.) 287–312 (AOCS Press, 2016).
136. Liu, Q., Huang, H., Chen, H., Lin, J. & Wang, Q. Food-grade nanoemulsions: Preparation, stability and application in encapsulation of bioactive compounds. *Molecules* **24**, 1–37 (2019).
137. McClements, D. J. & Decker, E. A. Lipid oxidation in oil-in-water emulsions: Impact of molecular environment on chemical reactions in heterogeneous food systems. *J. Food Sci.* **65**, 1270–1282 (2000).
138. Centritto, F. *et al.* Cellular and molecular determinants of all- trans retinoic acid sensitivity in breast cancer : Luminal phenotype and RAR a expression. **7**, 950–972 (2015).
139. Greenspan, P. *et al.* Nile Red A Selective Fluorescent Stain for Intracellular Lipid Droplets. *J. Cell Biol.***100**, 965–973 (1985).
140. Radde, B. N., Alizadeh-Rad, N., Price, S. M., Schultz, D. J. & Klinge, C. M. Anacardic Acid, Salicylic Acid, and Oleic Acid Differentially Alter Cellular Bioenergetic Function in Breast Cancer Cells. *J. Cell. Biochem.***12**, 2521–2532 (2016).
141. Marcial-medina, C. *et al.* Oleic acid induces migration through a FFAR1 / 4 , EGFR and AKT-dependent pathway in breast cancer cells. *Endocr Connect.* **8,** 252–265 (2019).
142. Yun, M. R. *et al.* Oleic acid enhances vascular smooth muscle cell proliferation via phosphatidylinositol 3-kinase/Akt signaling pathway. *Pharmacol. Res.***54**, 97–102 (2006).
143. Werlein, A., Peters, A., Ngoune, R., Winkler, K. & Pütz, G. Interference of phosphatidylcholines with in-vitro cell proliferation - No flock without black sheep. *Biochim. Biophys. Acta - Biomembr.***1848**, 1599–1608 (2015).
144. Hardy, S., St-Onge, G. G., Joly, É., Langelier, Y. & Prentki, M. Oleate promotes the proliferation of breast cancer cells via the G protein-coupled receptor GPR40. *J. Biol. Chem.* **280**, 13285–13291

(2005).
145. Rampersad, S. N. Multiple applications of alamar blue as an indicator of metabolic function and cellular health in cell viability bioassays. *Sensors (Switzerland)* **12**, 12347–12360 (2012).
146. Lupien, L. E. *et al.* Endocytosis of very low-density lipoproteins: An unexpected mechanism for lipid acquisition by breast cancer cells. *J. Lipid Res.***61**, 205–218 (2020).
147. Carmona-Ule, N. *et al.* Short-Term Ex Vivo Culture of CTCs from Advance Breast Cancer Patients: Clinical Implications. *Cancers (Basel).***13**, 2668 (2021).
148. Seyfried, T. N. & Huysentruyt, L. C. On the origin of cancer metastasis. *Crit. Rev. Oncog.***18**, 43–73 (2013).
149. De Bono, J. S. *et al.* Circulating tumor cells predict survival benefit from treatment in metastatic castration-resistant prostate cancer. *Clin. Cancer Res.***14**, 6302–6309 (2008).
150. Cohen, S. J. *et al.* Relationship of circulating tumor cells to tumor response, progression-free survival, and overall survival in patients with metastatic colorectal cancer. *J. Clin. Oncol.***26**, 3213–3221 (2008).
151. Yan, W. T. *et al.* Circulating tumor cell status monitors the treatment responses in breast cancer patients: A meta-analysis. *Sci. Rep.***7**, 1–12 (2017).
152. Alix-Panabières, C., Bartkowiak, K. & Pantel, K. Functional studies on circulating and disseminated tumor cells in carcinoma patients. *Mol. Oncol.***10**, 443–449 (2016).
153. Maheswaran, S. & Haber, D. A. Ex vivo culture of CTCs: An emerging resource to guide cancer therapy. *Cancer Res.***75**, 2411–2415 (2015).
154. Kowalik, A., Kowalewska, M. & Góźdź, S. Current approaches for avoiding the limitations of circulating tumor cells detection methods—implications for diagnosis and treatment of patients with solid tumors. *Translational Research* **185**, 58–84.e15 (2017).
155. Massagué, J. & Obenauf, A. C. Metastatic colonization by circulating tumour cells. *Nature* **529**, 298–306 (2016).
156. Fina, E. *et al.* Did circulating tumor cells tell us all they could? The

missed circulating tumor cell message in breast cancer. *Int. J. Biol. Markers* **30**, e429-33 (2015).
157. Xiao, J. *et al.* Efficient propagation of circulating tumor cells: A first step for probing tumor metastasis. *Cancers (Basel).***12**, 1–14 (2020).
158. Bobek, V. *et al*. Detection and Cultivation of Circulating Tumor Cells in Malignant Pleural Mesothelioma. *Anticancer Res.* **34**, 2565–2569 (2014).
159. Kolostova, K. *et al.* Detection and cultivation of circulating tumor cells in gastric cancer. *Cytotechnology* **68**, 1095–1102 (2016).
160. Zhang, Z. *et al.* Expansion of CTCs from early stage lung cancer patients using a microfluidic co-culture model. *Oncotarget* **5**, 12383–12397 (2014).
161. Zhang, Z., Shiratsuchi, H., Palanisamy, N., Nagrath, S. & Ramnath, N. Expanded Circulating Tumor Cells from a Patient with ALK-Positive Lung Cancer Present with EML4-ALK Rearrangement Along with Resistance Mutation and Enable Drug Sensitivity Testing: A Case Study. *J. Thorac. Oncol.***12**, 397–402 (2017).
162. Hamilton, G., Hochmair, M., Rath, B., Klameth, L. & Zeillinger, R. Small cell lung cancer: Circulating tumor cells of extended stage patients express a mesenchymal-epithelial transition phenotype. *Cell Adhes. Migr.***10**, 360–367 (2016).
163. Kolostova, K. *et al.* Circulating tumor cells in localized prostate cancer: Isolation, cultivation In Vitro and relationship to T-stage and gleason score. *Anticancer Res.***34**, 3641–3646 (2014).
164. Koch, C. *et al.* Characterization of circulating breast cancer cells with tumorigenic and metastatic capacity. *EMBO Mol. Med.***12**, 1–22 (2020).
165. Sheng, W. *et al.* Capture, release and culture of circulating tumor cells from pancreatic cancer patients using an enhanced mixing chip. *Lab Chip* **14**, 89–98 (2014).
166. Brungs, D. *et al.* Establishment of novel long-term cultures from EpCAM positive and negative circulating tumour cells from patients with metastatic gastroesophageal cancer. *Sci. Rep.***10**, 1–13 (2020).
167. Soler, A. *et al.* Autologous cell lines from circulating colon cancer cells captured from sequential liquid biopsies as model to study

therapy-driven tumor changes. *Sci. Rep.***8**, 15931 (2018).

168. Tellez-Gabriel, M. *et al.* Circulating Tumor Cell-Derived Pre-Clinical Models for Personalized Medicine. *Cancers (Basel)* **11**, 19 (2019).
169. Duval, K. *et al.* Modeling physiological events in 2D vs. 3D cell culture. *Physiology* **32**, 266–277 (2017).
170. Hoarau-Véchot, J., Rafii, A., Touboul, C. & Pasquier, J. Halfway between 2D and animal models: Are 3D cultures the ideal tool to study cancer-microenvironment interactions? *Int. J. Mol. Sci.***19**, 181 (2018).
171. Kapałczyńska, M. *et al.* 2D and 3D cell cultures – a comparison of different types of cancer cell cultures. *Arch. Med. Sci.***14**, 910–919 (2018).
172. Nath, S. & Devi, G. R. Three-dimensional culture systems in cancer research: Focus on tumor spheroid model. *Pharmacol. Ther.***163**, 94–108 (2016).
173. Al-Hajj, M., Wicha, M. S., Benito-Hernandez, A., Morrison, S. J. & Clarke, M. F. Prospective identification of tumorigenic breast cancer cells. *Proc. Natl. Acad. Sci. U. S. A.***100**, 3983–3988 (2003).
174. Tosoni, D., Di Fiore, P. P. & Pece, S. Functional Purification of Human and Mouse Mammary Stem Cells. In *Progenitor Cells: Methods and Protocols* (eds. Mace, K. A. & Braun, K. M.) 59–79 (Humana Press, Totowa, NJ, 2012).
175. Zhang, Y. *et al.* Microfluidic chip for isolation of viable circulating tumor cells of hepatocellular carcinoma for their culture and drug sensitivity assay. *Cancer Biol. \& Ther.***17**, 1177–1187 (2016).
176. Klameth, L. *et al.* Small cell lung cancer: model of circulating tumor cell tumorospheres in chemoresistance. *Sci. Rep.***7**, 5337 (2017).
177. Vishnoi, M. *et al.* The isolation and characterization of CTC subsets related to breast cancer dormancy. *Sci. Rep.***5**, 1–14 (2015).
178. Soeda, A. *et al.* Hypoxia promotes expansion of the CD133-positive glioma stem cells through activation of HIF-1alpha. *Oncogene* **28**, 3949–3959 (2009).
179. Ackermann, T. & Tardito, S. Cell Culture Medium Formulation and Its Implications in Cancer Metabolism. *Trends in Cancer* **5**, 329–332

(2019).
180. Kang, Q. *et al.* Comparative analysis of circulating tumor DNA stability In K3EDTA, Streck, and CellSave blood collection tubes. *Clin. Biochem.* **49**, 1354–1360 (2016).
181. Schneider, C. A., Rasband, W. S. & Eliceiri, K. W. NIH Image to ImageJ: 25 years of image analysis. *Nat. Methods* **9**, 671–675 (2012).
182. Che, J. *et al.* Classification of large circulating tumor cells isolated with ultra-high throughput microfluidic Vortex technology. *Oncotarget* **7**, 12748–12760 (2016).
183. Kulasinghe, A. *et al.* Short term ex-vivo expansion of circulating head and neck tumour cells. *Oncotarget* **7**, 60101–60109 (2016).
184. Kapeleris, J. *et al.* Ex vivo culture of circulating tumour cells derived from non-small cell lung cancer. *Transl. Lung Cancer Res.* **9**, 1795–1809 (2020).
185. Wang, R. *et al.* Cultured circulating tumor cells and their derived xenografts for personalized oncology. *Asian J. Urol.* **3**, 240–253 (2016).
186. Ginestier, C. *et al.* ALDH1 Is a Marker of Normal and Malignant Human Mammary Stem Cells and a Predictor of Poor Clinical Outcome. *Cell Stem Cell* **1**, 555–567 (2007).
187. Reduzzi, C. *et al.* The curious phenomenon of dual-positive circulating cells: Longtime overlooked tumor cells. *Semin. Cancer Biol.* **60**, 344–350 (2019).
188. Domingos Chinen, L. T. *et al.*Isolation, Detection, And immunomorphological characterization of circulating tumor cells (CTCs) from patients with different types of sarcoma using isolation by size of tumor cells: A window on sarcoma-cell invasion. *Onco. Targets. Ther.* **7**, 1609–1617 (2014).
189. Emerson, T. *et al.* Fourier-ring descriptor to characterize rare circulating cells from images generated using immunofluorescence microscopy. *Comput. Med. Imaging Graph.* **40**, 70–87 (2015).
190. Lazar, D. C. *et al.* Cytometric comparisons between circulating tumor cells from prostate cancer patients and the prostate-tumor-derived LNCaP cell line. *Phys. Biol.* **9**, 16002 (2012).
191. Boshuizen, R., Kuhn, P. & van den Heuvel, M. Circulating tumor

cells in non-small cell lung carcinoma. *J. Thorac. Dis.* **4**, 456–458 (2012).

192. Adams, D. L. *et al.* Circulating giant macrophages as a potential biomarker of solid tumors. *Proc. Natl. Acad. Sci. U. S. A.***111**, 3514–3519 (2014).
193. Pereira-Veiga, T. *et al.*CTCs Expression Profiling for Advanced Breast Cancer Monitoring. *Cancers (Basel).* **11**, 1941 (2019).
194. Cools-Lartigue, J. *et al.* Neutrophil extracellular traps sequester circulating tumor cells and promote metastasis. *J. Clin. Invest.* **123**, 3446–3458 (2013).
195. Aguirre, L. A. *et al.* Tumor stem cells fuse with monocytes to form highly invasive tumor-hybrid cells. *Oncoimmunology* **9**, 1773024 (2020).
196. Peake, B. F., Eze, S. M., Yang, L., Castellino, R. C. & Nahta, R. Growth differentiation factor 15 mediates epithelial mesenchymal transition and invasion of breast cancers through IGF-1R-FoxM1 signaling. *Oncotarget* **8**, 94393-94406 (2017).
197. Modi, A. *et al.* Growth differentiation factor 15 and its role in carcinogenesis: an update. *Growth Factors* **37**, 190–207 (2019).
198. Tanabe, S., Kawabata, T., Aoyagi, K., Yokozaki, H. & Sasaki, H. Gene expression and pathway analysis of CTNNB1 in cancer and stem cells. *World J. Stem Cells* **8**, 384–395 (2016).
199. Zhao, J. *et al.* Exogenous lipids promote the growth of breast cancer cells via CD36. *Oncol. Rep.* **38**, 2105–2115 (2017).
200. Li, L. & Li, W. Epithelial-mesenchymal transition in human cancer: Comprehensive reprogramming of metabolism, epigenetics, and differentiation. *Pharmacol. Ther.* **150**, 33–46 (2015).
201. Morel, A. P. *et al.* Generation of breast cancer stem cells through epithelial-mesenchymal transition. *PLoS One* **3**, 1–7 (2008).
202. Wilson, M. M., Weinberg, R. A., Lees, J. A. & Guen, V. J. Emerging Mechanisms by which EMT Programs Control Stemness. *Trends in Cancer* **6**, 775–780 (2020).
203. Xin, Y., Li, K., Yang, M. & Tan, Y. Fluid shear stress induces emt of circulating tumor cells via jnk signaling in favor of their survival during hematogenous dissemination. *Int. J. Mol. Sci.* **21**, 1–16

(2020).
204. Dicato, M., Plawny, L. & Diederich, M. Anemia in cancer. *Ann. Oncol.* **21**, vii167–vii172 (2010).
205. Lang, E., Bissinger, R., Qadri, S. M. & Lang, F. Suicidal death of erythrocytes in cancer and its chemotherapy: A potential target in the treatment of tumor-associated anemia. *Int. J. cancer* **141**, 1522–1528 (2017).
206. Lominadze, D. & Dean, W. L. Involvement of fibrinogen specific binding in erythrocyte aggregation. *FEBS Lett.* **517**, 41–44 (2002).
207. Gupta, G. P. & Massagué, J. Cancer Metastasis: Building a Framework. *Cell* **127**, 679–695 (2006).
208. Micalizzi, D. S., Maheswaran, S. & Haber, D. A. A conduit to metastasis: Circulating tumor cell biology. *Genes and Development* **31,** 1827-1840 (2017).
209. Palmirotta, R. *et al.* Liquid biopsy of cancer: a multimodal diagnostic tool in clinical oncology. *Therapeutic Advances in Medical Oncology* **10**, 1758835918794630 (2018).
210. Brock, G., Castellanos-Rizaldos, E., Hu, L., Coticchia, C. & Skog, J. Liquid biopsy for cancer screening, patient stratification and monitoring. *Translational Cancer Research* **4**, 280–290 (2015).
211. Alix-Panabières, C. & Pantel, K. Clinical applications of circulating tumor cells and circulating tumor DNA as liquid biopsy. *Cancer Discov.***6**, 479–491 (2016).
212. Sparano, J. *et al.* Association of Circulating Tumor Cells With Late Recurrence of Estrogen Receptor–Positive Breast Cancer: A Secondary Analysis of a Randomized Clinical Trial. *JAMA Oncol.***4**, 1700–1706 (2018).
213. Bidard, F. C., Proudhon, C. & Pierga, J. Y. Circulating tumor cells in breast cancer. *Molecular Oncology* **10**, 418–430 (2016).
214. Mazel, M. *et al.* Frequent expression of PD-L1 on circulating breast cancer cells. *Mol. Oncol.***9**, 1773–1782 (2015).
215. Cimadamore, A. *et al.* Update on Circulating Tumor Cells in Genitourinary Tumors with Focus on Prostate Cancer. *Cells* **9**, 1–18 (2020).
216. Pantel, K. *et al.* Circulating epithelial cells in patients with benign

colon diseases. *Clin. Chem.* **58**, 936–940 (2012).

217. Schulze, K. *et al.* Presence of EpCAM-positive circulating tumor cells as biomarker for systemic disease strongly correlates to survival in patients with hepatocellular carcinoma. *Int. J. Cancer* **133**, 2165–2171 (2013).
218. Rink, M. *et al.* Prognostic role and HER2 expression of circulating tumor cells in peripheral blood of patients prior to radical cystectomy: A prospective study. *Eur. Urol.***61**, 810–817 (2012).
219. Yu, M. *et al.* Circulating Breast Tumor Cells Exhibit Dynamic Changes in Epithelial and Mesenchymal Composition. *Science* **339**, 580–584 (2013).
220. Dongre, A. & Weinberg, R. A. New insights into the mechanisms of epithelial–mesenchymal transition and implications for cancer. *Nat. Rev. Mol. Cell Biol.* **20**, 69–84 (2019).
221. Joosse, S. A., Gorges, T. M. & Pantel, K. Biology , detection , and clinical implications of circulating tumor cells. **7**, 1–11 (2015).
222. Ferreira, M. M., Ramani, V. C. & Jeffrey, S. S. Circulating tumor cell technologies. *Molecular Oncology* **10**, 374–394 (2016).
223. Miller, M. C., Doyle, G. V. & Terstappen, L. W. M. M. Significance of Circulating Tumor Cells Detected by the CellSearch System in Patients with Metastatic Breast Colorectal and Prostate Cancer. *J. Oncol.***2010**, 1–8 (2010).
224. Stott, S. L. *et al.* Isolation of circulating tumor cells using a microvortex-generating herringbone-chip. *Proc. Natl. Acad. Sci.***107**, 18392 –18397 (2010).
225. Gwak, H. *et al.* Progress in Circulating Tumor Cell Research Using Microfluidic Devices. *Micromachines (Basel)* **9,** 353 (2018).
226. Armstrong, A. J. *et al.* Circulating tumor cells from patients with advanced prostate and breast cancer display both epithelial and mesenchymal markers. *Mol. Cancer Res.***9**, 997–1007 (2011).
227. Vila, A., *et al.* EGFR-Based Immunoisolation as a Recovery Target for Low-EpCAM CTC Subpopulation. *PLoS One* **11**, e0163705 (2016).
228. Rakha, E. A. *et al.*Prognostic markers in triple-negative breast cancer. *Cancer* **109**, 25–32 (2007).

229. Zou, Y., Xia, Y., Meng, F., Zhang, J. & Zhong, Z. GE11-Directed Functional Polymersomal Doxorubicin as an Advanced Alternative to Clinical Liposomal Formulation for Ovarian Cancer Treatment. *Mol Pharm.* **15,** 3664–3671 (2018).
230. Ding, J. *et al.* Construction of Epidermal Growth Factor Receptor Peptide Magnetic Nanovesicles with Lipid Bilayers for Enhanced Capture of Liver Cancer Circulating Tumor Cells. *Analytical chemistry* **88,** 8997–9003 (2016).
231. Bai, L. *et al.* Peptide-based isolation of circulating tumor cells by magnetic nanoparticles. *J. Mater. Chem. B* **2**, 4080–4088 (2014).
232. Sapsford, K. E. *et al.* Functionalizing nanoparticles with biological molecules: Developing chemistries that facilitate nanotechnology. *Chem. Rev.* **113**, 1904–2074 (2013).
233. Song, Y. *et al.* Chemical Science. *Chem. Sci.***8**, 1736–1751 (2017).
234. Rodahl, M., Höök, F., Krozer, A., Brzezinski, P. & Kasemo, B. Quartz crystal microbalance setup for frequency and Q-factor measurements in gaseous and liquid environments. *Rev. Sci. Instrum.* **66**, 3924–3930 (1995).
235. Peng, C., Mei, J., Huang, S., Chen, B. & Liu, J. Capture and biological release of circulating tumor cells in pancreatic cancer based on peptide-functionalized silicon nanowire substrate. *Int J Nanomedicine* **14,** 205–214 (2019).
236. Wu, L. *et al.* Fluidic Multivalent Membrane Nanointerface Enables Synergetic Enrichment of Circulating Tumor Cells with High Efficiency and Viability. *J. Am. Chem. Soc.* **142**, 4800–4806 (2020).
237. Zhou, J. *et al.* The label-free separation and culture of tumor cells in a microfluidic biochip. *Analyst* **145**, 1706–1715 (2020).
238. Chen, H. *et al.* Highly-sensitive capture of circulating tumor cells using micro-ellipse filters. *Sci. Rep.* **7,** 610 (2017).
239. Tayoun, T. *et al.* CTC-Derived Models: A Window into the Seeding Capacity of Circulating Tumor Cells (CTCs). *Cells* **8**, 1145 (2019).
240. Tagne, J. B., Kakumanu, S., Ortiz, D., Shea, T. & Nicolosi, R. J. A nanoemulsion formulation of tamoxifen increases its efficacy in a breast cancer cell line. *Mol. Pharm.* **5**, 280–286 (2008).
241. Han, B., Wang, T. & Wen, T. Elemene Nanoemulsion Inhibits

Metastasis of Breast Cancer by ROS Scavenging. *Int. J. Nanomedicine* **16**, 6035–6048 (2021).

242. Cruz, A. L. S., Barreto, E. de A., Fazolini, N. P. B., Viola, J. P. B. & Bozza, P. T. Lipid droplets: platforms with multiple functions in cancer hallmarks. *Cell Death Dis.* **11**, 105 (2020).
243. Feng, W. W. *et al.* CD36-Mediated Metabolic Rewiring of Breast Cancer Cells Promotes Resistance to HER2-Targeted Therapies. *Cell Rep.* **29**, 3405-3420.e5 (2019).
244. Giudetti, A. M. *et al.* A specific lipid metabolic profile is associated with the epithelial mesenchymal transition program. *Biochim. Biophys. Acta - Mol. Cell Biol. Lipids* **1864**, 344–357 (2019).

Liquid biopsy represents a powerful tool to support precision medicine, allowing the study of the Circulating Tumour Cells (CTCs). The objective of this thesis is to develop innovative nanoparticles that can address two of the critical points that make challenging the use of CTCs in translational studies of breast cancer: ex vivo culture and isolation. The use of proliferative nanoemulsions (NEs) was successfully translated to ex vivo CTC cultures from metastatic breast cancer patients to expand these cells for their characterization. Moreover, the NEs were functionalized with peptides (Pept-NEs)
to endow them with specific recognition capabilities and it was confirmed that Pept-NEs can be immobilized on surfaces
for their use as a potential isolation system.